

**A Simulation study on Distributed
Generation Systems with PEM Fuel
Cell and PV Cell for Power Quality
Enrichment**

**Thesis Submitted by
Sathyaprabakaran.B**

Doctor of Philosophy (Engineering)

**Department of Electrical Engineering
Faculty Council of Engineering and Technology
Jadavpur University
Kolkata, India**

2018

Jadavpur University
Kolkata-700032, India

Index No.136/11/E

1. Title of the thesis

A Simulation study on Distributed Generation Systems
with PEM Fuel Cell and PV Cell for Power Quality
Enrichment

2. Name, Designation and Institution of the Supervisors

Dr. Subrata Paul

Professor

Department of Electrical Engineering

Jadavpur University

Kolkata700032

3. List of Journal Publications

(i) Sathyaprabakaran.B.,Subrata Paul.,Debashis Chatterjee., ‘**A New Strategy for On-Line Droop Adjustment for Microgrid Connected DGs**’, *International Journal of Power Electronics and Drive System*,Vol.9, No.1, pp. 139-149, 2018.

4. List of Patents : Nil

5. List of presentations in National/International Conference/
workshops :

(i) Sathyaprabakaran.B.,Subrata Paul.,‘ **Modeling and Simulation of PEM Fuel Cell Based Power Supply and its Control**’, *IET Third International Conference on Sustainable Energy and Intelligent System*,pp.306-311, 2012.

CERTIFICATE FROM THE SUPERVISOR

This is to certify that the thesis entitled "**A Simulation study on Distributed Generation Systems with PEM Fuel Cell and PV Cell for Power Quality Enrichment**", submitted by **Shri.Sathyaprabakaran.B**, who got his name registered on 14th February , 2011, for the award of Ph.D.(Engg.) degree of Jadavpur University, is absolutely based upon his own work under the supervision of **Prof. Subrata Paul** and that neither his thesis nor any part of the thesis has been submitted for any degree/diploma or any other academic award any where before.

.....

Signature of the supervisor

with date & office seal

Acknowledgement

I am greatly indebted to my esteemed supervisor **Dr. Subrata Paul** for his infallible stewardship, kind guidance and valuable suggestions that enabled me to carry out this research. His rigorous attitude towards research and inspiring thinking to solve problems are invaluable for my career. I pay my humblest and sincere thanks to him for his interest, useful encouragement and unconditional blessings.

I convey my sincere thanks and gratitude to **Dr. Debashis Chatterjee** for kind help, and constant support rendered by him in the completion of the thesis. His expertise and dynamism in the field of Distributed Generation is just inimitable. Due to his great efforts and lot of enlightening ideas during the course of this research, it was possible to achieve the results in shortest time.

I also take the privilege of thanking **Dr. S. K. Goswami, Dr. Sunita Dey Halder, and Dr. Sudipta Nath** and **all the staff members** of Electrical Engineering Department, for their valuable suggestions and encouragement.

I am thankful to the **authorities of Jadavpur University** for providing the laboratory facilities for carrying out the research and allowing me to submit the Thesis for Ph.D. (Engineering) Degree.

I would like to extend my gratitude to **The Director, Principal, Dean, Head of EE** and **all faculty members** of **Electrical Engineering Department, Netaji Subhash Engineering College, Kolkata** for their constant support and encouragement.

My appreciation and special thanks to **Dr.Tribesh Nag** for his cordial help who helped me during my entire research work.

I would like to express my wholehearted thanks to my family especially to my wife and my children (**S.Varshitha** and **S.Logacharan**) for their love, patience and sacrifice throughout my entire life. Because of their unconditional love and prayers, I have the chance to complete this thesis.

I would like to appreciate the encouragement and prayers of my mother and my brothers for their support.

SATHYAPRABAKARAN.B

TABLE OF CONTENTS

	Page No.
ACKNOWLEDGEMENT	vi
TABLE OF CONTENTS	viii
LIST OF TABLES	xiii
LIST OF FIGURES	xiv
LIST OF ABBREVIATION	xix
ABSTRACT	xx
CHAPTER I : INTRODUCTION	
1.1	Distributed Energy Sources (DERs)..... 2
1.2	Distributed Energy Technologies..... 3
1.2.1	Fuel Cells..... 3
1.2.2	Gas Turbines..... 4
1.2.2.1	Micro Turbines..... 5
1.2.3	Photovoltaic Systems..... 5
1.2.4	Wind Energy Conversion Systems..... 6
1.3	Energy Storage Technologies..... 7
1.4	Basic concepts of Microgrid..... 7
1.4.1	Grid connected operation..... 10
1.5	Issues and challenging problems with DG..... 10
1.5.1	Anti- Islanding or Islanding Protection..... 11
1.5.2	Protection..... 13
1.5.3	Synchronization..... 13
1.5.4	Absence of standards..... 14
1.5.4.1	Grid- code requirements..... 14
1.5.6	Reconnection/Restoration..... 14

	Page No.
1.6 Power Quality and its issues.....	16
1.6.1 Power Quality problems.....	17
1.6.2 Power Quality disturbances.....	18
1.6.3 Frequency and voltage fluctuations.....	21
1.7 Control of Grid connected DGs.....	22
1.7.1 Overview of Grid – connected Inverter topology.....	23
1.7.1.1 dq-Control.....	23
1.7.1.2 $\alpha\beta$ –Control.....	24
1.7.1.3 abc – Control.....	25
1.7.2 Observations of performance of Conventional current controllers.....	26
1.8 Proposed Control methods.....	27
1.8.1 Outline of MPC.....	27
1.8.2 Glimpses of Load sharing.....	29
1.9 Objectives of study.....	30
1.10 Thesis Organization.....	31
 CHAPTER II : MODELING OF DG SOURCES	
2.1 Overview of PEM Fuel Cell.....	33
2.2. Detailed Model of PEMFC.....	36
2.3 Simulation results and discussion for modeling PEMFC.....	40
2.4 Photovoltaic (PV) Cell power system.....	43
2.4.1 PV Cell to Module to Array.....	43
2.4.2 Types of PV panels.....	45
2.5 Design of V-I characteristics of PV system.....	46

	Page No.
2.5.1	Current–Voltage Relationship For A Single PV Cell 46
2.5.2	Current–Voltage relationship for a PV module..... 47
2.5.3	Current–Voltage relationship for a photovoltaic array..... 48
2.5.4	Model Parameters of PV Cell to Module to Array 48
2.5.4.1	Ideality Factor(n)..... 48
2.5.4.2	Photocurrent (I_{ph})..... 49
2.5.4.3	Diode saturation current(I_o)..... 49
2.5.4.4	Temperature of cell (T)..... 49
2.5.4.5	Parallel leakage resistance and series resistance..... 50
2.6	Simulation Results and discussion..... 50
2.7	Conclusion..... 53

CHAPTER III : CONCEPTS OF CONTROL OF GRID -CONNECTED DGS WITH EMPHASIZE ON SRF

3.1	Overview of Proposed Grid connected structure..... 54
3.2	Three- Phase Grid connected topology..... 55
3.3	Pulse Width Modulation(PWM)..... 56
3.3.1	Sine Pulse Width Modulation(SPWM)..... 56
3.4	LC Filter Design..... 57
3.5	Proportional – Integral (PI) controller for Grid- connected Inverter....., 60
3.6	Phase locked Loop(PLL)..... 61
3.6.1	SRF- PLL..... 62
3.6.1.1	Stationary reference frame of $\alpha\beta$ 63

	Page No.
3.6.1.2 Synchronous rotating reference frame (SRF) of <i>abc</i> , $\alpha\beta$ and <i>dq</i>	64
3.7 Modeling of three-phase Grid-connected VSI system with SRF	64
3.8 Control of Grid Connected Converters.....	67
3.8.1 VSI control strategies.....	67
3.8.2 Active and Reactive Power (<i>PQ</i>) Control Strategy..	68
3.9 Simulation Results and discussion under balanced condition....	70
3.10 Conclusion.....	75

**CHAPTER IV : PROPOSED PREDICTIVE CURRENT CONTROL
METHOD FOR ANALYSIS UNDER UNBALANCED VOLTAGE DIP
CONDITIONS**

4.1 Predictive Current control method.....	76
4.2 Overview of Model Predictive Control.....	77
4.3 Predictive Control of a Three-Phase Inverter.....	78
4.3.1 Cost Function.....	79
4.3.2 Converter Model.....	80
4.3.3 Load Model.....	84
4.4 Discrete-Time Model for Prediction.....	85
4.5 Principle of MPC controller.....	86
4.6 Simulation Code.....	89
4.7 Results and discussion.....	91
4.8 Conclusion	97

**CHAPTER V :PROPOSED POWER SYSTEM CONTROL DESIGN
FOR PARALLEL INVERTERS**

5.1	Introduction.....	99
5.2	Various control methods of the Parallel Inverters.....	100
5.2.1	Instantaneous Current Sharing Using Master/Slave Method.....	100
5.2.2	Deviation from average Active/Reactive Powers Method.....	100
5.2.3	Harmonic and Reactive Current Injection Method	101
5.2.4	Frequency and Voltage Droop Method.....	101
5.3	Concise introduction of Droop Control.....	102
5.4	Load-sharing control of Parallel Power converters.....	105
5.4.1	Grid Impedance Influence on Droop Control.....	106
5.4.2	VSI control strategies.....	110
5.4.3	<i>P-Q</i> control strategies.....	110
5.4.4	<i>V-f</i> Control strategy.....	111
5.4.5	Control of the DC link voltage.....	113
5.5	Simulation results and discussion	114
5.6	Conclusion.....	121

CHAPTER VI : CONCLUSION

6.1	Conclusion.....	122
6.2	Future Scope of Study.....	123

REFERENCES		124
-------------------	--	-----

LIST OF TABLES

Table No.		Page No.
2.1	Fuel Cell types with its merits and demerits.....	35
2.2	Input parameters for PEMFC Model.....	41
2.3	Simulation Input for PV Model.....	51
3.1	Parameter Values for grid connected DGs under balanced condition.....	73
4.1	Predictive Control Algorithm.....	79
4.2	Switching states and voltage vectors for SVPWM.....	84
4.3	System parameters for MPC controlled DGs.....	91
5.1	System parameters for the droop controlled DGs.....	115

LIST OF FIGURE

Figure No.		Page No.
1.1	Technologies that support DER systems.....	2
1.2	Scheme of Fuel Cell system.....	4
1.3	Gas Turbines Electrical power Generation.....	5
1.4	Scheme of PV System.....	6
1.5	Block Diagram of Wind systems.....	6
1.6	Typical Microgrid Architecture.....	9
1.7	(a) Grid Connected Microgrid (b) Islanded Microgrid...	10
1.8	Block diagram of Grid restoration from Islanded mode to Grid- connected mode.....	11
1.9	Common behaviour of Electrical disturbances.....	17
1.10	Waveforms illustrating various Power Quality Disrurbances.....	18
1.11	Voltage variation waveform.....	21
1.12	General Structure of dqo control strategy.....	24
1.13	General Structure of $\alpha\beta$ control strategy.....	25
1.14	General Structure of abc control strategy.....	26
1.15	Basic structure of Model Predictive Control.....	28
1.16	Structure of P-f and Q-V Droop control.....	30
2.1	Basic Scheme of PEMFC.....	34
2.2	Equivalent circuit of PEMFC.....	37
2.3	Ideal Polarization curve of a FC.....	38
2.4	Simulated Fuel Cell stack voltage.....	41
2.5	Matlab simulated diagram of PEMFC stack.....	42

Figure No.		Page No.
2.6	PV Cell to Module to Array.....	43
2.7	Working model of single PV cell.....	44
2.8	Types of PV panels for home use.....	45
2.9	Equivalent circuit of PV cell.....	47
2.10	(a) Simulation Model of PV system	51
	(b)Sub-system.....	52
2.11	Simulated results of V-I and P-V characteristics of PV Array.....	52
3.1	Architecture of proposed scheme.....	55
3.2	A typical VSI structure.....	55
3.3	Sinusoidal Waveform of three phase SPWM.....	57
3.4	Types of Filter based on frequency and bandwidth and their characteristics.....	58
3.5	LC Filter.....	59
3.6	Structure of the SRF PLL.....	62
3.7	abc to dq transformation.....	62
3.8	Synchronous rotating reference frame.....	64
3.9	Schematic diagram of Three-phase grid-connected inverter.....	65
3.10	Control Structure of Grid-connected VSI.....	68
3.11	Decoupling control of active and reactive power.....	69
3.12	(a) Angular frequency of reference phase.....	69
	(b) Voltage characteristics of grid and Inverter synchronization by PLL.....	71
3.13	Simulated result measured at PCC point - Voltage characteristics.....	72

Figure No.	Page No.
3.14	Simulated result measured at PCC point - Current characteristics..... 72
3.15	Simulated results of Active power delivered by DGs..... 74
3.16	Simulated result of d- axis current delivered by DGs..... 74
4.1	Working principle of MPC..... 77
4.2	General MPC scheme..... 78
4.3	Predictive current control block diagram..... 80
4.4	Voltage Source inverter Power circuit..... 81
4.5	Equivalent load configurations for different switching states..... 82
4.6	Voltage vectors in complex plane..... 83
4.7	Structure of the proposed control scheme with a disturbance observer..... 87
4.8	Predictive control algorithm flow diagram..... 88
4.9	Simulation results of Three- phase Grid connected inverter: (a) DC link voltage measured across the capacitor..... 92 (b) Inverter current waveform..... 92
4.10	Simulation results of implementation of SRF: (a) Voltage wave form during voltage dip..... 93 (b) Corresponding current wave form during dip..... 93
4.11	Simulation results of Three- phase Grid connected inverter with MPC: (a) Phase voltage waveform 94

Figure No.	Page No.
(b)Line voltage waveform.....	94
(c) Line current waveform.....	95
4.12 Variations in the parameters of d and q values during the occurrence of disturbance in the system :	
(a) Direct axis Current.....	95
(b) Direct axis voltage.....	96
(c) Quadrature axis voltage.....	96
4.13 Simulink Model of proposed control scheme.....	98
5.1 Various power control strategies for an islanded microgrid.....	102
5.2 Power flow control between two voltage sources nodes.....	104
5.3 Parallel connection of two inverters to a common load.....	105
5.4 Simplified model of power convector connected to a distribution network:	
(a) Equivalent circuit.....	106
(b) Phasor diagram.....	107
5.5 Droop characteristics of voltage and frequency.....	108
5.6 Reference voltage and frequency of Droop characteristics.	109
5.7 Droop Control Structure of Grid-connected VSI.....	110
5.8 Structure of voltage and frequency droop control.....	112
5.9 Block diagram of Complete Control structure of the study	114
5.10 Simulation results of load sharing system during transition	
(a) voltage waveform.....	115
(b) current waveform.....	116
5.11 Simulation results of power sharing:	
(a) Active power.....	117

Figure No.	Page No.
(b) Reactive power	117
(c) Frequency.....	117
(d) Drop in Voltage.....	118
5.12 Variations in the parameters of d and q values during the occurrence of disturbance in the system :	
a) direct axis current	119
b) direct and quadrature axis voltage.....	119
5.13 Simulink Model of Complete Control structure of the study	120

LIST OF ABBREVIATIONS

CHP	combined heat and power
DER	Distributed energy resources
DG	distributed generation
FACTS	flexible AC transmission system
FC	Fuel cells
LV	low voltage
MG	Microgrid
MPC	Model predictive control
MPPT	maximum power point tracking
MV	medium voltage
PCC	Point of common Coupling
PEMFC	Proton exchange membrane fuel cell
PI	Proportional Integral
PLL	Phase Locked Loop
PV	Photovoltaic cell
PWM	Pulse Width Modulation
SPWM	Sine Pulse Width Modulation
SRF	Synchronous rotating reference frame
VSI	Voltage Source Inverter

ABSTRACT

The main focus of this thesis is fundamental investigations of control techniques of inverter-based microgrids. It aims to develop new and improved control techniques to enhance performance and reliability so as to improve the overall power quality. It focuses on analysis of power quality disturbances occurring in the microgrid.

Conventional current controllers are only effective when the grid voltage is ideally balanced and sinusoidal. Due to the popular use of nonlinear loads, the grid voltage at the point of common coupling (PCC) is typically not pure sinusoidal, but instead can be unbalanced or distorted. These abnormal grid voltage conditions can strongly deteriorate the performance of the regulating grid current. The control methods, MPC and Droop control however have been emerged as potential control power to achieve high quality grid current and to improve the system dynamic response, eliminate steady state error and to prevent the use of the feed-forward.

A current predictive based MPC method is proposed in our research work, which has demand to define cost functions and can further simplify the calculation process. MPC has been proposed for the current control, which is the preeminent powerful alternative to conventional method for the conventional current control. This control scheme predicts the future load current behaviour for each valid switching state of the converter, in terms of the measured load current and predicted load voltage. The predictions are evaluated with a cost function that minimizes the error between the predicted

currents and their references at the end of each sampling time. A nonlinear control technique has been developed for three-phase voltage-source converters. The converter switching states are selected from a switching table. This algorithm selects the appropriate voltage vectors and calculates duty cycles in every sampling period to minimize the errors of the instantaneous active and reactive power. Simulation studies are performed to verify the performance of the MPC control method and its strategy.

In inverter-based microgrids, the paralleled inverters need to work in both grid-connected mode and Islanded mode and should be able to transfer seamlessly between the two modes. In grid-connected mode, the inverters control the amount of power injected into the grid. In Islanded mode, however, the inverters control the island voltage while the output power is dictated by the load. This can be achieved using droop control.

This thesis proposes a simple and effective control technique for interconnection of DG resources to the power grid via interfacing converters based on Phase locked loop (PLL) and Droop control. The behaviour of a Microgrid (MG) system during the transition from islanded mode to grid-connected mode of operation has been studied. A dynamic phase shifted PLL technique is locally designed for generating phase reference of each inverter. Droop relations are established between the voltage and current in dq synchronous reference frame (SRF). To provide better dynamics and higher stability, the SRF voltage and current are decoupled by introducing a current vector, which is aligned with the voltage vector. The phase angle between filter capacitor voltage vector and d-axis is dynamically adjusted with the change in q-axis inverter current to generate the phase reference of each

inverter. During fluctuations in load capacity, the grid-connected system must be able to supply balanced power from the utility grid side and micro-grid side. Therefore, droop control is implemented to maintain a balanced power sharing.

An adjusted droop control method for equivalent load sharing of parallel connected Inverters, without any communication between individual inverters, has been presented. The control loops are tested with aid of MATLAB Simulink tool during several operating conditions.

Chapter I

Introduction

Energy plays its continuous role in all domains of human life, since the industrial revolution started and the world started looking towards productivity and modernity. The main sources of power generation are fossil fuels (coal, oil and natural gas) and nuclear power plants. These sources may be sufficient for our generation; however for future generations there is necessity to look for sustainability and finding new solutions to resolve the problem of increasing energy demand and exhaustible fossil fuels resources [1]-[5].

Further, generation of electric power via conventional means is unsustainable, it is considered as the main source of greenhouse gases mainly CO₂ which harms the environment drastically and causes global warming, ozone depletion and climate change. Thus one of the major priorities worldwide is focusing on the sustainability terms; Renewable Energy (RE), Energy Efficiency Improvements (EEI) and Energy Saving (ES), which are representing interesting areas for researchers and engineers to overcome these problems by introducing solutions for maintaining the environment and looking for sustainability [6]-[8].

Clean Energy (CE) is generated by Renewable Energy Sources (RES) like solar energy, wind energy, geothermal and other forms like biomass. These kinds of sources have been used in the past just for special purposes, for supplying rural areas with electricity, wherein supplying these areas from utility grids requires more infrastructures like transmission lines and transformers with more losses and huge investment costs. Nowadays renewable energy is commonly used in different applications mainly in grid connected systems [9].

The utility grid in the decade became the main power supply mode in the world with the growing demand for electricity. However, it has gradually revealed some problems, such as difficulty in running and high cost, and it is also difficult to meet the safety and reliability

requirement in load with the increasingly high demand. The interconnection of distributed generators (DGs) to the utility grid through power electronic converters has raised concern about proper load sharing between different DGs and the grid. The reduction in global emissions and energy losses make the Microgrid (MG) a promising alternative to traditional power distribution systems.

1.1 Distributed energy resources (DERs)

Distributed energy resources (DER) refers to electric power generation resources that are directly connected to medium voltage (MV) or low voltage (LV) distribution systems, rather than to the bulk power transmission systems [10]. DER includes both generation units such as fuel cells, micro-turbines, photovoltaic, etc., and energy storage technologies like batteries, flywheels, superconducting magnetic energy storage, to mention but a few. Further explanation of each of these is presented in the following sections. Figure 1.1 illustrates the technologies that can support DER systems.

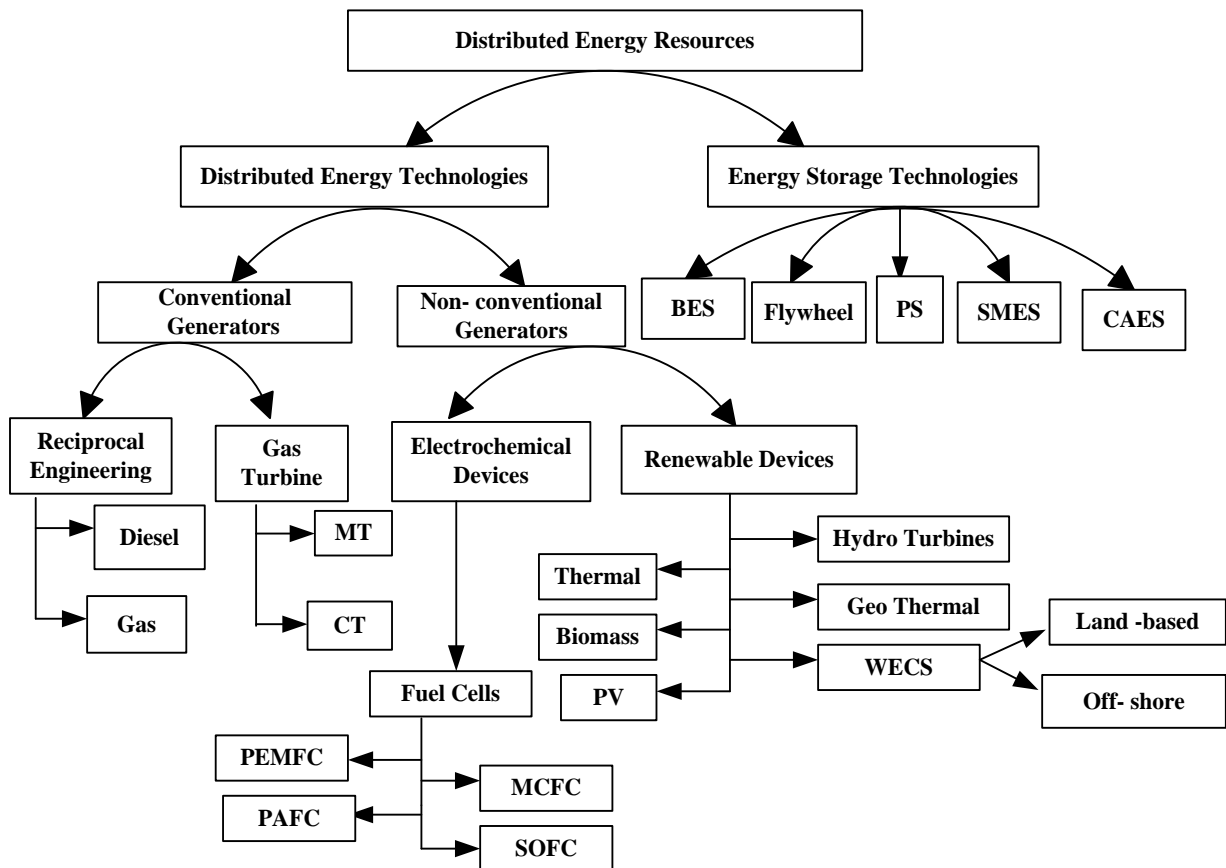


Figure 1.1 Technologies that support DER systems

The exact definition of DG varies somewhat between sources and capacities; however, it is defined as any source of electric power of limited capacity, directly connected to the power system distribution network where it is consumed by the end users. DG can be powered by micro-turbines, combustion engines, fuel cells, wind turbines, geothermal, photovoltaic system, etc. DG takes place on two-levels: the local level and the end-point level. Local level power generation plants often include renewable energy technologies that are site specific, such as wind turbines, geothermal energy production, solar systems (photovoltaic and combustion), and some hydro-thermal plants. At the end-point level, the individual energy consumer can apply many of these same technologies with similar effects [11].

1.2 Distributed Energy Technologies

In this section, the brief overviews of some of the renewable and non- renewable Distributed Energy systems are presented.

1.2.1 Fuel cells (FCs)

Fuel cells convert chemical energy directly into electrical energy and heat. This process has got the similarities with that of batteries, since both use electrochemical process, between hydrogen and oxygen to generate a DC current [12]. These two devices (batteries and fuel cells) consist of two electrodes, separated by an electrolyte. Eq. (1.1) shows the overall chemical reaction in fuel cells.



Fuel cells are generally characterized by the material of electrolyte used. Major types of fuel cells in different stages of commercial availability are discussed detail in chapter II.

To obtain AC current from fuel cell technology, power conditioning equipment is required to handle the inversion of DC current generated by fuel cell to AC current that is required to be integrated into the distribution network [12]. Physically a fuel cell plant consists of three major parts: a fuel processor that removes fuel impurities and may increase concentration of hydrogen in the fuel; a power section (fuel cell itself) which consists of a set

of stacks containing catalytic electrodes, generating the electricity; and a power conditioner that converts the direct current produced in the power section into alternating current to be connected to the grid [10],[13]. Resulting advantages of this technology are high efficiency, almost low emissions, and noiselessness as a result of non-existence of moving parts, and free adjustable ratio (50 kW–3 MW) of electric and heat generation. The energy savings result from the high conversion efficiency, is typically 40% or higher, depending on the type of fuel cell. When utilized in a cogeneration application by recovering the available thermal energy output, fuel cell’s overall energy utilization efficiencies can be in the order of 85% or more. Fuel cell fed into the grid is depicted in figure 1.2.

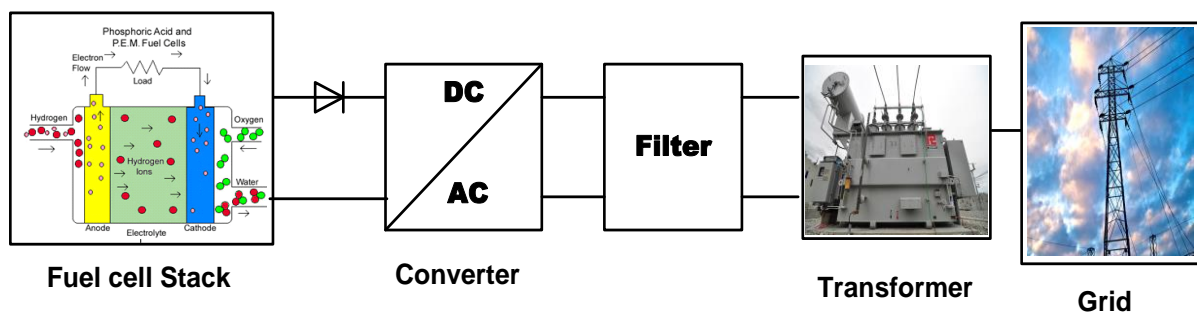


Figure 1.2 Scheme of Fuel Cell system

1.2.2 Gas Turbines (GT)

A gas turbine, otherwise known as a combustion turbine, is a rotary engine that extracts energy from a flow of combustion gas. It has a combustion chamber in-between the upstream compressor coupled to a downstream turbine. Gas turbines are generally divided into three main categories, namely: heavy frame, aero derivative, and micro-turbine. The micro-turbines (MT) that are commercially viable are available in the 27–250 kW range. The technology is largely based upon aircraft auxiliary power units and automotive style turbochargers. Energy is added to the gas stream in the combustor, where air is mixed with fuel and ignited. Combustion increases the temperature, velocity and volume of the gas flow. This is directed through a nozzle over the turbine’s blades, spinning the turbine and powering the compressor. Energy is extracted in the form of shaft power, compressed air and thrust, in any combination, and used to power aircraft, trains, ships, generators, and even tanks. The working principle is depicted in figure 1.3.

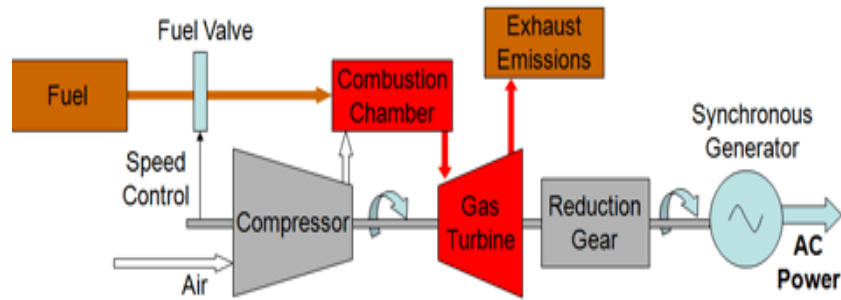


Figure 1.3 Gas Turbines Electrical power Generation

1.2.2.1 Micro-turbines (MT)

Application of Micro-turbines are becoming widespread for distributed power and combined heat and power applications as they can start quickly. They are one of the most promising technologies for powering hybrid electric vehicles. Generally micro-turbine systems range from 30 to 400 kW, while conventional gas turbines range from 500 kW to more than 300MW. Part of their success is due to advances in power electronics, which enables unattended operation and interfacing with the commercial power grid. Typical micro-turbine efficiencies are between 33% and 37%, especially with 85% effective recuperate, but could achieve efficiencies of above 80% in a combined heat and power (CHP) application.

1.2.3 Photovoltaic systems (PVs)

Conversion of solar energy directly to electricity has been technologically possible since the late 1930s, using photovoltaic systems (PVs). These systems are commonly known as solar panels. PV solar panels consist of discrete multiple cells, connected together either in series or parallel, that convert light radiation into electricity. PV technology could be stand-alone or connected to the grid [6]. The output power of PV panels is directly proportional to the surface area of the cells and footprint sizes. Therefore, footprint needs to be relatively large (0.02 kW/m²). Even though the operating efficiency of this technology may be relatively low (10–24%), nevertheless, it cannot be compared with non-renewable systems. Since the output current of PVs is a function of solar radiation and temperature, a maximum power point tracking (MPPT) stage is required in the converter to always obtain the maximum power output [13]-[16]. PV units are integrated into the grid as depicted in Figure.1.4.

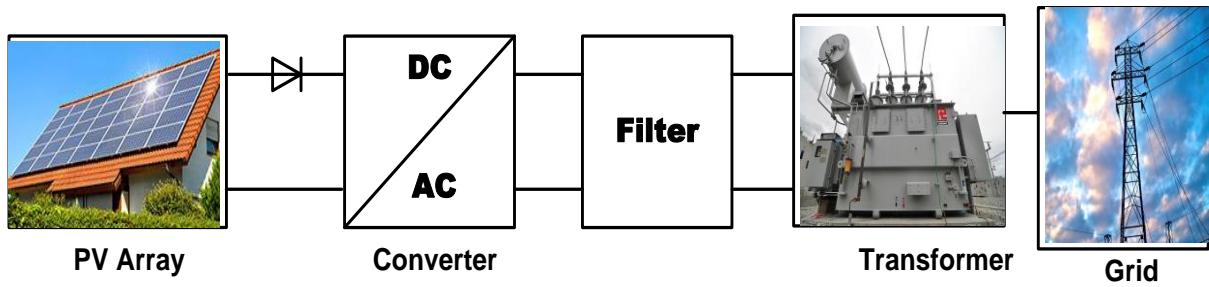


Figure 1.4 Scheme of PV System

1.2.4 Wind energy conversion system (WECS)

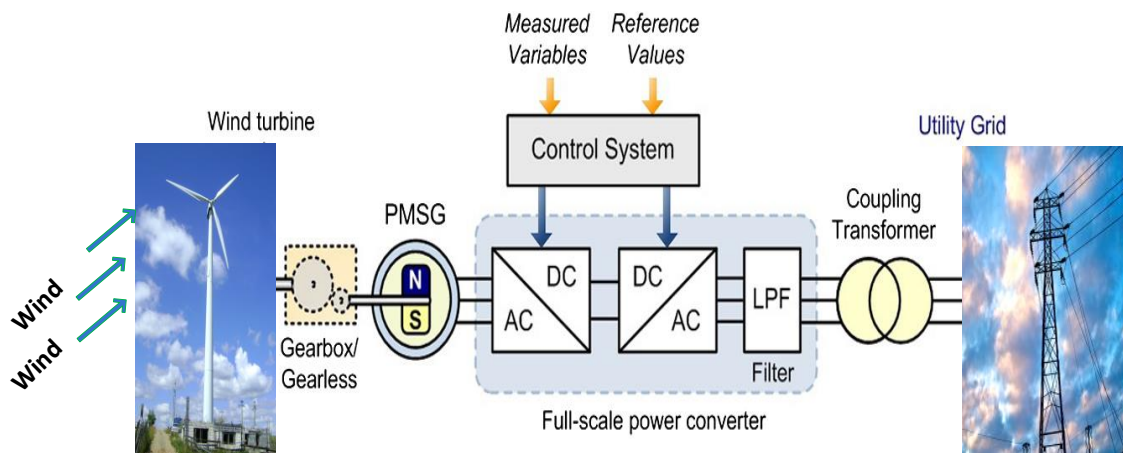


Figure 1.5 Block Diagram of Wind systems

Windmills or wind turbines convert the kinetic energy of the streaming air to electric power. Investigation has revealed that power is produced in the wind speed of 4–25 m/s range. The size of the wind turbine has increased rapidly during the last two decades with the largest units now being about 4 MW compared to the 1970s in which unit sizes were below 20 kW. For wind turbines above 1.0MW size to overcome mechanical stresses, they are equipped with a variable speed system incorporating power electronics. Single units can normally be integrated to the distribution grid of 10–20 kV, though the present trend is that wind power is being located off shore in larger parks that are connected to high voltage levels, even to the transmission system. The power quality depends on the system design. Direct connection of synchronous generators may result in increased flicker levels and relatively large active power variation. At present, wind energy has been found to be the most

competitive among all renewable energy technologies. Figure 1.5 presents the schematic block diagram of WECS connection to the power grid.

1.3 Energy storage Technologies

The Energy storage devices are one of the main critical components to rely on for successful operation of a microgrid that provides the user with dispatch capability of the distributed resources (PV and wind etc.) and to be the caretaker in balancing the power and energy demand with generation. It is easier to integrate into a dc system. The stored energy can then be used to provide electricity during periods of high demand. Energy storage devices take this responsibility in three necessary scenarios:

- Ensure the power balance in a microgrid despite load fluctuations and transients since DGs with their lower inertia lack the capability for fast responding to these disturbances;
- Provides ride-through capability when there are dynamic variations in intermittent energy sources and allows the DGs to operate as dispatchable units;
- Provides the initial energy requirement for a seamless transition between grid-connected to/from islanded operation of microgrids.

But its disadvantage is that the electrical energy needs to be stored in battery banks requiring more space and maintenance.

1.4 Basic concepts of Microgrid

The rapid development of DG generations has not only provided a lot of clean and efficient energy for the community, but has also brought great challenges to the existing power system. In order to reduce the adverse impact on the existing distribution network brought by DG, Microgrid concepts is new approach to the integration of DER due to the rapid growth of systems of decentralized energy production and thus opening promising perspectives in the sustainable energy sector. A microgrid can be considered as a local grid, it is formed by integrating loads, multiple DGs, ESS could also be used to control the net power flows to and from the utility in the grid connected mode [12], Such MGs also include the flexible AC transmission system (FACTS) control devices such as power flow controllers and voltage regulators as well as protective relays and circuit breakers[20] ,the MG is able to operate either in grid-connected or islanded mode, with possibility of seamless transitions between them[26].

The microgrid concept acts as solution to the problem of integrating large amount of micro generation without interrupting the utility network's operation. The microgrid or distribution network subsystem will create less trouble to the utility network than the conventional micro generation if there is proper and intelligent coordination of micro generation and loads. In case of disturbances on the main network, microgrid could potentially disconnect and continue to operate individually, which helps in improving power quality to the consumer [3].

The U. S. Department of Energy (DOE) has provided the following definition of Microgrids

“A Microgrid, a local energy network, offers integration of distributed energy resources (DER) with local elastic loads, which can operate in parallel with the grid or in an intentional island mode to provide a customized level of high reliability and resilience to grid disturbances. This advanced, integrated distribution system addresses the need for application in locations with electric supply and/or delivery constraints, in remote sites, and for protection of critical loads and economically sensitive development. (Myles, et al. 2011)”

The Congressional Research Service (CRS) presents following definition for Microgrid. It has a slight difference with the above description:

“A Microgrid is any small or local electric power system that is independent of the bulk electric power network. For example, it can be a combined heat and power system based on a natural gas combustion engine (which cogenerates electricity and hot water or steam from water used to cool the natural gas turbine), or diesel generators, renewable energy, or fuel cells. A Microgrid can be used to serve the electricity needs of data centres, colleges, hospitals, factories, military bases, or entire communities.”

Different scenarios for future architectures of electricity systems recognize a fundamental fact that with increased levels of DG penetration; the distribution network can no longer be considered as a passive appendage to the transmission network. The entire distributed system has to be designed/operated as an integrated unit.

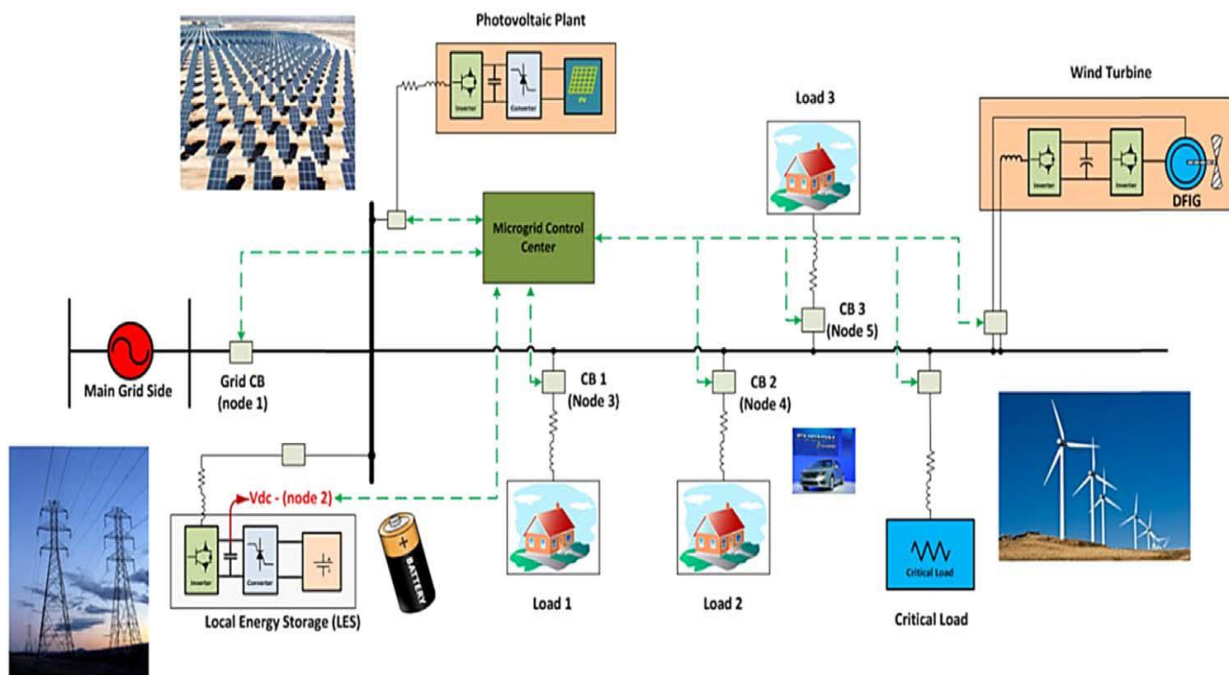


Figure 1.6 Typical Microgrid Architecture

The microgrid is an interconnection of distributed energy sources, such as micro turbines, wind turbines, fuel cells and PVs integrated with storage devices, such as batteries, flywheels and power capacitors on low voltage distribution systems [17]. Each feeder has circuit breaker and power flow controller. The basic microgrid architecture along with DGs connected to utility grid is shown in Figure 1.6.

An important advantage of MGs is improvement of energy efficiency with the system of producing CHP combined, which captures thermal energy resulting from the production of electricity for a variety of heating needs (hot water steam, heating and cooling). The microgrid is responsible to provide and ensure these following criteria

- To ensure that the micro sources feed the electrical loads; offers and optimizes heat utilization for local installation
- To ensure that the microgrid satisfies operational contracts with the utility;
- To minimize emissions and/or system losses;
- To enhance the robustness of the distribution system and maximize the operational efficiency and local reliability;
- To facilitate greater use of renewable (wind and PV systems);

- To ensure that the active and reactive powers are transferred according to necessity of the microgrids and/or the distribution system;
- Disconnection and reconnection processes are conducted seamlessly;
- In case of general failure, the microgrid is able to operate through black-start.

1.4.1 Microgrid operation

Two operation modes of microgrid can be defined as follows [31]:

• **Grid-connected Mode:** The microgrid is connected to the upstream network. The MG can receive totally or partially the energy by the main grid (depending on the power sharing). On the other hand, the power excess can be sent to the main grid (when the total production exceeds consumption).

• **Islanded Mode:** when the upstream network has a failure (fault) known as unscheduled Islanding, or there are some planned actions (for example, in order to perform maintenance actions) known as pre-scheduled Islanding, the MG can smoothly move to islanded operation [32]. Thus, the MG operate autonomously, is called island mode, in a similar way to the electric power systems of the physical islands.

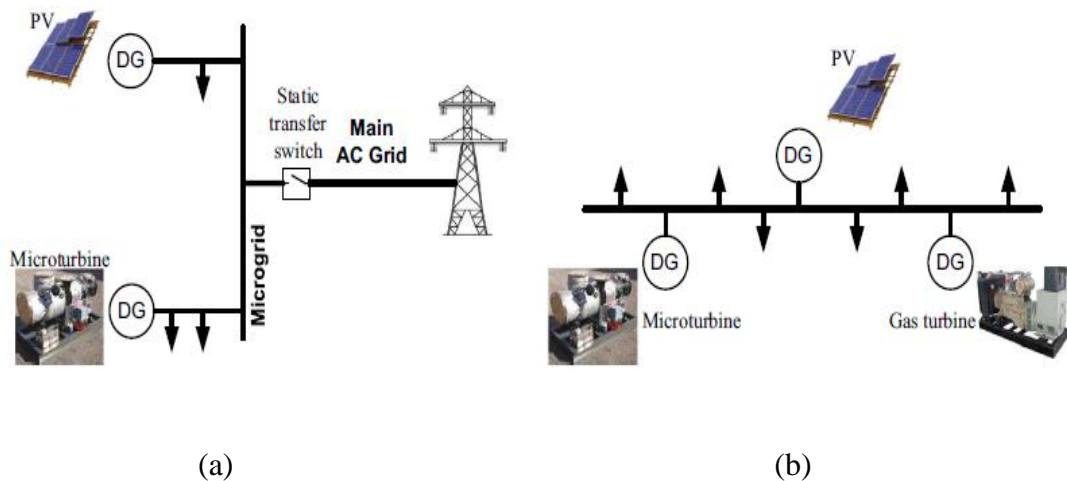


Figure 1.7 (a) Grid Connected Microgrid (b) Islanded Microgrid

1.5 Issues and Challenging problems with DG

Despite the fact that the Microgrid system has a large number of benefits, its application involves several disadvantages. The challenging problems are listed below:

- Anti-Islanding protection
- Auto reconnection after a trip
- Short circuit capacity
- AC and DC Isolation
- Installation safety requirements
- Voltage regulation
- Harmonics
- Flicker, unbalance
- Over-voltage from direct/indirect lightning
- Transient over voltage in grid
- DC injection and power factor

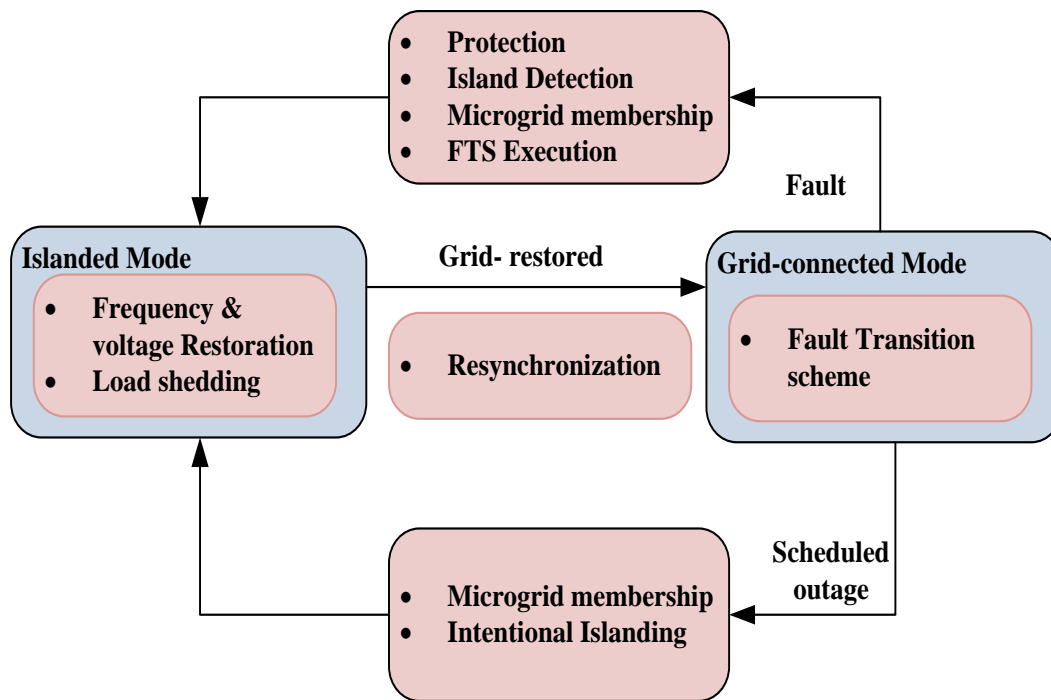


Figure 1.8 Block diagram of Grid restoration from Islanded mode to Grid- connected mode

The detailed discussion of some of the challenges, difficulties and potential drawbacks faced by Microgrid are presented below.

1.5.1 Anti- Islanding or Islanding Protection

Islanding refers to the condition when a portion of the grid becomes temporarily isolated from the main grid but remains energized by its own DGs. For example DGs like

solar panel or wind turbine continues to generate power and feed the grid, even though the electricity power from the electrical utility is no longer present. Also it exposes utility workers to life critical dangers of shocks and burns, who may think that there is no power once the utility power is shut down, but the grid may still be powered due to the distributed generators.

Islanding may be unintentional or intentional.

(i) ***Intentional Islanding***

The intentional islanding is preferably done with a minimal load flow to or from the main grid due to intentional disconnect for rectifying the sags, scheduled outage or for servicing the power lines. Controlled islands are more stable than the unintentionally formed islands. They are also less prone to collapse and do not aggravate existing conditions that lead to blackouts. However, these islands may still suffer from generation-load imbalances. To eliminate undesired consequences of a power imbalance, load or generation shedding is executed.

(ii) ***Unintentional Islanding***

The main hazards and problems associated with unintentional islanding are:

- *Violation of the acceptable limits* for voltage, frequency, unbalance, harmonics, flicker and other *PQ* parameters which can lead to malfunction or damage of network and customer equipment. Usually this hazard is restricted by the tripping limits of protective relays (voltage and frequency) implemented at the generator site.
- *Uncleared faults* (earth or phase faults) due to too low short-circuit capacity or unearthed operation. Possible damage of network equipment, or sustained fault currents.
- *Out-of-phase re-closing* of circuit breakers may damage circuit breaker equipment and cause high transient in rush currents which may damage the generator. Of particular relevance for networks with an automatic re-closing facility.
- *Electric shock* due to touching of live conductors assumed to be dead. Only relevant for LV networks and depending on the safety practices applied for working on the line.

To avoid this problem, all distributed generators should be equipped with devices to prevent islanding. Thus, distributed generators must detect islanding and immediately

disconnect from the circuit. The act of preventing islanding from happening is also called anti-islanding.

To detect the islanding event, islanding detection technique commonly uses frequency, voltage, active power, and reactive power parameters. The type of loads, affects all of these parameters which in turn affect the performance of islanding. There are many ways to detect islanding. a) Active islanding detection; b) Passive detection methods

(a) Active islanding detection

Active detection methods involve the technique of constantly sending a signal back and forth between the distributed generator and the grid to ensure the status of electrical supply.

(b) Passive islanding detection

Passive detection methods make use of transients in the electricity (such as voltage, current, frequency, etc.) for detection.

1.5.2 Protection

To ensure reliable, safe operation of the power system network proper protective devices with better selectivity, fast operation, simplicity, flexibility, different setting opportunities and low price has to be chosen. The traditional protection schemes designed for radial flow with high fault current for distribution network will not operate faithfully to MG because of bidirectional power flow, dynamic characteristics of DGs, intermittent nature of the DG and variation in fault current. The major challenges faced in the protection of microgrid are

- (a) Dynamics in fault current magnitude
- (b) Loss of Mains (LOM)
- (c) Unnecessary disconnections (lack of selectivity)
- (d) Blinding of protection

1.5.3 Synchronization

Converter interfaced DG units must be synchronized with the utility system. Grid synchronization is a challenging task especially when the utility signal is polluted with disturbances and harmonics or distorted frequency. A phase detecting technique provides a

reference phase signal synchronized with the grid voltage that is required to control and meet the power quality standards. This is critical in converter interfaced DG units where the synchronization scheme should provide a high degree of insensitivity to power system disturbances, unbalances, harmonics, voltage sags, and other types of pollutions that exist in the grid signal. In general, a good synchronization scheme must

- proficiently detect the phase angle of the utility signal,
- track the phase and frequency variations smoothly,
- forcefully reject disturbances and harmonics.

1.5.4 Absence of standards

Since this is a new potential area, there are not yet available standards for several crucial issues as power quality data for several micro source generation, standards and protocols to enable the integration of micro sources in electricity markets. Safety guidelines and protection guidelines are also lacking.

1.5.4.1 Grid code requirements

A grid code is an 'interconnecting guidelines' or instructions, which specify technical and operational characteristic requirements of power plants. It is the specification which defines the parameters a facility connected to an electric network has to meet to ensure safe, secure and proper economic functioning of the electric system. These include voltage regulation, reactive power supply and power factor limits, response to a system fault (short-circuit), response to changes in the frequency on the grid, and requirement to "ride through" short interruptions of the connection [13].

1.5.5 Reconnection/Restoration

Currently, MGs are being phased in slowly due in part to the difficulty of operating sub networks independently as well as determining when they can be reconnected to the main grid. Upon reconnection of an islanded sub-network to the main grid, instability can cause damage on both ends. It is important to track instabilities on both the microgrid and main grid upon reconnection to accurately depict the outcome of reconnection. Effort has been directed at creating control schemes to minimize power flow at the point of common coupling (PCC)

using direct machine control, load shedding, as well as energy storage, to aid in smooth reconnection .

Black - start - The process of restoring an electric power station or a part of an electric grid to operation without relying on the external electric power transmission network is known as **blackstart**. Normally, the electric power used within the plant is provided from the station's own generators. If all of the plant's main generators are shut down, station service power is provided by drawing power from the grid through the plant's transmission line. However, during a wide-area outage, off-site power from the grid is not available. In the absence of grid power, a so-called black start needs to be performed to bootstrap the power grid into operation.

Not all generating plants are suitable for black-start capability. Wind turbines are not suitable for black start because wind may not be available when needed. Wind turbines, mini-hydro, or micro-hydro plants, are often connected to induction generators which are incapable of providing power to re-energize the network. The black-start unit must also be stable when operated with the large reactive load of a long transmission line. Many high-voltage direct current converter stations cannot operate into a "dead" system, either, since they require commutation power from the system at the load end.

During restoration process of the islands back to the power transmission system, two main issues have to be considered, voltage control and frequency control. Since the islands were formed to eliminate the risk of blackout during a contingency, it has to be integrated to the main grid as soon as the fault is cleared. After restoration of the tie lines, if the system is found to be stable, the load can be restored according to the load priority. And if the system is found to be unstable, the next line according to the line priority is restored instead of restoring the load.

The major steps required for restoration are:

- 1) Islands which have survived need to be stabilised for frequency and need to be used for starting other units.
- 2) Hydro/Gas units which require less startup power need to be started using in-house DG sets.
- 3) Larger thermal units need to be fed "startup power" from: a) Islands which have survived b) Blackstarted generators c) Other synchronous grids.

- 4) Started units are synchronised with one another.
- 5) Loads and Generation have to be matched as much as possible to avoid large frequency variations.

1.6 Power Quality and its issues

Power Quality is a combination of voltage profile, Frequency profile, Harmonics contain and reliability of power supply.

Power quality is often defined as the electrical network's or the grid's ability to supply a clean and stable power supply. In other words, power quality ideally creates a perfect power supply that is always available, has a pure noise-free sinusoidal wave shape, and is always within voltage and frequency tolerances.

Power Quality problem is defined as “Any power problem manifested in voltage/current or leading to frequency deviations that result in failure or misoperation of customer equipment”. i.e. the decisive measurement of power quality is taken from the performance and productivity of end-user equipment (customer). If the electric power is inadequate for those needs, the quality is said to be “lacking”.

The definition of the IEEE Standard 1100 (“IEEE Recommended Practice for Powering and Grounding Sensitive Electronic Equipment”, also known as “Emerald Book”) for Power quality is “the concept of powering and grounding sensitive equipment in a matter that is suitable to the operation of that equipment”.

Apart from natural phenomena that cannot be avoided, e.g. lightning, a usual procedure is the customers and utilities blaming each other. Some cases can be identified as typical:

- Remote faults in the system can make the voltage drop at the point where a critical customer is connected. Although the utility might not detect any abnormality on the feeder to this customer due to the suitable action of the protection system, the voltage drop might be sufficient to cause an adjustable speed drive (ASD) of a motor to trip off.
- Despite being originally supplied by a voltage with “good quality”, wrong manoeuvres, equipment malfunction or high non-linear loads at the industrial plant can also

be the source of power quality problems to other customers supplied by an electrically close feeder.

- The owner of the equipment at an industrial plant, which is a utility customer, usually buys equipment at lowest cost. Suppliers of equipment do not feel encouraged to add extra features to the equipment in order to bear common disturbances, as these features would increase the equipment cost and final price. Moreover, many manufacturers are unable to identify the power system disturbances that can affect their equipment [27-28].

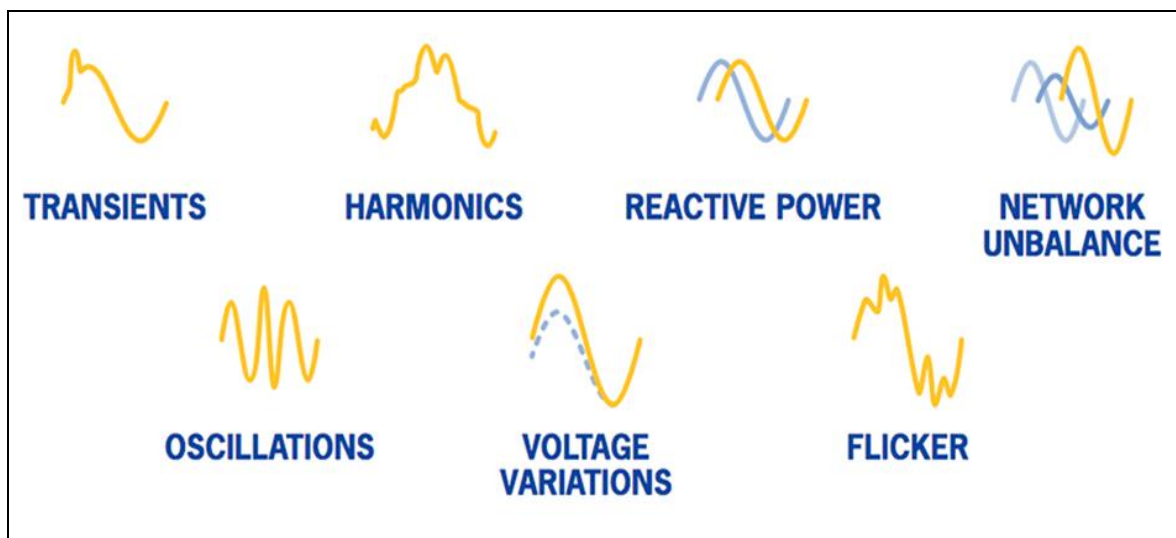


Figure 1.9 Common behaviour of Electrical disturbances

1.6.1 Power Quality Problems

Power Quality problems exist when atleast one of the following conditions is present and significantly affect the normal operation of the system [22], [26], [28]:

- (a) The system frequency has deviated from the nominal value of 50Hz;
- (b) Voltage magnitudes are outside their allowable range of varieties;
- (c) Harmonic Frequencies are present in the system;
- (d) There is imbalance in the magnitude of the phase voltage;
- (e) The phase displacement between the voltages is not equal to 120^0 ;
- (f) Voltage fluctuations cause flicker that is outside the allowable flicker severity lines; or
- (g) High- Frequency over voltages are present in the Distribution systems.

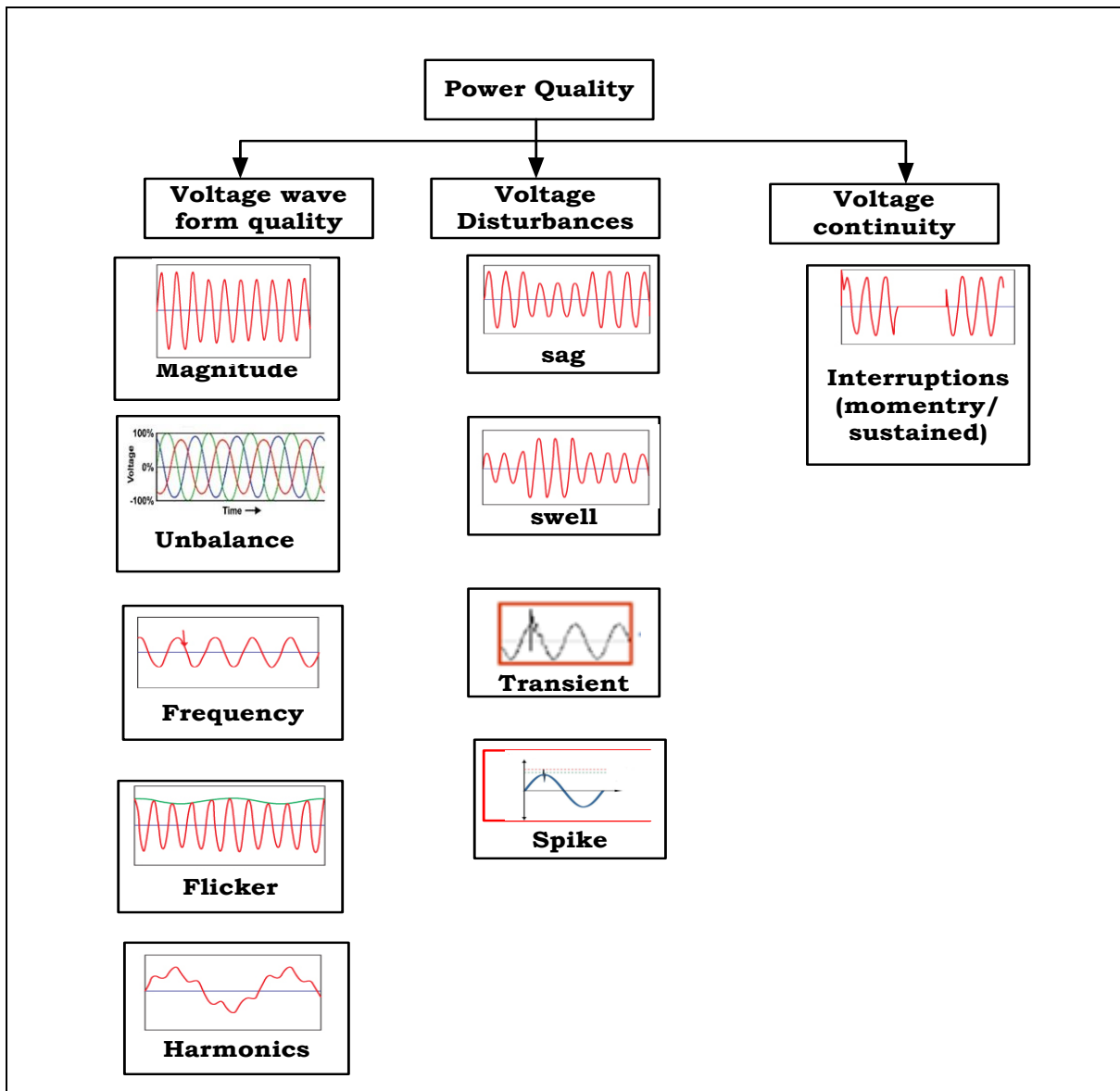
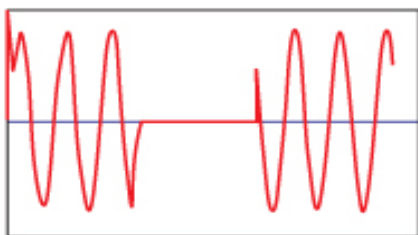


Figure 1.10 Waveforms illustrating various power Quality disturbances

1.6.2 Power Quality disturbances


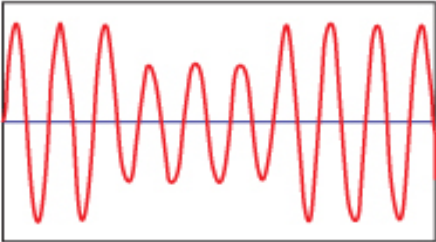
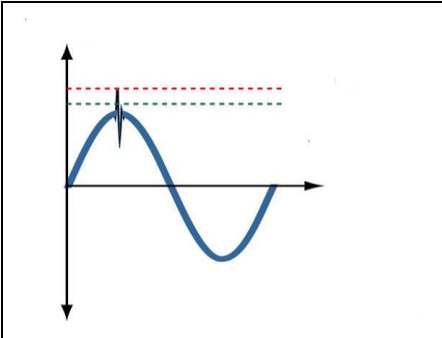
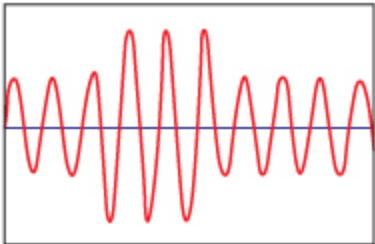
1. Very short interruptions



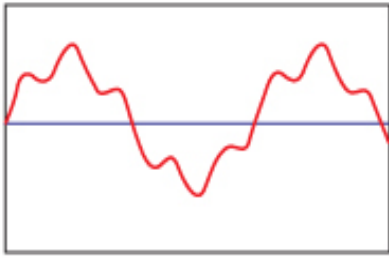
Description: Total interruption of electrical supply for duration from few milliseconds to one or two seconds.

Causes: Mainly due to the opening and automatic reclose of relays. The main fault causes are insulation failure, lightning and insulator flashover.

Consequences: Tripping of protection devices.

<p>2.Long interruptions</p> 	<p>Description: Total interruption of electrical supply for duration greater than 1 to 2 seconds.</p> <p>Causes: Equipment failure in the power system network, storms, fire, human error, failure of protection devices.</p> <p>Consequences: Stoppage of all equipment.</p>
<p>3.Voltage sag</p> 	<p>Description: A decrease of the normal voltage level between 10 and 90% of the nominal rms voltage at the power frequency, for durations of 0.5 cycle to 1 minute.</p> <p>Causes: Faults on the transmission or distribution, Faults in consumer's installation, Connection of heavy loads and start-up of large motors.</p> <p>Consequences: Malfunction of microprocessor-based control systems. Tripping of contactors and electromechanical relays. Disconnection and loss of efficiency in electric rotating machines.</p>
<p>4. Voltage Spike</p> 	<p>Description: Very fast variation of the voltage value for durations from a several microseconds to few milliseconds. These variations may reach thousands of volts, even in low voltage.</p> <p>Causes: Lightning, switching of lines or power factor correction capacitors, disconnection of heavy loads.</p> <p>Consequences: Destruction of components (particularly electronic components) and of insulation materials, electromagnetic interference.</p>
<p>5. Voltage Swell</p> 	<p>Description: Momentary increase of the voltage, at the power frequency, outside the normal tolerances, with duration of more than one cycle and typically less than a few seconds.</p> <p>Causes: Start/stop of heavy loads, badly dimensioned power sources, badly regulated transformers.</p> <p>Consequences: Data loss, flickering of lighting and screens, stoppage or damage of sensitive equipment, if the voltage values are too high.</p>

7. Harmonic distortion

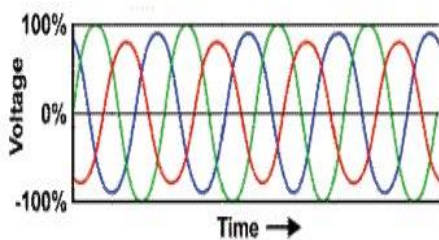


Description: Voltage or current waveforms having frequencies that are multiples of power system frequency.

Causes: All non-linear loads, such as power electronics equipment, SMPS, data processing equipment.

Consequences: Increased probability in occurrence of resonance, overload in 3-phase systems, overheating of all cables and equipment, electromagnetic interference with communication systems.

7. Voltage Unbalance



Description: Voltage variation in a power system in which the voltage magnitudes or the phase angle differences between them are not equal.

Causes:

- Small unbalances are primarily caused by single-phase loads operating on a three-phase circuit.
- If the reactance of three phase is not same; it will result in varying current flowing in three phases and give out system unbalance.
- Any large single phase load, or a number of small loads connected to only one phase cause more current to flow from that particular phase causing voltage drop on line.
- Switching of three phase heavy loads results in current and voltage surges and cause unbalance.
- Unequal impedance in the power transmission or distribution system cause differentiating current in three phases.

Consequences: Tripping of protection devices, damage of loads

Although all disturbances mentioned above are of concern in the power quality context, the most problematic issue is the occurrence of faults. System faults can produce voltage variations at different points of the system with different magnitudes and time scales,

depending on how far the analyzed point is from the fault location, the fault clearing procedure, and system impedances.

In the research work, we have considered the voltage and frequency fluctuation which drastically affects the power quality and load sharing between the DGs for load demand in main grid.

1.6.3 Frequency and Voltage Fluctuations

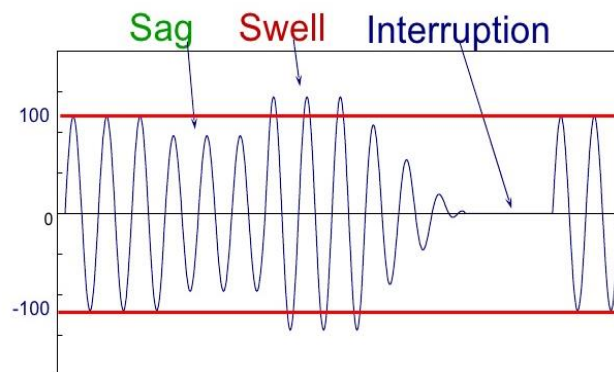


Figure 1.11 Voltage variation waveform

Frequency and voltage fluctuations can be again classified as

1. Grid-derived voltage fluctuations
2. Voltage imbalance
3. Voltage rise and reverse power flow
4. Power factor Correction

(i) Grid- derived Voltage Fluctuations

Inverters are generally configured to operate in grid ‘voltage-following’ mode and to disconnect DG when the grid voltage moves outside set parameters. Where there are large numbers of DG systems or large DG systems on a particular feeder, their automatic disconnection due to the grid voltage being out of range can be problematic because other generators on the network will suddenly have to provide additional power.

Inverters operating in voltage-regulating mode help boost network voltage by injecting reactive power during voltage sags, as well as reduce network voltage by drawing

reactive power during voltage rise. Thus, connection standards need to be developed to incorporate and allow inverters to provide reactive power where appropriate, in a manner that did not interfere with any islanding detection systems.

(ii) Voltage Imbalance

Voltage imbalance is when the amplitude of each phase voltage is different in a three-phase system or the phase difference is not exactly 120° . Single phase systems installed disproportionately on a single phase may cause severely unbalanced networks leading to damage to controls, transformers, DG, motors and power electronic devices. Thus, at high PV penetrations, the cumulative size of all systems connected to each phase should be as equal as possible. All systems above a minimum power output level of between 5-10kW typically should have a balanced three phase output.

(iii) Voltage rise and Reverse power flow

Traditional centralized power networks involve power flow in one direction only: from power plant to transmission network, to distribution network, to load. In order to accommodate line losses, voltage is usually supplied at 5-10% higher than the nominal end use voltage. Voltage regulators are also used to compensate for voltage drop and maintain the voltage in the designated range along the line.

(iv) Power Factor Correction

Because of poor power factor, line losses increases and voltage regulation become difficult. Poor power factor on the grid increases line losses and makes voltage regulation more difficult. Inverters configured to operate in voltage-following have unity power factor, while inverters in voltage-regulating following mode provide current that is out of phase with the grid voltage and so provide power factor correction.

1.7 Control of Grid connected DGs

The inverter output voltage is the vector sum of the AC grid voltage and the series drop of the filter as well as the grid impedances. Therefore the current controller algorithm

should estimate the converter output voltage for a given power reference accounting the filter drop and maintains the power flow to follow the reference. There are various type of current controllers used with various reference frames adapted by various authors in the literature for grid connected converters [14-15]. The PI controller in the synchronously rotating ($d-q$) reference frame and the PR controller in the stationary ($\alpha-\beta$) reference frame, Natural reference frame controller(abc) are commonly adopted to achieve a high-quality grid current. In this subsection, the conventional current control strategies for the grid -connected operations of DG, which supports DGs to transfer a sinusoidal current to utility grid are discussed in detail.

1.7.1 Overview of Grid Connected Inverter Topology

To study stationary and dynamic regimes in three-phase systems, the application of “vector control” (Park vector) is a powerful tool for the analysis and control of DC-AC converters, enabling abstraction of differential equations that govern the behaviour of the three-phase system in independent rotating shafts. The main disadvantage of using this control method is that it introduces a nonlinear part, a rotation of axes (mathematical transformations), which requires a lot of computing power, an issue that is solved with existing microcontrollers and digital signal processing(DSP).

1.7.1.1 dq control

The concept of decoupled active and reactive power control of three-phase inverter is realized in the synchronous reference frame (SRF) or dq control by using the $abc-dq$ transformation for converting the grid current and voltages into a rotating reference system with the grid voltage, these variable control values are transformed into continuous. In this way, the AC current is decoupled into active and reactive power components, I_d and I_q , respectively. These current components are then regulated in order to eliminate the error between the reference and measured values of the active and reactive powers. In most cases, I_d is regulated through a DC-link voltage control aiming at balancing the active power flow in the system [22],[25] .

As shown in Figure 1.12, the power control loop is followed by a current control system. By comparing the reference and measured currents, the current controller should generate the proper switching states for the inverter to eliminate the current error and produce

the desired ac current waveform [26]. In the case that the reactive power has to be controlled, a reactive power reference must be imposed to the system. Linear PI controller is an established reference tracking technique associated with the d - q control structure due their satisfactory combinational performance.

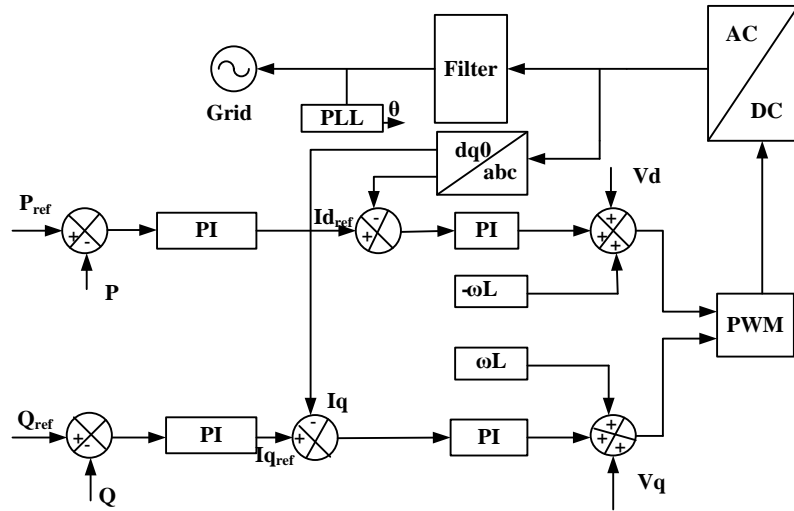


Figure.1.12 General Structure of $dq0$ control strategy

The transfer function on the d - q coordinate structure is given as

$$G(s) = \begin{bmatrix} K_p + \frac{K_I}{s} & 0 \\ 0 & K_p + \frac{K_I}{s} \end{bmatrix} \quad (1.2)$$

where K_p is the proportional gain and K_I is the integral gain of the controller.

For improving the performance of Proportional Integral (PI) controller, cross-coupling terms and voltage feed forward are usually used [23]. In any case, with all these improvements, the compensation capability of the low-order harmonics in the case of PI controllers is very poor. The phase-locked loop (PLL) technique is usually used in extracting the phase angle of the grid voltages in the case of PV systems [24].

1.7.1.2 $\alpha\beta$ -Control

The grid currents are transformed into a stationary reference frame using the abc - $\alpha\beta$ module, as shown in figure 1.13. The abc control is to have an individual controller for each

grid current; that achieves a very high gain around the resonance frequency, thus capable of eliminating the steady-state error between the controlled signal and its reference. High dynamic characteristics of the Proportional Resonant (PR) controller have been reported in different works, and which is gaining common popularity in the current control for networked systems, is an alternative solution for performance under the PI controller. The basic operation of the PR controller is based on the introduction of an infinite gain at the resonant frequency to eliminate the steady state error at this frequency between the control signal and the reference. It does not require the use of feed forward [16],[30].

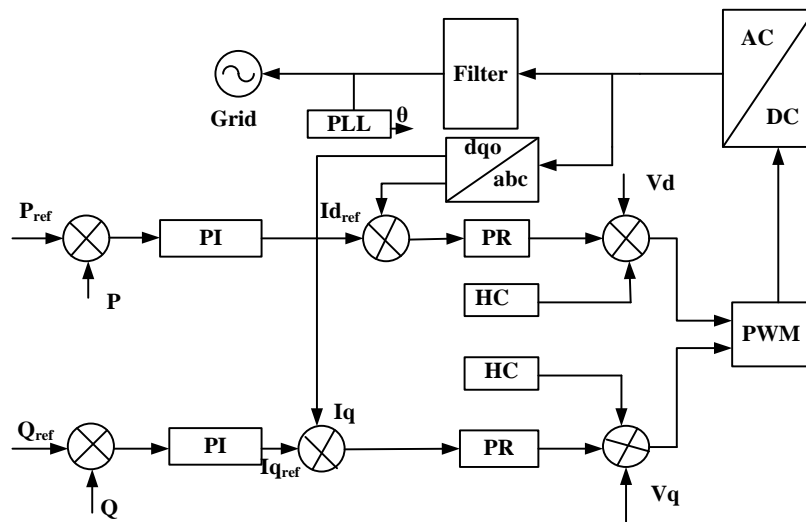


Figure.1.13 General Structure of $\alpha\beta$ control strategy

The transfer matrix of the PR controller in the stationary reference frame is given by,

$$G(s) = \begin{bmatrix} K_P + \frac{K_I}{s^2 + \omega^2} & 0 \\ 0 & K_P + \frac{K_I}{s^2 + \omega^2} \end{bmatrix} \quad (1.3)$$

1.7.1.3 abc control

It is a structure where nonlinear controllers like hysteresis or dead beat are preferred due to their high dynamics. The performance of these controllers is proportional to the sampling frequency. Hence, the rapid development of digital systems such as digital signal processors or field programmable gate array is an advantage for such an implementation. A possible implementation of *abc* control is depicted in figure 1.14, where the output of DC-

link voltage controller sets the active current reference. Using the phase angle of the grid voltages provided by a PLL system, the three current references are created. Each of them is compared with the corresponding measured current, and the error goes into the controller. If hysteresis or dead-beat controllers are employed in the current loop, the modulator is not necessary. The output of these controllers is the switching states for the switches in the power converter. In the case that three PI or PR controllers are used, the modulator is necessary to create the duty cycles for the PWM pattern. The PI controller is widely used in conjunction with the dq control, but its implementation in the abc frame is also possible as described in [17-19].

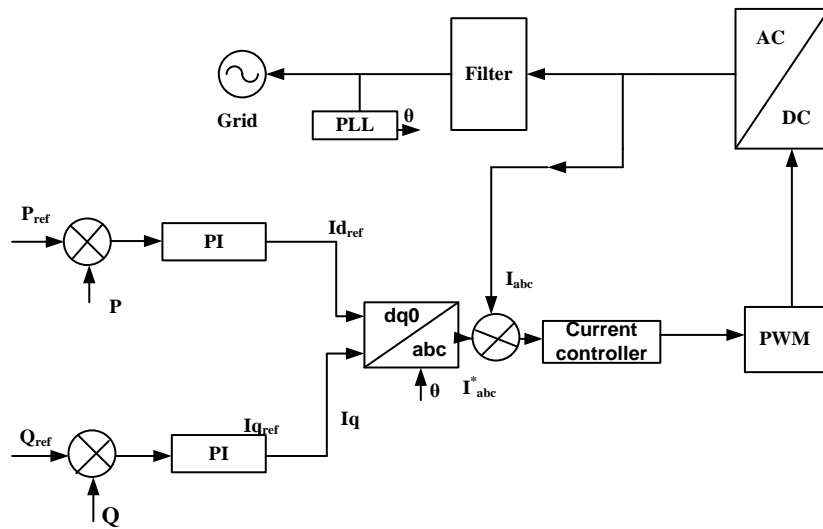


Figure.1.14 General Structure of abc control strategy

The implementation of PR controller in abc can be expressed as,

$$G(s) = \begin{bmatrix} K_P + \frac{K_I}{s^2 + \omega^2} & 0 & 0 \\ 0 & K_P + \frac{K_I}{s^2 + \omega^2} & 0 \\ 0 & 0 & K_P + \frac{K_I}{s^2 + \omega^2} \end{bmatrix} \quad (1.4)$$

1.7.2 Observations of performance of Conventional current controllers

The general drawbacks of the conventional controllers are:

- (1) slow dynamic response;
- (2) high computational requirement;
- (3) complex computational process;
- (4) method is impractical in accuracy;
- (5) intricate to implement.

Dependence on voltage feed-forward and cross-coupling blocks are the major drawbacks of the control structure implemented in synchronous reference (dq) frame. The phase angle of the grid voltage should be extracted in this implementation. In the stationary reference frame ($\alpha\beta$), if PR controllers are used for current regulation, the complexity of the control becomes less compared to the structure implemented in the dq frame. Also, the phase angle information is not necessary and filtered grid voltages can be used as templates for the reference current waveform. In the natural frame (abc), the control system complexity will be increased if an adaptive hysteresis band controller is used for current regulation [50-61].

These current controllers discussed above are only effective when the grid voltage is ideally balanced and sinusoidal. Due to the popular use of nonlinear loads, the grid voltage at the point of common coupling (PCC) is typically not pure sinusoidal, but instead can be unbalanced or distorted. These abnormal grid voltage conditions can strongly deteriorate the performance of the regulating grid current [62-70].

1.8 Proposed Control Methods

The following control methods, MPC and Droop control however have been emerged as potential control power to achieve high quality grid current and to improve the system dynamic response, eliminate steady state error and to prevent the use of the feed-forward. The brief justification of the implementation of these proposed methods in our research study are discussed in forthcoming sections.

1.8.1 Outline of MPC

Model predictive control (MPC) is one of the main process control techniques explored in the recent past. MPC offers an alternative to overcome the drawbacks of classical techniques to satisfy fast dynamic response, flexibility in the definition of the control objectives, and the easy inclusion of nonlinearities. It is the amalgamation of different technologies used to predict future control action and future control trajectories knowing the current input and output variables and the future control signals. It can be said that the MPC scheme is based on the explicit use of a process model and process measurements to generate values for process input as a solution of an on-line (real-time) optimization problem to predict future process behaviour [72-76].

MPC is a powerful technique that involves the use of a mathematical model of the controlled system to find an optimal control solution for a predefined time horizon. Modulation technique is not required for MPC since the output command is directly applied to the power electronics. There are many advantages in this method such that when compared to VOC, MPC does not require rotary transformation, inner current loop, or PWM block and promising alternative to control power converters, and this method eliminates the requirement for linear modulators and provides, in principle, superior dynamic performance [77-88].

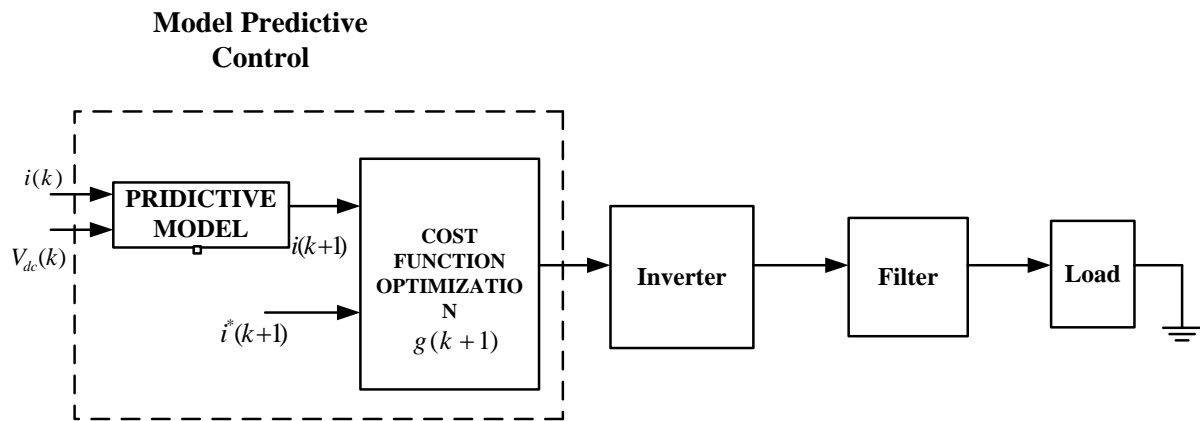


Figure.1.15 Basic structure of MPC

In this study, the concept of nonlinear model-based predictive control (MPC) with continuous set has been proposed for the current control of three-phase voltage-source converters to deal the issues like stability, efficient computation, constraints, and others. The converter switching states are selected from a switching table. This algorithm selects the appropriate voltage vectors and calculates duty cycles in every sampling period to minimize the errors of the instantaneous active and reactive power. It directly selects the desired voltage vector to regulate both active power and reactive power based on a predefined switching table, despite the merits of simple structure, quick response, and strong robustness.

One of the remarkable aspects of MPC is the use of costs assigned to each objective to achieve reference tracking, balance in the DC link, and a reduction in the switching frequency. This method establishes cost functions and compares the function values, according to the current predictive results, to select the optimal switching states. Figure 1.15, describes the simple structure of proposed current prediction control method for

nonlinearities, In current prediction of the MPC, the prediction step has to be taken for all alternative output levels, and the predictive results should be compared with each other to determine the best choice.

1.8.2 Overview of Load sharing

The control schemes can be classified into two main groups with regard to the use of control wire interconnections. The first technique is based on active load sharing, and average power sharing. Although these control schemes achieve both good output-voltage regulation and equal current sharing, they need critical intercommunication lines among modules that could reduce the system reliability and expandability.

The second control scheme for the parallel operation of inverters is mainly based on the droop method. In inverter-based microgrids, the paralleled inverters need to work in both grid-connected mode and Islanded mode and should be able to transfer seamlessly between the two modes. In grid-connected mode, the inverters control the amount of power injected into the grid. In Islanded mode, however, the inverters control the island voltage while the output power is dictated by the load. This can be achieved using droop control [93-98].

In an islanding microgrid, all the DGs are responsible for maintaining the system voltage and frequency while sharing the active and reactive power. Load sharing without communication between converters is the most desirable option as the network can be complex and can span over a large geographic area. A common approach to achieve this is through the use of frequency droop characteristics so that the parallel converters can be controlled locally to deliver desired real and reactive power to the system. This technique consists of adjusting the frequency and voltage amplitude in terms of the active and reactive power injected by the inverter. The droop method is more reliable and flexible than the communication based methods, as it utilizes the local measurements [99-101].

The reactive power sharing via the conventional droop control method has some shortcomings. Unless the determination of line parameters is very accurate, the power sharing is not done correctly and is degraded. This can result in an unbalance of reactive power flow for loads that are located closer to one converter than another despite both converters having the same droop coefficients. To overcome this problem, the P-f and Q-V droop control scheme are proposed in for active and reactive power sharing among parallel-connected inverters where the parallel-connected inverters can operate as grid-forming with droop

characteristics and achieve good active and reactive current sharing without any central controlling or telecommunication links between VSIs [102-105]. The general structure of frequency and voltage droop adjustment is shown in figure 1.16.

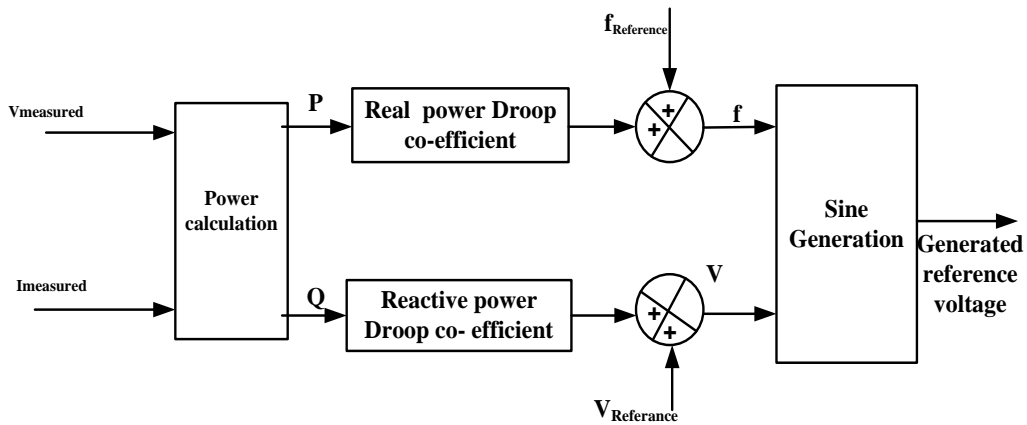


Figure 1.16 Structure of $(P-f)$ & $(Q-V)$ droop control

1.9 Objectives of the study

Although the term “power quality” encompasses all disturbances encountered in a power system, it has been found that voltage sags and unbalance are the most relevant types of phenomena in distribution systems affecting the quality of the service provided by a utility. This thesis, therefore, reports the development of new strategies for grid- connected converter control, namely MPC and droop control, to deal with unbalanced dip in voltage and proper load sharing between DGs respectively.

The main task of this research is to design an improved control strategy for grid-connected inverters within microgrid considering various factors which affects the power quality and load sharing.

To validate the proposed method, the following studies have been done.

Two DG sources (DG1 – PV, DG2- PEMFC) are connected to grid and tested under various loads in balanced condition using convention PI method and the characteristics of active power and reactive power were studied at PCC.

The behaviour is studied by adopting MPC for unbalanced voltage dip condition. MPC is used for the current control, which is the preminent powerful alternative to conventional method for the conventional current control. This control scheme predicts the future load current behaviour for each valid switching state of the converter, in terms of the measured load current and predicted load voltage. The predictions are evaluated with a cost function that minimizes the error between the predicted currents and their references at the end of each sampling time.

When working in the grid-connected mode, the utility grid will support the stable voltage and frequency to the microgrid. However, when operating in islanded mode, microgrid needs to maintain its stable voltage and frequency. Thus, the droop control is used in the islanded mode to make sure that microgrid can provide the stabilized electrical power with steady voltage and frequency for loads. The improved droop control method is applied to achieve better load sharing with low voltage and frequency deviation in microgrid, and to get a better reactive power sharing.

1.10 Thesis Organization

Chapter I: Introduction

This chapter includes brief introduction of DERS; brief overview of DG sources; basic concepts of Microgrids, Challenges difficulties, Potential drawbacks to attain Power quality in microgrid.

Chapter II: Modeling of DGs

This chapter includes overview of DGs- PEMFC, PV; Simulation results and discussion of modeling of PEMFC and PV.

Chapter III: Concepts of Control of Grid -connected DGs with emphasize on SRF

This chapter includes the overview design of proposed model, Three- phase inverter topology, concepts of PWM, design of LC filter; discussion of PLL, control loops of grid connected DGs and their simulation results and discussion.

Chapter IV: Proposed Predictive Current Control Method for analysis under unbalanced voltage dip conditions

This chapter includes overview of MPC, predictive control, of three phase inverter, cost function, discussion of SVPWM, discrete time model of prediction, principle of MPC controller, complete control structure and simulation study.

Chapter V: Proposed power system Control design for Parallel Inverters

This chapter includes various control methods of parallel inverters, load sharing control of power converts, grid impedance droop control, droop implemented control strategy, control of DC link voltage, simulation results and discussion

Chapter VI: Conclusion.

Chapter II

Modeling of DG sources

Among the various DERs discussed in previous chapter, two DERs – PEMFC and PV are considered as DGs in this research work. PEMFC and PV show greater interest due to the high benefits and more scope for future development in power sector. Modeling and simulated results are discussed in detail.

2.1 Overview of PEM Fuel Cell (PEMFC)

Fuel cells have received more attention during the past decade and appear to have the potential to become the power source of the future. Fuel cells are electrochemical devices that convert chemical energy of a fuel directly into DC electricity. All fuel cells comprise two electrodes (Anode and Cathode) and an electrolyte (e.g. a membrane) that separates the electrodes. The oxidation of fuel (mainly hydrogen) at the anode produces electrons which are guided via an external conductor to the cathode where they reduce the oxidant and produce electricity. Unlike batteries, FC can produce electrical energy for as long as fuel and oxidant are supplied to the electrodes. To increase the low voltage of a single fuel cell, many cells are connected in series to form a fuel cell stack [35-37].

Fuel cells have various advantages compared to conventional power sources, such as internal combustion engines or batteries [38]. Benefits include:

- Fuel cells have a higher efficiency than diesel or gas engines.
- Most FCs are noiseless, ideally suited for use within buildings such as hospitals.
- FC can eliminate pollution caused by burning fossil fuels; for hydrogen fuelled fuel cells, the only by-product at point of use is water.
- If the hydrogen comes from the electrolysis of water driven by renewable energy, then using FC eliminates greenhouse gases over the whole cycle.

- FCs do not need conventional fuels such as oil or gas
- Since hydrogen can be produced anywhere where there is water and a source of power, generation of fuel can be distributed and does not have to be grid-dependent.
- The use of stationary FCs to generate power at the point of use allows for a decentralised power grid that is potentially more stable.
- Low temperature FC (PEMFC, DMFC) has low heat transmission which makes them ideal for military applications.
- Higher temperature FC produce high-grade process heat along with electricity and are well suited to cogeneration applications.

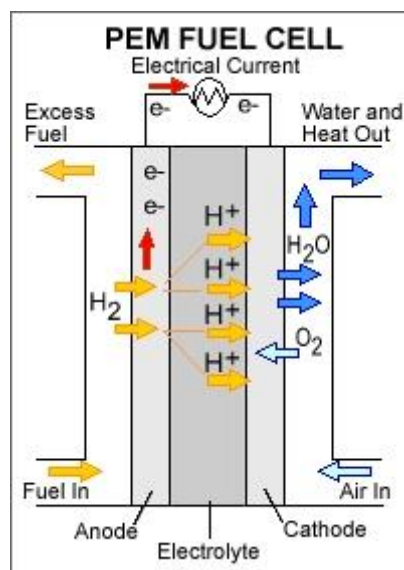


Figure 2.1 Basic Scheme of PEMFC

The basic scheme for a single FC is represented in Figure 2.1 and the reactions involved in the anode side, the cathode side and the overall reaction of the process are described by the eq. (2.1 - 2.3) follows

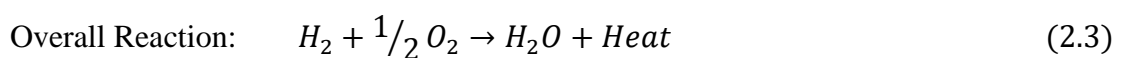
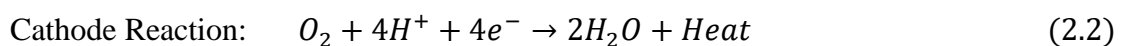
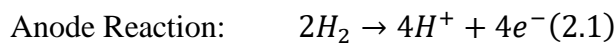


Table 2.1 Fuel Cell Types and its merits, demerits

	Low Temperature Fuel Cells			High Temperature Fuel Cells		
	DMFC	PEMFC	AFC	PAFC	MCFC	SOFC
Electrolyte	Proton-conducting membrane usually polymer poly-perfluorosulfonic acid		Caustic potash solution	Concentrated phosphoric acid	Molten carbonate	Ceramic
Temperature Range	50 - 100°C	50 - 100°C	90 - 100°C	150 - 200°C	~ 650°C	800-1,000°C
Fuel	Methanol	Hydrogen	Hydrogen	Hydrogen	Natural gas, coal	Natural gas, coal
System Output	Up to 1.5kW	<1kW – 250kW	10kW – 100kW	50kW – 1MW	<1kW – 1MW	5kW – 3MW
Electrical efficiency	20 - 25%	60% (direct) 25-40% (reformed)	60%	32-38%	45-47%	35-43%
Application Examples	<ul style="list-style-type: none"> ▪ Vehicles, ▪ Small appliances- Laptops, Mobile phones 	<ul style="list-style-type: none"> ▪ Vehicles, ▪ small generators ▪ domestic supply ▪ power stations 	Military Space	Block type heat, power stations	Power plants, CHP	Power plants, CHP
Advantages	<ul style="list-style-type: none"> ▪ High energy storage ▪ No reforming needed ▪ Easy storage and transport 	<ul style="list-style-type: none"> ▪ Solid electrolyte reduces corrosion ▪ Electrolyte management 	<ul style="list-style-type: none"> ▪ Cathode reaction faster in alkaline electrolyte, ▪ higher performance 	<ul style="list-style-type: none"> ▪ Higher overall efficiency with CHP ▪ Increased tolerance to impurities in hydrogen 	<ul style="list-style-type: none"> ▪ High efficiency ▪ Fuel flexibility ▪ Can use a variety of catalysts ▪ Suitable for CHP 	<ul style="list-style-type: none"> ▪ High efficiency ▪ Fuel flexibility ▪ Can use a variety of catalysts ▪ Solid electrolyte reduces electrolyte management problems ▪ Suitable for CHP Hybrid/GT cycle
Disadvantages	<ul style="list-style-type: none"> ▪ Low power output ▪ Methanol is toxic and flammable 	<ul style="list-style-type: none"> ▪ Requires expensive catalysts ▪ High sensitivity to fuel impurities ▪ Not suitable for CHP 	<ul style="list-style-type: none"> ▪ Expensive removal of CO₂ from fuel ▪ Electrolyte management 	<ul style="list-style-type: none"> ▪ Requires expensive platinum catalysts ▪ Low current and power ▪ Large size/Weight 	<ul style="list-style-type: none"> ▪ High temperature speeds corrosion and breakdown of cell component ▪ Complex electrolyte management ▪ Slow start-up 	<ul style="list-style-type: none"> ▪ High temperature enhances corrosion and breakdown of cell components. ▪ Slow start-up ▪ Brittleness of ceramic electrolyte with thermal cycling

Depending on the type of electrolyte used, different types of fuel cells are classified as Proton exchange membrane fuel cell (PEMFC), Alkaline electrolyte fuel cell (AFC), Phosphoric acid electrolyte fuel cell (PAFC), Molten carbonate electrolyte fuel cell (MCFC),

Direct methanol fuel cell (DMFC), Solid oxide fuel cell (SOFC). The advantages and disadvantages are given in Table 2.1.

Among the different fuel cells, the PEMFC and SOFC show great potential in transportation and distributed generation applications. In this thesis, the PEMFC is considered because of its excellent load following capability and high power density, rapid start-up, high efficiency as well as low operating conditions which provide the possibility of using cheaper components [39-40].

2.2 Detailed Model of PEMFC

The FC system model parameters used in this model are as follows:

B, C	Constants to simulate the activation over voltage in PEMFC system [V];	q_{O_2}	input molar flow of oxygen [kmol/s];
CV	conversion factor [kmol of Hydrogen per methane];	$q_{methane}$	methane flow rate [kmol/s];
E	Nernst instantaneous voltage [V];	$q_{H_2}^{in}$	hydrogen input flow [kmol/s];
E^0	standard no load voltage [V];	$q_{H_2}^{out}$	hydrogen output flow [kmol/s];
F	Faraday's constant [C/kmol];	$q_{H_2}^r$	hydrogen flow that reacts [kmol/s];
I'_{FC}	FC system feedback current [A];	$q_{H_2}^{req}$	amount of hydrogen flow required to meet the load change [kmol/s];
K_1	Proportional-integral (PI) gain;	R	universal gas constant [(1atm)/(kmol·K)];
K_{an}	anode valve constant [$\sqrt{kmol \cdot Kg(atm \cdot s) - I}$];	R^{int}	FC internal resistance [Ω];
K_{H_2}	hydrogen valve molar constant [kmol/(atm·s)];	T	absolute temperature [K];
$K_{H_2O} K_{O_2}$	water valve and oxygen valve molar constant [kmol/(atm·s)];	U	utilization rate;
K_r	modeling constant [kmol/(s·A)];	V_{an}	volume of the anode [m^3];
M_{H_2}	molar mass of hydrogen [kg·kmol ⁻¹];	V_{cell}	dc output voltage of FC system [V];
N_O	number of series fuel cells in stack;	τ_1, τ_2	reformer time constants [s];
p_{H_2}	hydrogen partial pressure [atm];	τ_3	time constant of the PI controller [s];
$P_{H_2O} P_{O_2}$	water and oxygen partial pressure [atm];	$\tau_{H_2} \tau_{O_2}$	hydrogen and oxygen time constant [s];
q_{H_2}	molar flow of hydrogen [kmol/s];	τ_{H_2O}	water time constant [s];
		η_{act}	activation over voltage [V];
		η_{ohmic}	ohmic over voltage [V]

In a PEM fuel cell, the two electrodes are separated by a solid membrane which only allows the H^+ ions to pass, but prevents the motion of electrons. The electrons at the anode will flow through the external load and comes to the surface of the cathode, to which the protons of hydrogen will be attracted at the same time. Thus, two charged layers of opposite polarity are formed across the boundary between the porous cathode and the membrane. These two layer separated by the membrane act as double charged layer, which can store electrical energy, due to this property this can be treated as a capacitor.

The simplified model represents a particular fuel cell stack operating at nominal conditions of temperature and pressure, can be represented by an electrical equivalent circuit as shown in Figure 2.2.

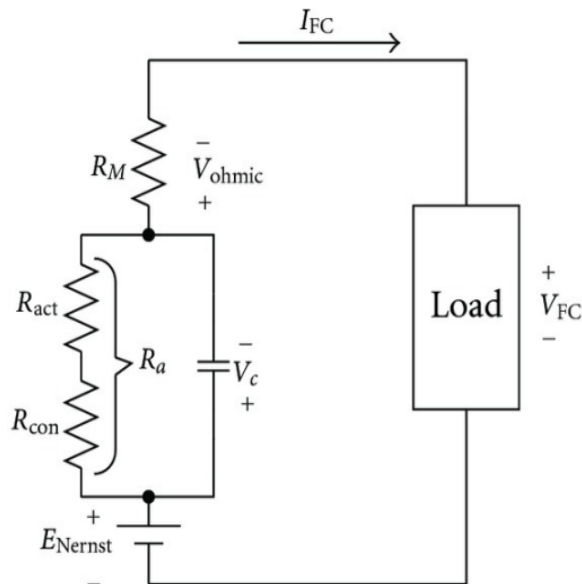


Figure 2.2 Equivalent circuit of PEMFC

A typical polarization curve of PEMFC is shown in figure 2.3 and it comprises of three voltage drop region, namely [40]

- (a) Activation voltage drop \rightarrow due to the slowness of the chemical reactions taking place at electrode surfaces. Depending on the temperature and operating pressure, type of electrode, and catalyst used, this region is more or less wide.
- (b) Ohmic voltage drop \rightarrow the resistive losses due to the internal resistance of the fuel cell stack.
- (c) Concentration voltage drop \rightarrow mass transport losses resulting from the change in concentration of reactants as the fuel is used.

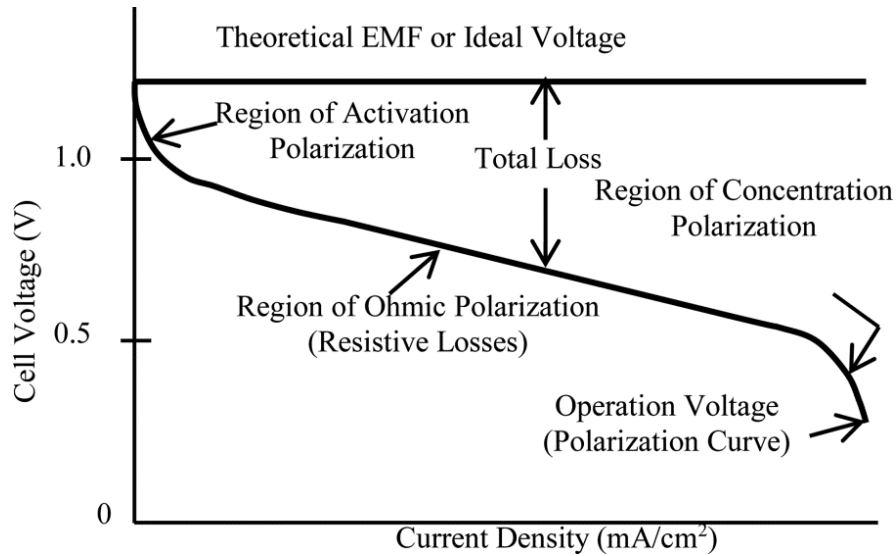


Figure 2.3 Ideal Polarization curve of a FC

A mathematical approach is presented for building a dynamic model for a PEM fuel-cell stack. To simplify the analysis, the following assumptions are made.

- One-dimensional treatment,
- Ideal and uniformly distributed gases,
- Constant pressures in the fuel-cell gas flow channels,
- The fuel is humidified and the oxidant is humidified air. Assume the effective anode water vapour pressure is 50% of the saturated vapour pressure while the effective cathode water pressure is 100%.
- The fuel cell works under 100⁰C and the reaction product is in liquid phase.
- Thermodynamic properties are evaluated at the average stack temperature, temperature variations across the stack are neglected, and the overall specific heat capacity of the stack is assumed to be a constant.
- A fuel cell stack is represented by combining parameters for individual cells

The relationship between the molar flow of any gas (hydrogen) through the valve and its partial pressure in pressure inside the channel can be expressed as

$$\frac{q_{H_2}}{p_{H_2}} = \frac{K_{an}}{\sqrt{M_{H_2}}} = K_{H_2} \quad (2.4)$$

For hydrogen molar flow, there are three significant factors: (i) Hydrogen input flow, (ii) hydrogen output flow, and (iii) hydrogen flow during the reaction .The relationship among these factors can be written as

$$\frac{d}{dt} p_{H_2} = \frac{RT}{V_{an}} (q_{H_2}^{in} - q_{H_2}^{out} - q_{H_2}^r) \quad (2.5)$$

According to the basic electrochemical relationship between the hydrogen flow and the FC system current, the flow rate of reacted hydrogen is given by

$$q_{H_2}^r = \frac{N_o I'_{FC}}{2F} = 2K_r I'_{FC} \quad (2.6)$$

Using (2.4) and (2.6), and applying Laplace transform, the hydrogen partial pressure can be obtained in the s domain as

$$p_{H_2} = \frac{1/K_{H_2}}{1 + \tau_{H_2} s} (q_{H_2} - 2K_r I'_{FC}) \quad (2.7)$$

where

$$\tau_{H_2} = \frac{V_{an}}{K_{H_2} RT} \quad (2.8)$$

Similarly, water partial pressure and oxygen partial pressure can be obtained. The polarization curve for the PEMFC is obtained from the sum of the Nernst's voltage, the activation over voltage, and the ohmic over voltage. Assuming constant temperature and oxygen concentration, the FC output voltage may be expressed as

$$V_{cell} = E + \eta_{act} + \eta_{ohmic} \quad (2.9)$$

where

$$\eta_{act} = -B \ln(C I'_{FC}) \quad (2.10)$$

and

$$\eta_{ohmic} = -R^{int} I'_{FC} \quad (2.11)$$

Now, the Nernst's instantaneous voltage may be expressed as

$$E = N_o \left[E_o + \frac{RT}{2F} \log \left[\frac{p_{H_2} \sqrt{P_{O_2}}}{p_{H_2O}} \right] \right] \quad (2.12)$$

The fuel cell system consumes hydrogen, according to power demand and the reformer continuously generates hydrogen for stack operation. The mathematical form of the reformer model can be expressed as

$$\frac{q_{H_2}}{q_{methanol}} = \frac{CV}{\tau_1 \tau_2 s^2 + (\tau_1 + \tau_2)s + 1} \quad (2.13)$$

During operational conditions, to control the hydrogen flow rate according to the output power of the FC system, a PI control system is used. To achieve this feedback control, FC current from the output is taken back to the input while converting the hydrogen into molar form as given as

$$q_{H_2}^{req} = \frac{N_o I'_{FC}}{2FU} \quad (2.14)$$

The amount of hydrogen available from the reformer can be used to control the methane flow rate by using a PI controller, expressed as

$$q_{methanol} = \left(k_1 + \frac{k_1}{\tau_3 s} \right) \left(\frac{N_o I'_{FC}}{2FU} - q_{H_2}^{in} \right) \quad (2.15)$$

2.3 Simulation Results and discussion for modelling PEMFC

The MATLAB and Simulink based FC system model as shown in figure 2.5 is developed from the above equations and the simulated PEMFC stack output voltage is shown in figure 2.4. The parameters used in the study is shown in the Table 2.2. The DC output voltage of PEMFC connected to the utility grid using DC to AC converter and power control loops. The control details are discussed in forthcoming chapter.

Table 2.2 Simulation input for PEMFC model

B	0.0477[A ⁻¹]	τ_{O_2}	6.74[s]
C	0.0136[V]	K_{O_2}	2.11 x 10 ⁻⁵ [k _{mol} (s atm) ⁻¹]
CV	2	R_{int}	0.00303[
F	96484600[C k _{mol} ⁻¹]	R	8314.47[J(k _{mol} k) ⁻¹]
τ_{H_2}	3.37[s]	T	343[k]
K_{H_2}	4.22 x 10 ⁻⁵ [k _{mol} (s atm) ⁻¹]	U	0.8
r_{h-o}	1.168	$\tau_{H_2 O}$	18.418[s]
K_r	1.8449 x 10 ⁻⁶ [k _{mol} (sA) ⁻¹]	$K_{H_2 O}$	7.716 x 10 ⁻⁶ [k _{mol} (s atm) ⁻¹]
$q_{methref}$	0.000015[k _{mol} S ⁻¹]	X	0.5Ω
E_o	0.6[V]	k_5, k_7	0.2
N_o	1250	k_6, k_8	10

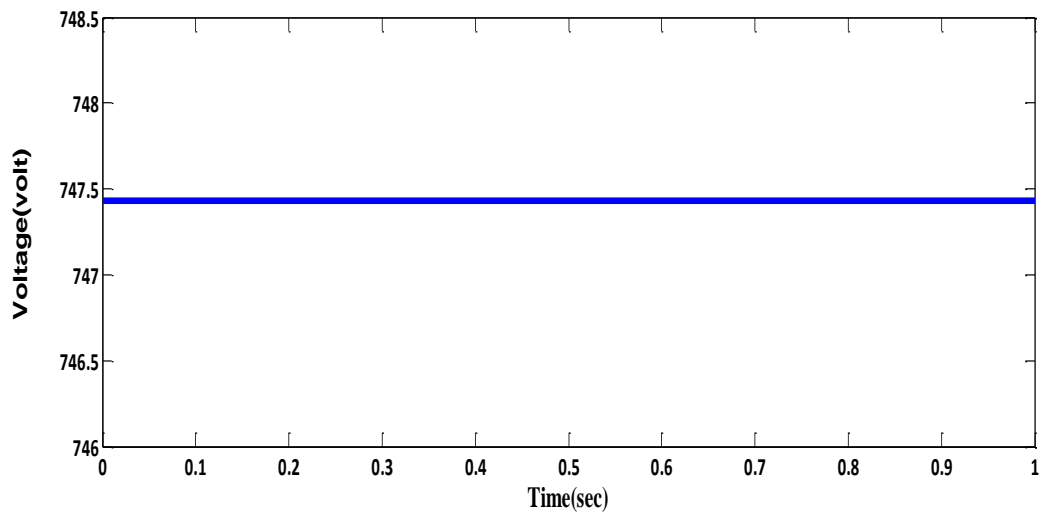
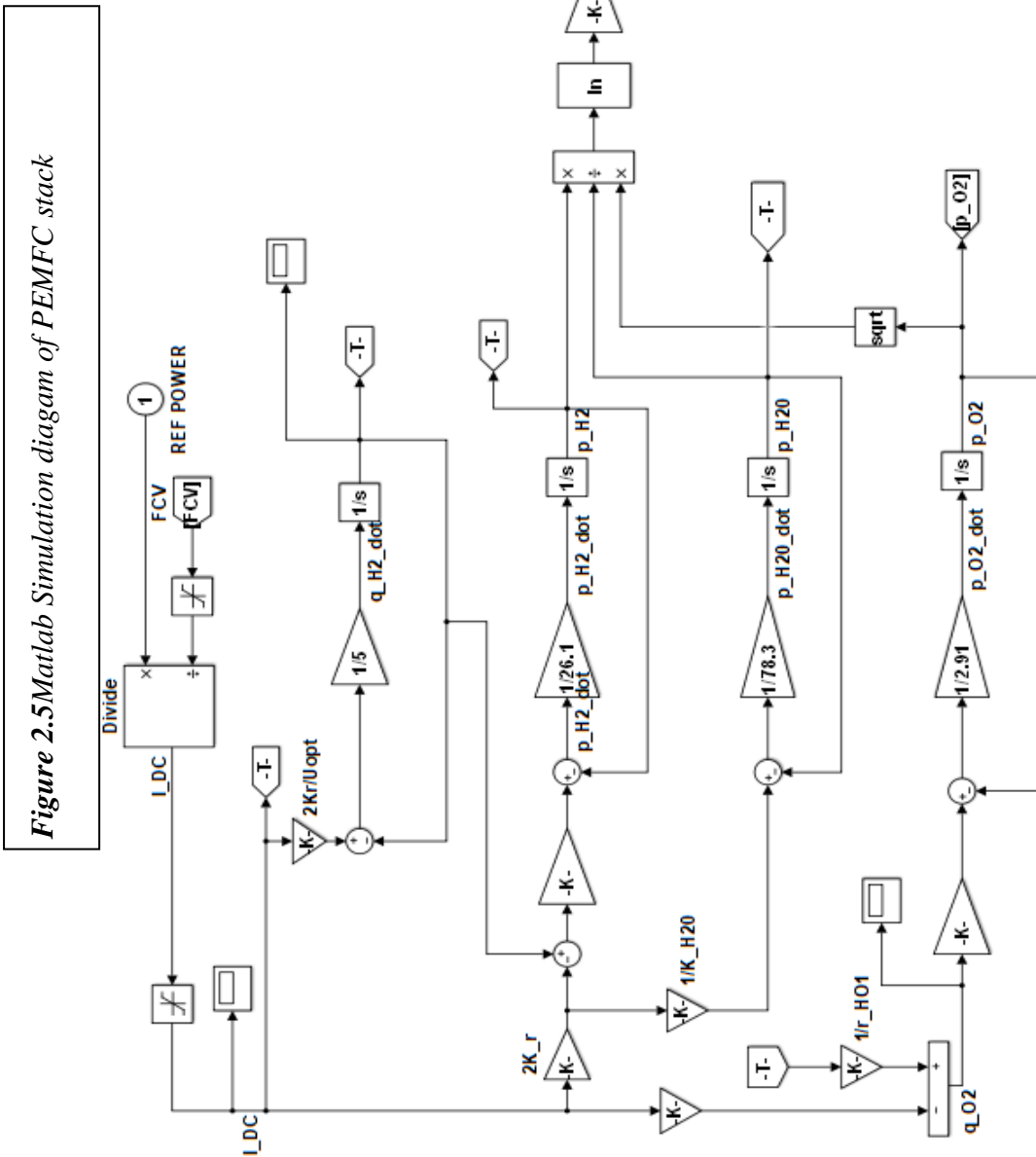


Figure 2.4 Simulated Fuel Cell stack voltage

As depicted in the figure 2.4, the single cell simulated FC voltage connected to series and parallel combination to obtain desired power and voltage. Approximately 1250 cells are connected in Fuel cell stack to achieve Nernst's (E_o) voltage.

behavior



2.4 Photovoltaic (PV) Cell Power System

Growing interest in renewable energy resources has caused the photovoltaic (PV) power market to expand rapidly, especially in the area of distributed generation because of its being environmentally friendly, sustainable, and fuel cost-free.

A PV system or solar power system is a power system designed to supply usable solar power by means of photovoltaic. It consists of an arrangement of several components, including solar panels to absorb and convert sunlight into electricity, a solar inverter to change the electric current from DC to AC, as well as mounting, cabling, and other electrical accessories to set up a working system. It may also use a solar tracking system to improve the system's overall performance and include an integrated battery solution. PV systems have been used in many applications such as satellite systems, communication systems, water pumps, electric vehicle applications, and solar power plants [41].

The two most important factors determining energy outputs of PV are radiation and cell temperature. PV cell performances under standard test conditions given as - radiation 1000W/m^2 and the temperature 25°C).

2.4.1 PV Cell to Module to Array

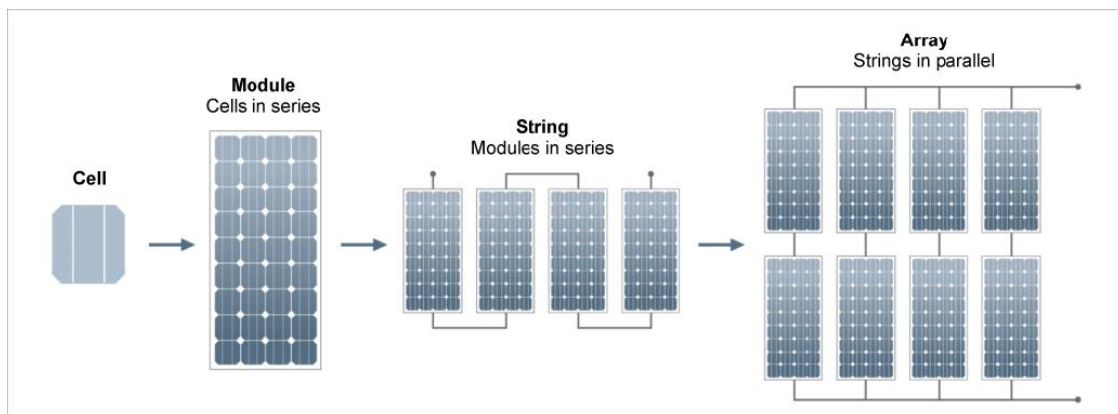


Figure 2.6 PV Cell to Module to Array

All PV cell consists of two or more thin layers of semi- conducting material, most commonly silicon. When the semiconductor is exposed to light, electrical charges are generated and can be conducted away by metal contacts as DC. The electrical output from a single cell is small, so multiple cells are connected to form a ‘string’, which produces a direct current. ‘Strings’ are encapsulated (usually behind glass) to form a module. A PV module

refers to a number of cells connected in series and in a PV array, modules are connected in series and in parallel [42],[43-45].

- **PV cell**

Solar cells are the building blocks of a PV array. These are made up of semiconductor materials like silicon etc. A thin semiconductor wafer is specially treated to form an electric field, positive on a side and negative on the other. Electrons are knocked loose from the atoms of the semiconductor material when light strikes upon them. If an electrical circuit is made attaching a conductor to the both sides of the semiconductor, electrons flow will start causing an electric current. It can be circular or square in construction.

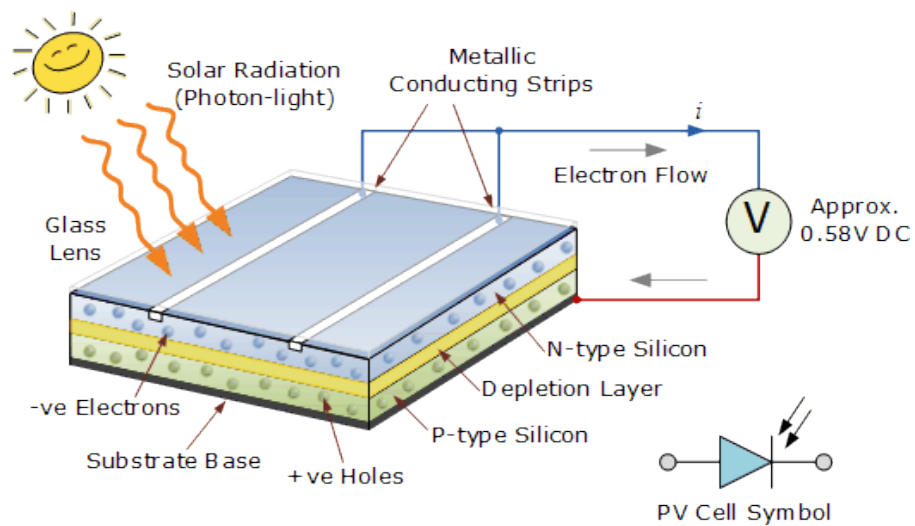


Figure 2.7 Working model of single PV cell

- **PV Module**

The voltage generated by a single solar cell is very low, around 0.5V. So, a number of solar cells are connected in both series and parallel connections to achieve the desired output. In case of partial shading, diodes may be needed to avoid reverse current in the array. Good ventilation behind the solar panels are provided to avoid the possibility of less efficiency at high temperature

- **PV Array**

The power produced by a single module is not sufficient to meet the power demands for most of the practical purposes. PV arrays can use inverters to convert the DC output into

AC and use it for motors, lighting and other loads. The modules are connected in series for more voltage rating and then in parallel to meet the current specifications.

2.4.2 Types of PV Panels

Some of the commercially available types of PV cell or film, used on an active solar roof are (a) monocrystalline, (b) polycrystalline, and (c) thin film.

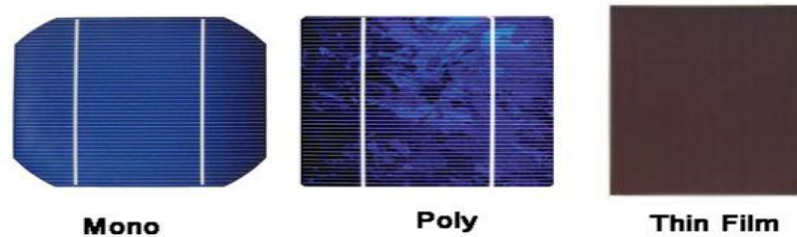


Figure 2.8 Types of PV panels for home use

(a) Mono crystalline silicon PV panels

These are made using cells sliced from a single cylindrical crystal of silicon. This is the most efficient photovoltaic technology, typically converting around 15% of the sun's energy into electricity. The manufacturing process required to produce monocrystalline silicon is complicated, resulting in slightly higher costs than other technologies.

(b) Polycrystalline silicon PV panels

Also known as multicrystalline cells, polycrystalline silicon cells are made from cells cut from an ingot of melted and recrystallised silicon. The ingots are then saw-cut into very thin wafers and assembled into complete cells. They are generally cheaper to produce than monocrystalline cells, due to the simpler manufacturing process, but they tend to be slightly less efficient, with average efficiencies of around 12%.

(c) Thin-film PV panels

A thin-film solar cell is a second generation solar cell made by depositing one or more thin layers, or thin film (TF) of photovoltaic material on a substrate, such as glass, plastic or metal. Thin-film solar cells are commercially used in several technologies, including

cadmium telluride (CdTe), copper indium gallium diselenide (CIGS), and amorphous thin-film silicon (a-Si, TF-Si).

Film thickness varies from a few nanometers (nm) to tens of micrometers (μm), much thinner than thin-film's rival technology, the conventional, first-generation silicon solar cell (c-Si), that uses wafers of up to 200 μm . This allows thin film cells to be flexible, and lower in weight. It is used in building integrated PVs and as semi-transparent, PV glazing material that can be laminated onto windows. Thin-film technology has always been cheaper but less efficient than conventional c-Si technology. However, it has significantly improved over the years.

2.5 Design of V-I characteristics of PV system

<i>Nomenclature</i>			
α_T ,	temperature and relative	β_T, β'_T	temperature and relative
α'_T	temperature coefficient of short circuit system;		temperature coefficient of open circuit system
N_S, N_M	cells in series, modules connected in series	N_C, N_P	cells in series in each module, No. of strings in parallel
I_{pv}	PV output current	q	electron charge $1.6 \times 10^{-23}(C)$;
I_M, I_A	Module current , Array current	R_s	series resistance
I_{ph}	photo current or irradiance current	R_{sh}	shunt resistance
I_D	current thro' anti- parallel diode	T	Cell temperature
I_{sh}	shunt current	V_{pv}	PV output voltage
I_o	diode saturation current	V_M, V_A	module voltage , array voltage
I_{SC}	short circuit current	V_{OC}, V_{MP}	Open circuit voltage , maximum power point voltage
k	Boltzmann's constant $1.38 \times 10^{-19}(J/k)$	n	Ideality factor

2.5.1 Current–voltage relationship for a single PV cell

PV cell is traditionally represented by an equivalent circuit composed of a current source, an anti-parallel diode [48], a series resistance and a shunt resistance. As shown in

Figure.2.9, a PV cell can be modeled as a current source connected with one diode and two resistors. The characteristic equation can be derived as follows,

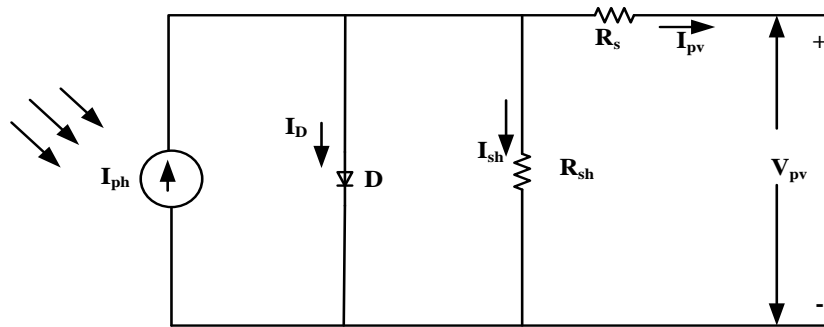


Figure 2.9 Equivalent circuit of PV cell

According to Kirchoff's current law,

$$I_{pv} = I_{ph} - I_D - I_{sh} \quad (2.16)$$

where I_{ph} is the photo current or irradiance current, generated when the cell is exposed to sunlight. I_{ph} varies linearly with solar irradiance for a certain cell temperature. I_D is the current flowing through the anti-parallel diode, which induces the non-linear characteristics of the solar cell. I_{sh} is shunt current due to the shunt resistor R_{sh} . Substituting relevant expressions for I_D and I_{sh} , we get

$$I_{pv} = I_{ph} - I_0 \left\{ \exp \left[\frac{q(V_{pv} + R_s I_{pv})}{nkT} \right] - 1 \right\} - \frac{V_{pv} + R_s I_{pv}}{R_{sh}} \quad (2.17)$$

where V is output voltage, I is output current, I_0 is cell reverse saturation current, I_{ph} is light-generated current, q is electron charge 1.6×10^{-19} (C), T is cell temperature in Celsius, k is Boltzmann's constant 1.38×10^{-19} (J/k), R_{sh} is shunt resistance, R_s is series resistance, ideality factor n is introduced in the denominator of the exponent [50].

2.5.2 Current–voltage relationship for a PV module

A PV module is typically composed of a number of solar cells in series. N_s represents the number of solar cells in series for one module. When N_s solar cells are connected in series to build up a module, the output current I_M and output voltage V_M of the module have the following relationship.

$$I_M = I_{ph} - I_0 \left[\exp \left(\frac{q(V_M + I_M N_S R_S)}{N_S n k T} \right) - 1 \right] - \frac{V_M + I_M N_S R_S}{N_S R_{sh}} \quad (2.18)$$

Eq.(2.18) can be expanded to any number of cells in series (N_S), and thus not restricted to one module. If there are N_M modules connected in series, and there are N_C cells in series in each module, then

$$N_S = N_M \times N_C \quad (2.19)$$

2.5.3 Current–voltage relationship for a photovoltaic array

In an array, PV modules are connected in series and in parallel. It is important to consider the effects of those connections on the performance of the array. The current–voltage relationship for groups of strings connected in parallel (an array) as shown in figure. 2.6. The output current I_A and output voltage V_A of a PV array with N_S cells in series and N_P strings can be expressed by the following equation,[43],[46-47].

$$I_A = N_P I_{ph} - N_P I_0 \left[\exp \left(\frac{q \left(V_A + I_A \frac{N_S}{N_P} R_S \right)}{N_S n k T} \right) - 1 \right] - \frac{V_A + I_A \frac{N_S}{N_P} R_S}{\frac{N_S}{N_P} R_{sh}} \quad (2.20)$$

2.5.4 Model Parameters of PV Cell to Module to Array

2.5.4.1 Ideality Factor (n)

The ideality factor (n) accounts for the different mechanisms responsible for moving carriers across the junction. The parameter n is 1 if the transport process is purely diffusion and $n \approx 2$ if it is primarily recombination in the depletion region. Some research papers suggest an n of 1.3 for silicon. The parameter n represents one of the unknowns of the cell-to-module-to-array model. In our work, n is assumed to be related only to the material of the PV cell and be independent of temperature and solar irradiation. If values for the photocurrent (I_{ph}), diode saturation current (I_0), series resistance (R_S), and shunt resistance (R_{sh}) are known, along with the operational data V_{OC} , I_{SC} , I_{MP} , V_{MP} , β_T , α_T ; ideality factor(n) can be solved. No matter the operating condition, the values of n will not change. The value of n compared to the value of n_{ref} at Standard Reference Conditions (SRC) is given by,

$$n = n_{ref} \quad (2.21)$$

where the solar irradiation is $G_{ref} = 1000 \text{ W/m}^2$ and the cell temperature is $T_{ref} = 298 \text{ K}$ or 25°C at SRC.

2.5.4.2 Photocurrent (I_{ph})

The photocurrent (I_{ph}), depends on the solar irradiance G and cell temperature T is given by

$$I_{ph} = I_{ph,ref} \left(\frac{G}{G_{ref}} \right) [1 + \alpha'_T (T - T_{ref})] \quad (2.22)$$

where $I_{ph,ref}$ is the photo current at SRC. α'_T is the relative temperature coefficient of the short-circuit current, which represents the rate of change of the short-circuit current with respect to temperature. The relationship between α'_T and α_T is given as

$$\alpha_T = \alpha'_T I_{ph,ref} \quad (2.23)$$

2.5.4.3 Diode saturation current (I_o)

I_o is primarily dependent on the temperature of the cell expressed as

$$I_o = I_{o,ref} \left[\frac{T}{T_{ref}} \right]^3 \exp \left[\frac{E_{g,ref}}{kT_{ref}} - \frac{E_g}{kT} \right] \quad (2.24)$$

Where $I_{o,ref}$ is the diode saturation current for the cell temperature at SRC, T_{ref} . E_g is the bandgap energy and for silicon to be

$$E_g = 1.16 - 7.02 \times 10^{-4} \left(\frac{T^2}{T - 1108} \right) \quad (2.25)$$

2.5.4.4 Temperature of cell (T)

Variation in cell temperature occurs due to changes in the ambient temperature as well as changes in the insolation as

$$T = T_{amb} + \left(\frac{NOCT - 20^\circ\text{C}}{0.8} \right) G \quad (2.26)$$

where T_{amb} is the ambient temperature and $NOCT$ represents the nominal operating cell temperature. G represents the solar irradiation at the ambient temperature, T_{amb} .

2.5.4.5 Parallel leakage resistance R_{sh} and series resistance R_s

The parallel leakage resistance or shunt resistance R_{sh} and series resistance R_s are the last two unknown parameters in the cell-to-module-to-array model [49]. Approximately,

$$R_{sh} > \frac{10 V_{OC}}{I_{SC}} \quad (2.27)$$

where V_{OC} and I_{SC} are open circuit voltage and short circuit current respectively.

The relationship relating the shunt resistance to irradiation at operating conditions and SRC can be expressed as,

$$\frac{R_{sh}}{R_{sh,ref}} = \frac{G}{G_{ref}} \quad (2.28)$$

Finally,

$$R_{sh} < \frac{0.1 V_{OC}}{I_{SC}} \quad (2.29)$$

Assuming the R_s to be independent and irradiation at both operating conditions and SRC,

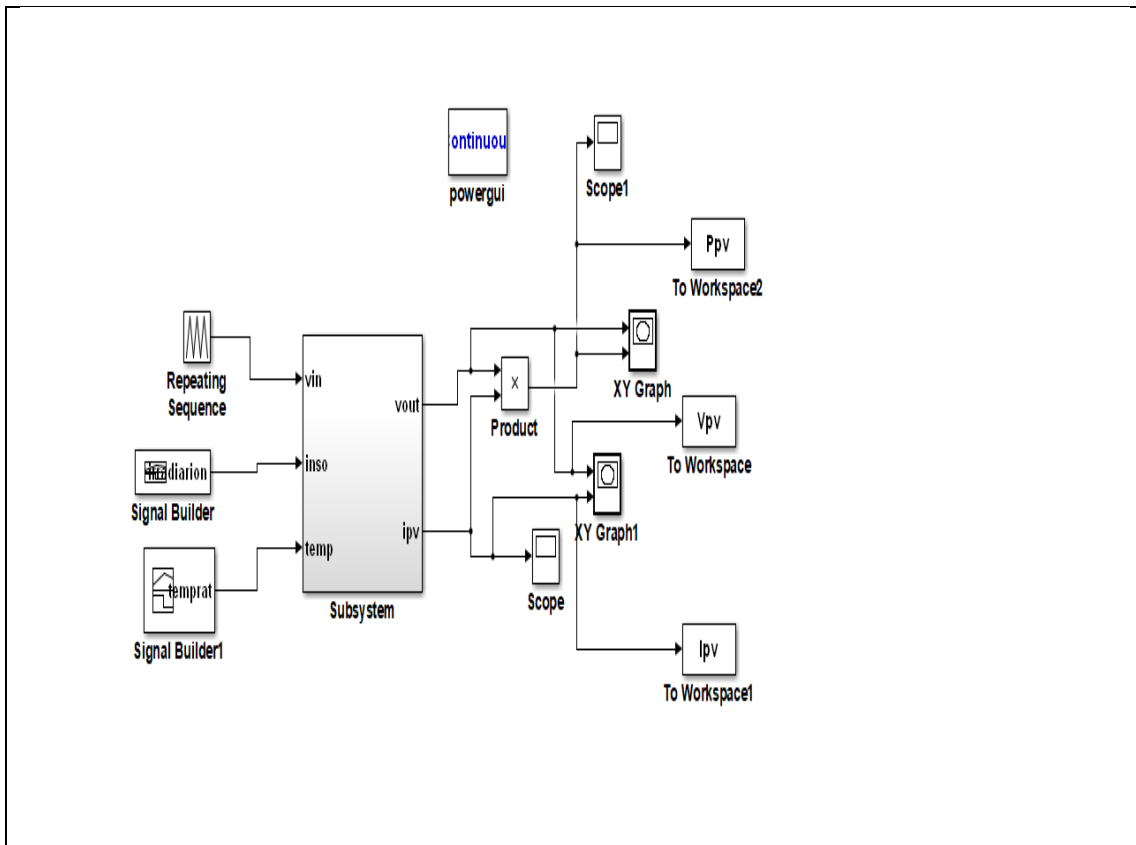
$$R_s = R_{s,ref} \quad (2.30)$$

2.6 Simulation results and discussion

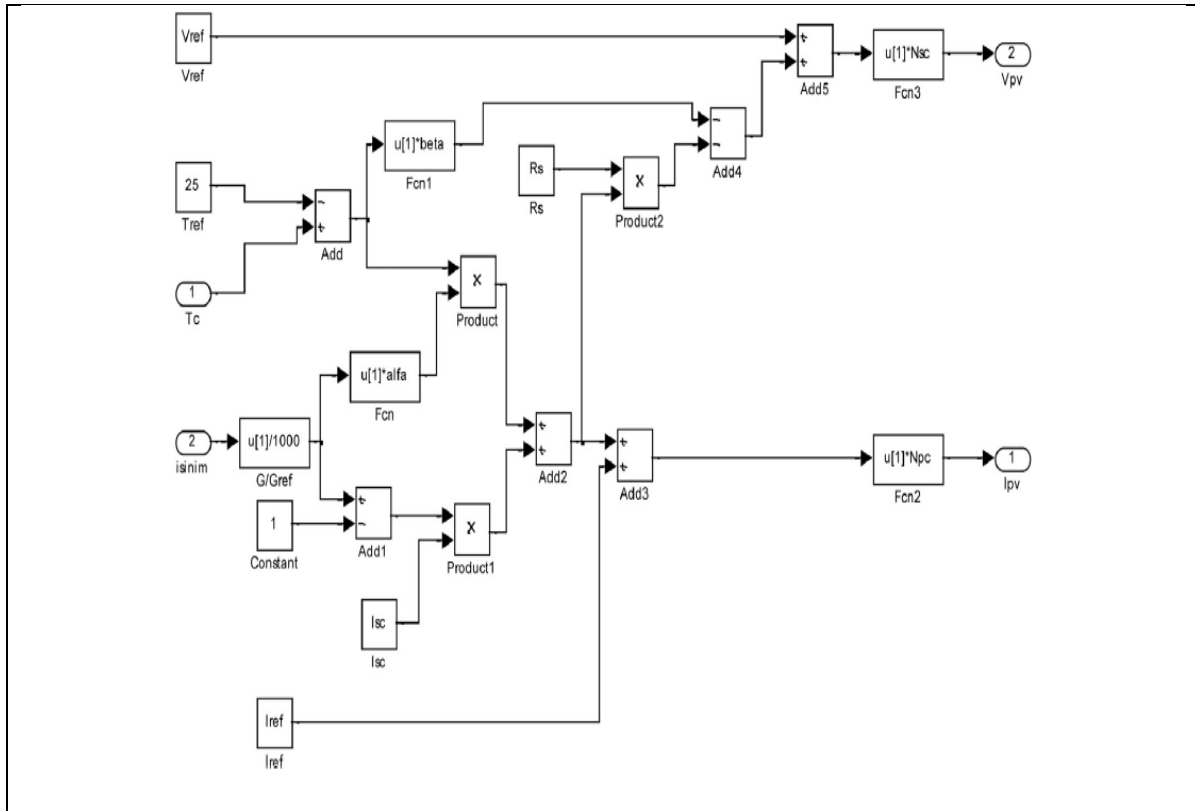
Based on the above mathematical equations of a PV module is simulated aided by Matlab/Simulink. The parameters taken for the simulation is given in Table 2.3. V-I characteristics and P-V characteristics of module is shown in figure 2.12. It is observed that the change of voltage and the current values depends on the value of irradiation vice versa power. The Simulink module is built as shown in figure 2.10(a) and its subsystem details given in 2.10(b)

Table 2.3 Simulation input for PV model

parameter	values
Number of cell per Module	96
Open circuit voltage(V_{oc})	64 volt
Short circuit current(I_{sc})	6 amp
Maximum module voltage(V_M)	54.5 volt
Maximum module current(I_M)	5.58 amp
Series resistance(R_s)	0.0387 Ω
Parallel resistance(R_p)	950 Ω
Photon current (I_{ph})	5.96 amp
Saturation current(I_o)	1.175e-08 amp
Number of series connected module per string	12
Number of parallel string	68



(a)



(b)

Figure 2.10(a) Simulation Model of PV system (b)Sub-system

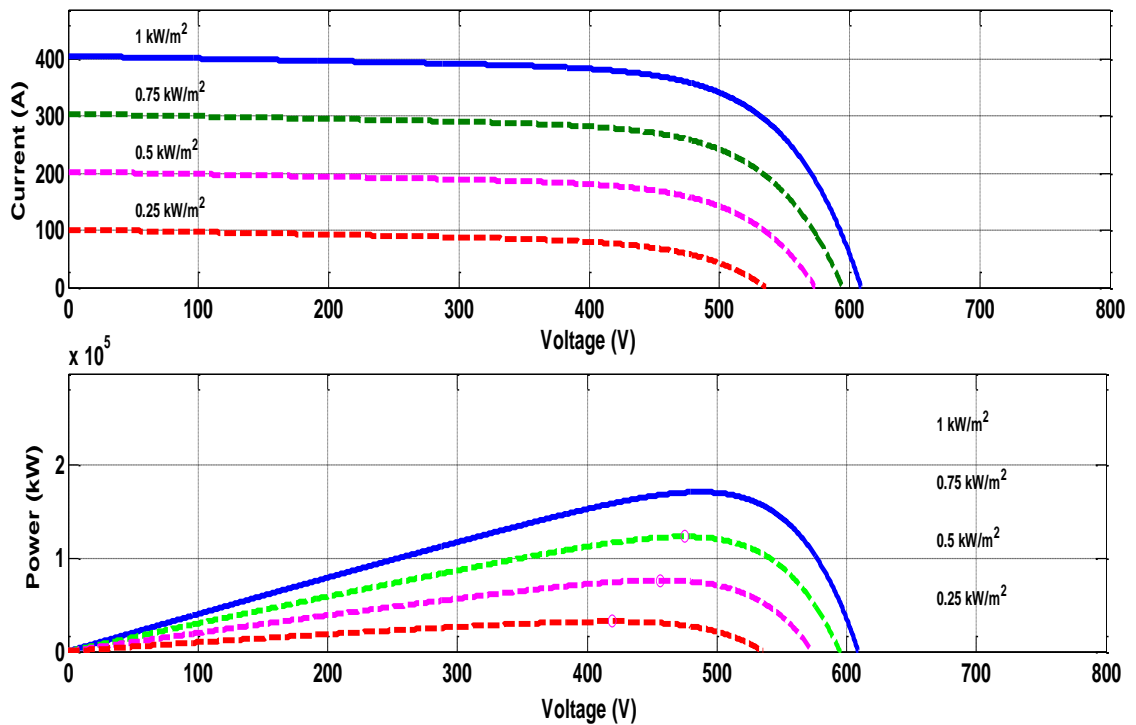


Figure 2.11 Simulated results of V-I and P-V characteristics of PV array

2.7 Conclusion

In this study, two DG units were projected-PEMFC and PV cell. The overview of different types of fuel cells, and merits of PEMFC in comparison to other fuel cell types were provided in detail. The mathematical model of PEMFC and characteristics of fuel stack voltage were deliberated. The simulation results and discussions on stack voltage of PEMFC were presented. Similarly, an over view of DG (PV) and working principle of different types of PV cells were discussed. The mathematical model, voltage -current characteristics, power –voltage characteristics, the performance of PV array for different temperatures were analysed in detail. The simulation parameters of DGs and its diagrams have been given in detail.

Chapter III

Concepts of Control of Grid -connected DGs with emphasize on SRF

In this chapter, the proposed grid – connected structure and the different concepts of control strategies adopted in this study are presented. The power conversion technology and power converter applications are discussed in detail for deep understanding of the idea.

The VSIs are the dominant inverters applying to parallel inverters applications. Power converters topologies and PWM modulation strategies for VSIs are illustrated. Several techniques are available in the literature for obtaining the instantaneous phase information of the grid voltage, but synchronous-reference-frame (SRF) Phase Locked Loop (PLL) (SRF-PLL) are reported to be the state of the art technique and so the same is utilized in the present research work. AC filters topologies with focusing in LC filter design and its dynamic behaviour is analysed. Synchronization with PLLs are described and discussed. Besides, since the current and voltage control loops system has a considerable effect on power sharing between inverters the design process for this control structure is also discussed in detailed. The model is validated under balanced condition and briefly discussed.

3.1 Overview of proposed Grid connected structure

The detailed structure of proposed model is given in Figure 3.1. As it shown, PV system is considered as DG1 and PEMFC system is considered as DG2. In our study, these DGs are integrated with utility grid at PCC through link impedance along with power control loop current controllers.

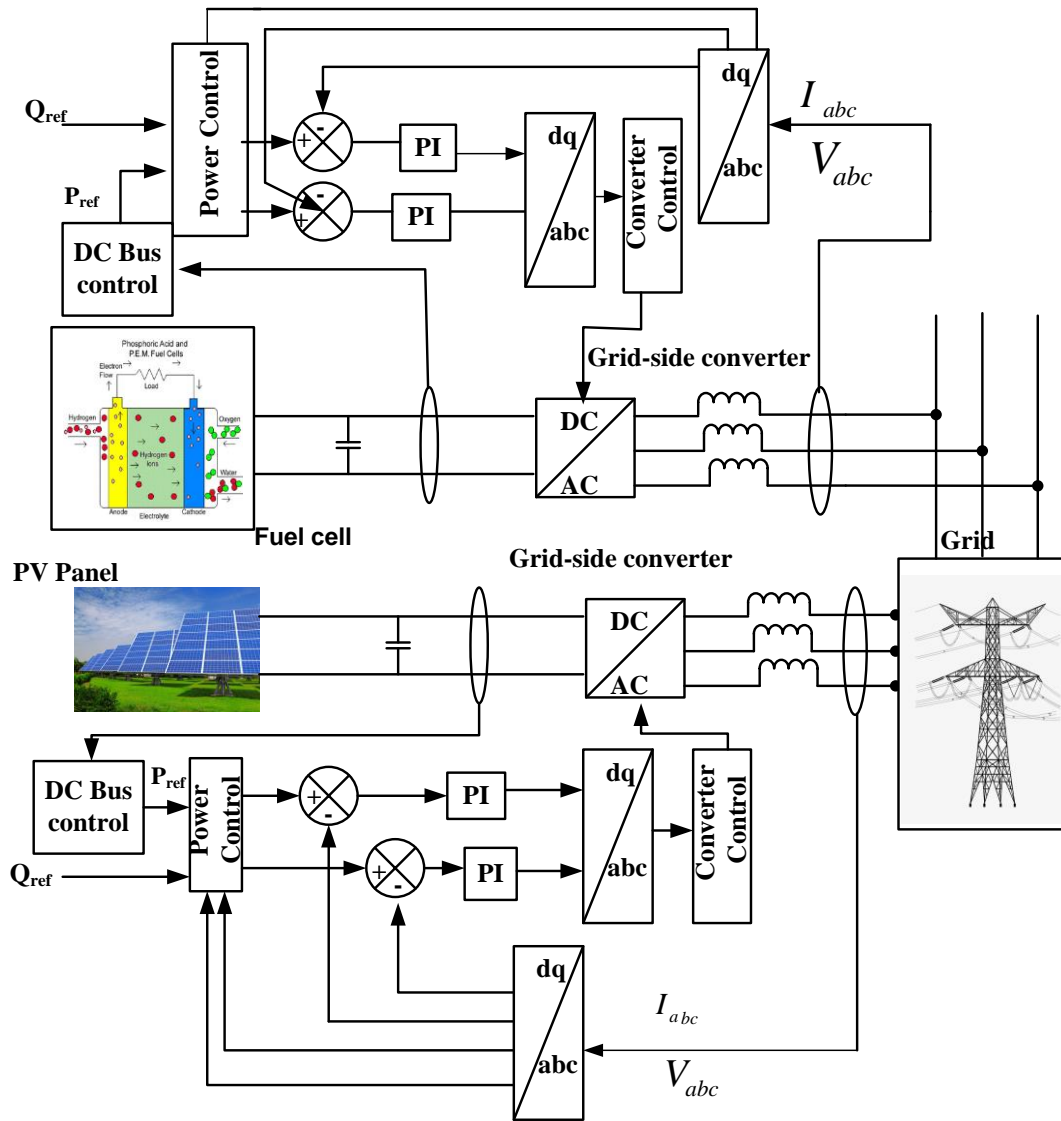


Figure 3.1 Architecture of proposed scheme

3.2 Three-Phase VSIs Topology

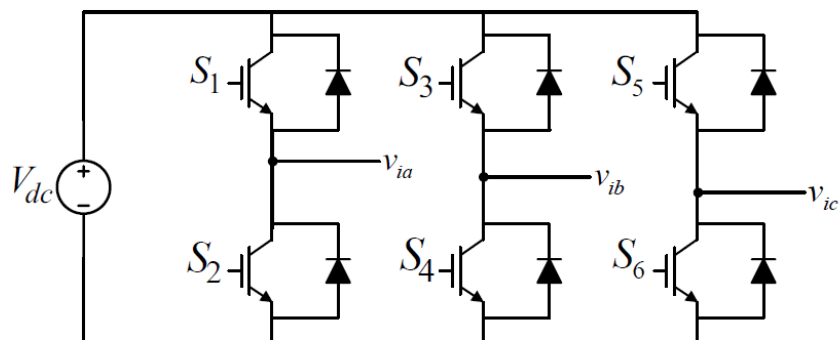


Figure 3.2 A typical VSI structure

Three-phase inverters are usually applied to the high power applications. These inverters can be formed by connecting three single-phase inverters in parallel or using a three-phase bridge. Figure. 3.2 shows the VSI structure in which V_{dc} represents the DC link voltage provided by a DG sources, (S1,...S6) denoted the power electronics device or static switches. The switching signals are applied to the switches using PWM technique [51-52].

3.3 Pulse Width Modulation (PWM)

PWM is used to control the amplitude and frequency of the output. PWM strategy plays an important role for harmonics and switching losses minimization in power converters. The main goal of any modulation strategy is to obtain a variable output with a maximum fundamental component and minimum harmonics. There are two major types of PWM techniques widely used for the control of DC-AC converter. (i) Sine Pulse Width Modulation (SPWM) (ii) State Vector Pulse Width Modulation (SVPWM).

Even though the DC bus voltage utilization for SPWM is low, the technique is widely used in industrial applications since it can be easily implemented [53].

In this study, we have considered SPWM for inverter switching control for the case of balanced load assumed. SVPWM is used for the case of unbalanced load and the details are discussed in next chapter.

3.3.1 Sine Pulse Width Modulation (SPWM)

The SPWM principle is based on the comparison of a carrier signal and pure sinusoidal control signals, as shown in Figure 3.3. For three phase VSI, the three modulating sinusoidal signals, with 120 degrees phase shift, are compared with a triangular waveform or carrier signal which is with higher frequency [54]. Figure3.3 shows the firing pulse generation for S1 and S4 using a three-phase PWM, and the L - L voltage (V_{ab}).

The ratio between the amplitude of the reference signal A_r , and carrier signal A_c is defined as the inverter modulation index

$$m = A_r/A_c \quad (3.1)$$

$$V_{out} = m \times V_{dc} \quad (3.2)$$

where V_{out} is the inverter output voltage amplitude. As long as the modulation index is less than unit ($m < 1$), the amplitude of the output voltage fundamental component is linearly proportional to the modulation index [55].

By changing the modulation index m , between 0 and 1 which is called the linear region, the widths of pulses vary, which results in variations in the amplitude of the output voltage. The maximum output voltage when ($m=1$) is given as

$$V_{ab} = \frac{\sqrt{3}}{2\sqrt{2}} mV_{dc} = 0.61V_{dc} \quad (3.3)$$

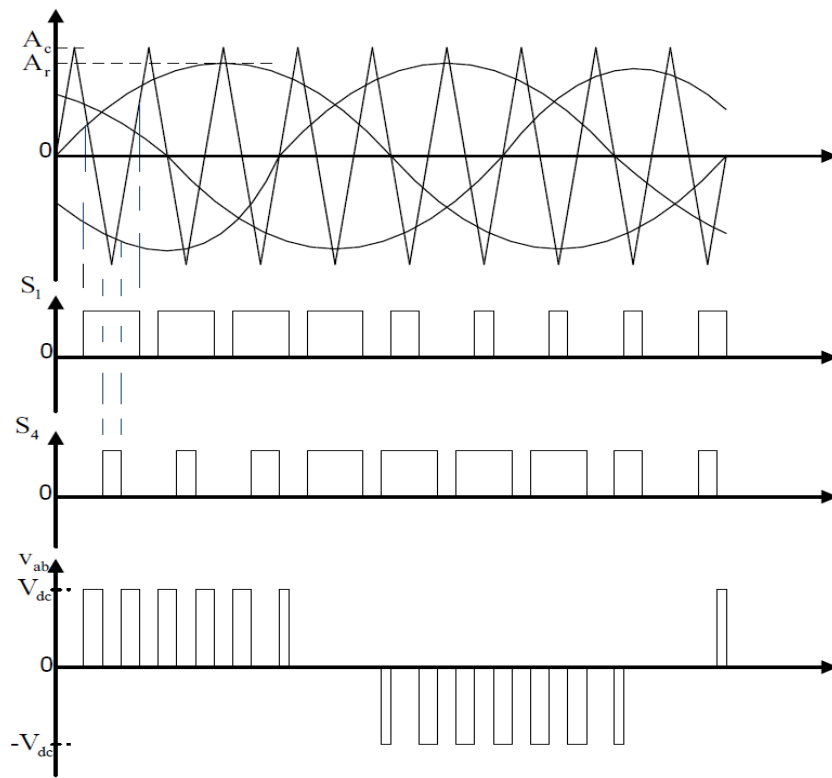


Figure 3.3 Sinusoidal Waveform of three phase SPWM

3.4 LC filter Design

A filter is a circuit capable of passing (or amplifying) certain frequencies while attenuating other frequencies. Thus, a filter can extract important frequencies from signals that also contain undesirable or irrelevant frequencies.

Filters can be classified on the following basis:

On the basis of Electrical components used	<ul style="list-style-type: none"> • Active Filter • Passive Filter
On the basis of signal transmitted	<ul style="list-style-type: none"> • Digital Filters(Buttersworth Filter, Chbyshev Filter, Comb Filter) • Analog Filter
On the basis of frequency and bandwidth rejected or accepted (see Figure 3.4)	<ul style="list-style-type: none"> • Low Pass filter • High Pass Filter • Band Pass Filter • All Pass Filter
On the basis of ripple reduction in AC current in rectifier circuit	<ul style="list-style-type: none"> • L-Filter • C- Filter • LC- Filter (see Figure 3.5) • L-type LC- Filter

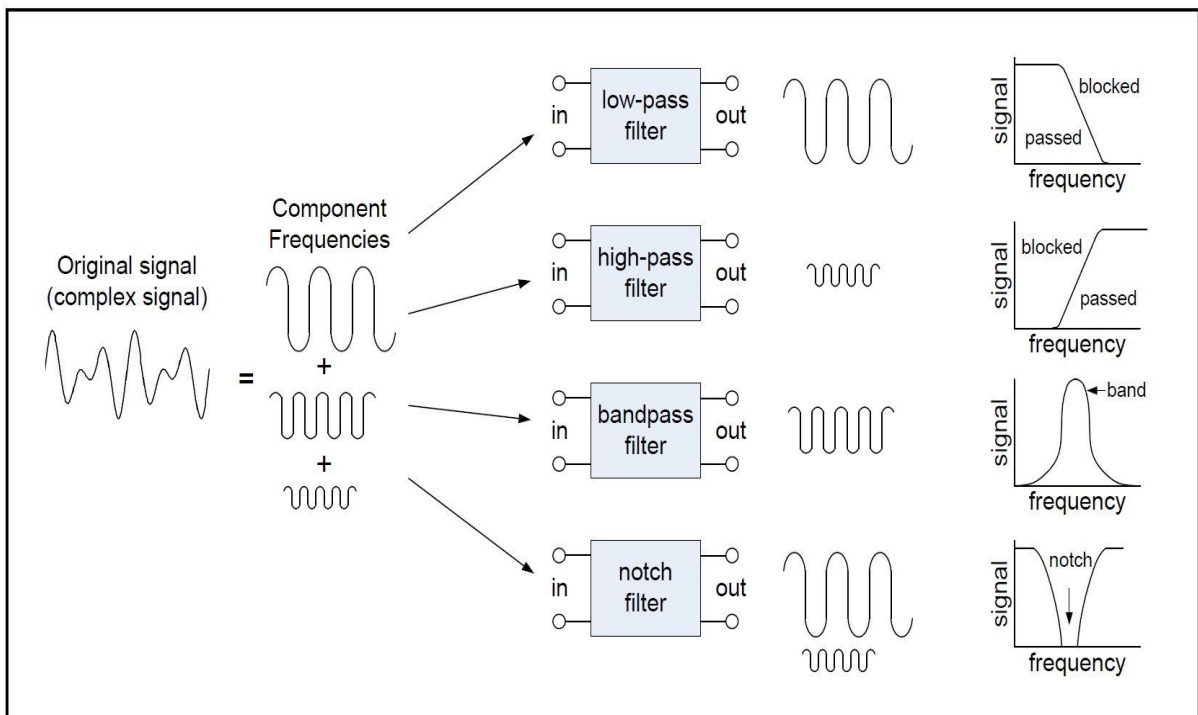


Figure 3.4 Types of Filter based on frequency and bandwidth and their characteristics

The output power of converters, synthesized by using PWM which has high frequency harmonics, needs to connect AC filter across the converter. In order to establish a voltage with low harmonic content, the LC filters is used in our study, at the output of the

inverters. The LC filter design for the inverter which using the Sinusoidal Pulse Width Modulation (SPWM) is imperative. This modulation method will produce a lot of harmonic in the switching frequency.

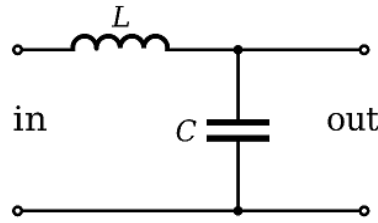


Figure 3.5 LC Filter

The relationship between filter cut-off frequency and its components is given as

$$f_c = \frac{1}{(2\pi\sqrt{L_f C_f})} \quad (3.4)$$

$$10f_m \leq f_r \leq \frac{f_c}{10} \quad (3.5)$$

where f_r is the resonant frequency of LC filter is, f_m is the frequency of modulating wave, and f_c is the frequency of SPWM carrier wave.

The function between filter output voltage $V_{f_{out}}$ and input voltage $V_{f_{in}}$ is

$$G(j\omega) = \frac{V_{f_{out}}}{V_{f_{in}}} = \frac{1/j\omega C_f}{j\omega L_f + 1/j\omega C_f + R_f} \quad (3.6)$$

Let $\omega_o = \frac{1}{\sqrt{L_f C_f}}$ and $\xi = \frac{R_f}{2} \sqrt{\frac{C_f}{L_f}}$, we get,

$$G(j\omega) = \frac{\omega_o^2}{(j\omega)^2 + j\omega * 2\xi C_f + R_f} \quad (3.7)$$

By using equations (3.4 ~ 3.7), the parameter of the LC filter is designed to make sure that the voltage drop in inductance cannot be exceed the 3% value of the system voltage [56-57].

3.5 Proportional- Integral (PI) Controller for grid- connected Inverter

In general P,PI,PD,PID controllers are used to improve steady state accuracy by decreasing the steady state errors; to improve the stability; to reduce the offsets produced in the system, to control the maximum overshoot of the system; to reduce the noise signals produced in the system; to make the system faster during the slow response of the over damped system.

In our research work P-I controller is chosen since P-I control provides better stability, eliminates the steady state error i.e offset, good transient response and stabilizes the controller design.

PI controllers have two tuning parameters to adjust. While this makes more challenging to tune than a P-only controller, they are not as complex as the three parameter PID controller. The main advantage of the PI controller is that there will be no remaining control error after a set point change or a process disturbance. PID controller is more sensitive and lead to sustained oscillations about the set point. PID produces offset if set point is changed from the design value and if K_p is increased about is set point. Hence, PI control is suitable for noisy processes, integrating processes, and processes resembling Ist order system.

Current loop adjuster use PI regulator to control d and q axis current and the PI controller transfer function is given as

$$G_{pi}(s) = K_p \left(1 + \frac{1}{T_i s} \right) = K_p + \frac{K_I}{s} \quad (3.8)$$

where T_i id the integral time or reset time. The constants K_p (proportional gain) and K_I (integral gain) decides the transfer function and the location of the poles and zeros of the PI compensator.

The closed loop transfer function of the current controller is given by

$$\frac{G_{pi}(s) G_m(s) \frac{1}{R_f + sL_f}}{1 + G_{pi}(s) G_m(s) \frac{1}{R_f + sL_f}} = \frac{1}{\tau_1 s(\tau_2 s + 1) + 1} \quad (3.9)$$

where $G_{pi}(s)$ is the PI controller transfer function of the current controller and $G_m(s)$ is measurement filter transfer function . τ_1 is the time constant corresponding to the bandwidth.

Simplifying the terms in (3.9) we get

$$\frac{R_f + sL_f}{G_{pi}(s) G_{inv}(s)} = \tau_1 s \quad (3.10)$$

Rearranging above equation,

$$K_p = \frac{L_f}{\tau_1}, K_I = \frac{R_f}{\tau_1} \quad (3.11)$$

3.6 Phase Locked Loop (PLL)

PLL is essential for inverter synchronization with the utility grid. The synchronization algorithm for attaining a controllable power factor must detect the phase angle of the three-phase utility grid voltage with optimal dynamic response and reliability in order to obtain the synchronization of the controlled three-phase inverter current and to ensure the proper behavior of the inverter control strategy.

It is a control system that generates an output signal whose phase is related to the phase of an input "reference" signal. This circuit compares the phase of the input signal with the phase of the signal derived from its output oscillator and adjusts the frequency of its oscillator to keep the phases matched. The output signal from the phase detector is used to control the oscillator in a feedback loop. Frequency is the time derivative of phase. Keeping both the input and output phase in lock step implies keeping the input and output frequencies in lock step. Consequently it can track an input frequency or it can generate a frequency that is a multiple of the input frequency [58].

To connect a power plant to the grid the output voltage from the inverter must have the same frequency for each of the three phases. This is achieved if the phase angle of the grid voltage is tracked. In the control system for the inverter a sine wave is created with selected phase difference as control wave for the SPWM. This is a real time process constantly working in order to keep the output from the inverters synchronized with the grid.

PLLs are available mainly with three types for phase tracking:

- (i) Synchronous rotating reference frame (SRF),
- (ii) Stationary reference frame

(iii) Zero crossing.

SRF PLL gives the best performance under non-ideal grid conditions; hence we have considered SRF-PLL in our study.

3.6.1 SRF- PLL or dq PLL

The SRF PLL is the one among the above mentioned with the best performance under distorted and non-ideal grid conditions and is therefore the PLL system to be further investigated in this report. The basic idea of the PLL system is a feedback system with a PI-regulator tracking the phase angle. Input is the three phases of the grid voltage and output from the PLL is the phase angle of one of the three phases. In the power supply substation there will be one inverter leg for each of the three phases. There are two alternatives, either assuming the grid voltages are in balance and track only one of the phases and then shift with 120 degrees for each of the other two phases or having three PLL systems, one for each phase[59].

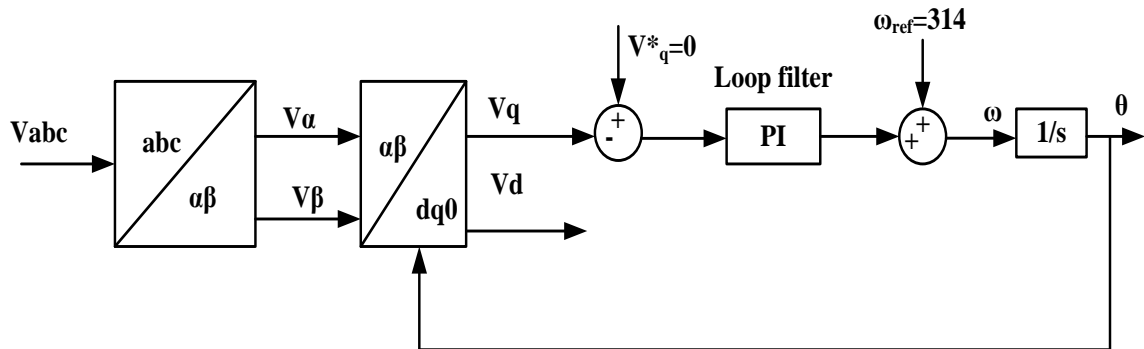


Figure 3.6 Structure of the SRF PLL

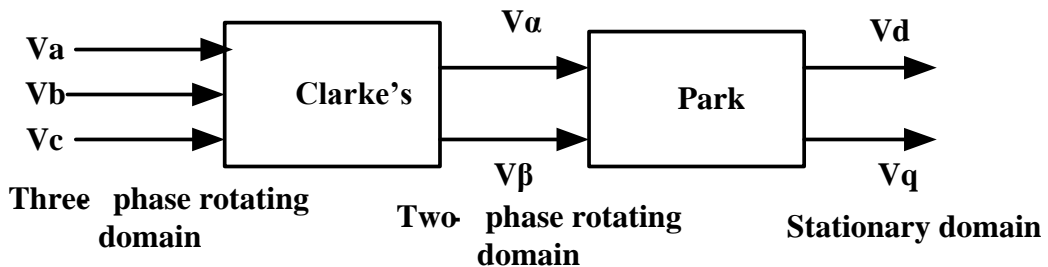


Figure 3.7 abc to dq transformation

A three-phase SRF-PLL structure is shown in Figure 3.6, consisting of Clark's and Park's transformations (also known as abc to dq transformation) (see figure 3.7), the PI regulator as the loop filter, and an integrator as the voltage-controller oscillator (VCO). The input variables are three phase utility grid voltages (V_a , V_b , V_c) and output variable is the phase angle (θ)

3.6.1.1 Stationary reference frame of $\alpha\beta$

To track the phase angle the three phase voltage signals V_a , V_b and V_c are transferred from three phases to a stationary system of two phases V_α and V_β , in order to avoid coupled AC currents and voltages [60]. Therefore voltage and current can be transformed from abc to $\alpha\beta$ and the grid voltages are given as

$$V_a = V_m \sin(\theta) \quad (3.12)$$

$$V_b = V_m \sin\left(\theta - \frac{2\theta\pi}{3}\right) \quad (3.13)$$

$$V_c = V_m \sin\left(\theta + \frac{2\pi}{3}\right) \quad (3.14)$$

where θ is the phase angle. Using Clarke's transformation, the balanced three phase quantities converted into balanced two phase orthogonal quantities. The $\alpha\beta$ -transformation matrix is given as

$$T_{\alpha\beta} = \frac{2}{3} \begin{bmatrix} 1 & -\frac{1}{2} & \frac{1}{2} \\ 0 & -\frac{\sqrt{3}}{2} & \frac{\sqrt{3}}{2} \end{bmatrix} \quad (3.15)$$

Carrying out the matrix multiplication $V_{\alpha\beta} = T_{\alpha\beta} V_{abc}$ produces

$$\begin{bmatrix} V_\alpha \\ V_\beta \end{bmatrix} = \begin{bmatrix} V_m \sin(\theta) \\ V_m \cos(\theta) \end{bmatrix} \quad (3.16)$$

3.6.1.2 Synchronous rotating reference frame (SRF) of abc , $\alpha\beta$ and dq

One of the issues associated with stationary reference frames (abc and $\alpha\beta$) is the steady state reference tracking error when the PI controllers are employed to control the signals. To overcome this issue while still using the PI controllers the sinusoidal signals can be transferred to DC signals using synchronous reference frame transformations. Figure. 3.8 shows this transformation graphically, as it can be seen the three-phase balanced sinusoidal signals (a, b, and c) are transformed to two rotating DC signals (d and q) with the angular velocity ω . The phase angle θ is tracked by synchronizing the voltage space vector along q or d axis in the SRF. Here the voltage space vector is synchronized with the q-axis[60],[61].

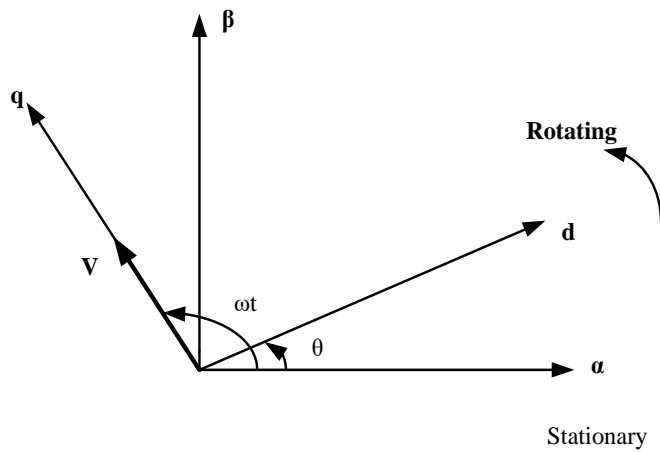


Figure 3.8 Synchronous rotating reference frame

3.7 Modeling of three-phase Grid-connected VSI system with SRF

A typical model of a three-phase grid connected VSI with an LC filter is depicted in Figure 3.7, whereas R_f , L_f , C_f represent the equivalent lumped resistance, an inductance of the filter and capacitance of the filter, respectively. I_{abc} is the grid current and V_{abc} is the grid voltage [62].

If the voltage space vector is to be synchronized with the q-axis the transformation matrix is

$$T_{dq} = \begin{bmatrix} \sin\theta^* & \cos\theta^* \\ -\cos\theta^* & \sin\theta^* \end{bmatrix} \quad (3.17)$$

where θ^* is the estimated phase angle output of the PLL system. Carrying out the transformation $V_{dq} = T_{dq}V_{\alpha\beta}$ and using the trigonometric addition formulas produces

$$\begin{bmatrix} V_d \\ V_q \end{bmatrix} = \begin{bmatrix} V_m \sin(\theta - \theta^*) \\ -V_m \cos(\theta - \theta^*) \end{bmatrix} \quad (3.18)$$

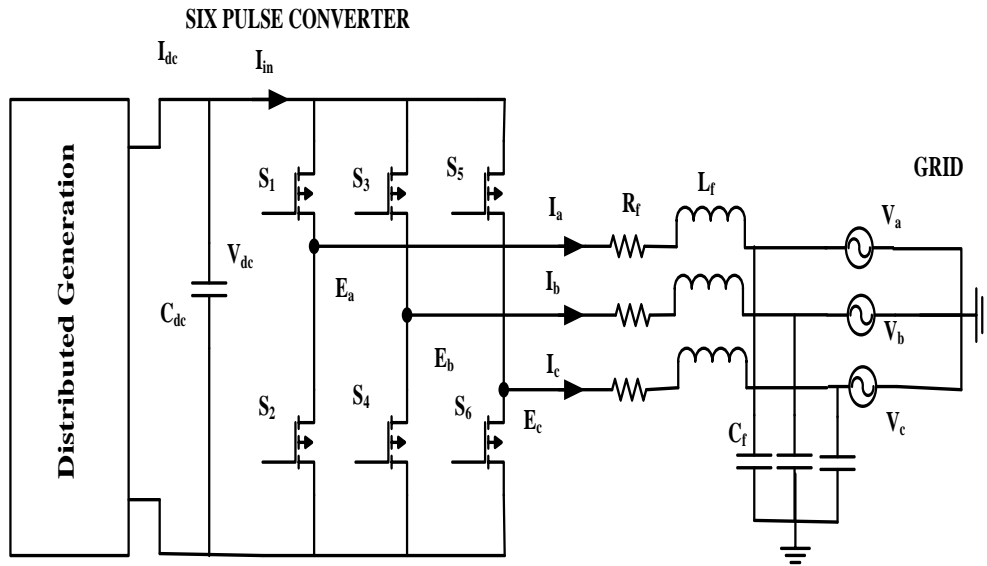


Figure 3.9 Schematic diagram of Three-phase grid-connected inverter

The phase angle θ is estimated with θ^* which is the integral of the estimated frequency. The estimated frequency ω_{ref} is the sum of the PI-output and the feed forward frequency ω . Gains of the PI-regulator are then designed so that V_q follows the reference value $V_q^* = 0$. If $V_q = 0$, then the space voltage vector is synchronized along the q -axis and the estimated frequency ω_{ref} is locked on the system frequency ω . This results in an estimated phase angle θ^* that equals the phase angle θ . If $\theta^* \approx \theta$ then the small angle approximation for sinus function yields $V_q = -V_m(\theta - \theta^*)$. The purpose of the feed forward frequency, ω , is to have the PI-regulator control for an output signal that goes to zero[63].

The SRF transformation is realizable using the transformation matrix,

$$T_{abc-dq} = \frac{2}{3} \begin{bmatrix} \cos(\theta) & \cos\left(\theta - \frac{2\pi}{3}\right) & \cos\left[\theta - \frac{4\pi}{3}\right] \\ -\sin(\theta) & -\sin\left(\theta - \frac{2\pi}{3}\right) & -\sin\left(\theta - \frac{4\pi}{3}\right) \end{bmatrix} \quad (3.19)$$

Where $\theta = \int \omega dt$, and the DC- rotating signals, which are called d and q , can be calculated as

$$\begin{bmatrix} V_d \\ V_q \end{bmatrix} = T_{abc-dq} \begin{bmatrix} V_a \\ V_b \\ V_c \end{bmatrix} \quad (3.20)$$

$$\begin{aligned} & [T_{dq-abc}] \begin{bmatrix} V_d \\ V_q \end{bmatrix} - [T_{dq-abc}] \begin{bmatrix} V C_{fd} \\ V C_{fq} \end{bmatrix} \\ &= R_f [T_{dq-abc}] \begin{bmatrix} I C_{fd} \\ I C_{fq} \end{bmatrix} + L_f \frac{d}{dt} ([T_{dq-abc}]) \begin{bmatrix} I C_{fd} \\ I C_{fq} \end{bmatrix} + L_f ([T_{dq-abc}]) \frac{d}{dt} \begin{bmatrix} I C_{fd} \\ I C_{fq} \end{bmatrix} \end{aligned} \quad (3.21)$$

where V_d and V_q are the inverter output voltage d and q components, $V C_{fd}$ and $V C_{fq}$ are the filter capacitor voltage in synchronous reference frame, and $I C_{fd}$ and $I C_{fq}$ are the d and q components of the filter inductor current[64-65] .

$$\text{By considering } [T_{abc-dq}][T_{dq-abc}] = \begin{bmatrix} 1 & 0 \\ 0 & 1 \end{bmatrix}, [T_{abc-dq}] \frac{d}{dt} [T_{dq-abc}] = \omega \begin{bmatrix} 0 & -1 \\ 1 & 0 \end{bmatrix},$$

and multiplying $[T_{abc-dq}]$ by equation 3.17, it can be refined as

$$\begin{bmatrix} V_d \\ V_q \end{bmatrix} = R_f \begin{bmatrix} I C_{fd} \\ I C_{fq} \end{bmatrix} + L_f \frac{d}{dt} \begin{bmatrix} I C_{fd} \\ I C_{fq} \end{bmatrix} + L_f \omega \begin{bmatrix} -I C_{fd} \\ I C_{fq} \end{bmatrix} + \begin{bmatrix} V C_{fd} \\ V C_{fq} \end{bmatrix} \quad (3.22)$$

The Inverse Park Transform block converts the time-domain direct, quadrature, and zero components in a rotating reference frame to the components of a three-phase system in an abc reference frame. The block can preserve the active and reactive powers with the powers of the system in the rotating reference frame by implementing an invariant version of the Park transform. For a balanced system, the zero component is equal to zero. In the abc reference frame, the state space equations of the system equivalent circuit are given as

$$\frac{d}{dt} \begin{bmatrix} I_a \\ I_b \\ I_c \end{bmatrix} = \frac{R_f}{L_f} \begin{bmatrix} I_a \\ I_b \\ I_c \end{bmatrix} + \frac{1}{L_s} \left(\begin{bmatrix} E_a \\ E_b \\ E_c \end{bmatrix} - \begin{bmatrix} V_a \\ V_b \\ V_c \end{bmatrix} \right) \quad (3.23)$$

Using Park's transformation, (3.19) can be expressed in the dq reference frame as

$$\frac{d}{dt} \begin{bmatrix} I_p \\ I_q \end{bmatrix} = \begin{bmatrix} -\frac{R_f}{L_f} & \omega \\ -\omega & -\frac{R_S}{L_S} \end{bmatrix} \begin{bmatrix} I_p \\ I_q \end{bmatrix} + \frac{1}{L_S} \left(\begin{bmatrix} E_d \\ E_q \end{bmatrix} - \begin{bmatrix} V_p \\ V_q \end{bmatrix} \right) \quad (3.24)$$

where ω is the coordinate angular frequency, and the Park's transformation can be defined as

$$I_{dq0} = T I_{abc} \quad (3.25)$$

$$\text{where, } I_{dq0} = \begin{bmatrix} I_p \\ I_q \\ I_0 \end{bmatrix}, I_{abc} = \begin{bmatrix} I_a \\ I_b \\ I_c \end{bmatrix}, T = \frac{2}{3} \begin{bmatrix} \cos\theta & \cos\left(\theta - \frac{2\pi}{3}\right) & \cos\left(\theta + \frac{2\pi}{3}\right) \\ -\sin\theta & \sin\left(\theta - \frac{2\pi}{3}\right) & -\sin\left(\theta + \frac{2\pi}{3}\right) \\ \frac{1}{2} & \frac{1}{2} & \frac{1}{2} \end{bmatrix}$$

and $\theta = \omega_s t + \theta_0$ is the synchronous rotating angle, θ_0 represents the initial value.

3.8 Control of Grid Connected Converters

Grid connected VSIs are controlled with different control strategies. These control strategies are used to perform the control of the DC-link voltage, active and reactive power injected to the grid, grid synchronization and power quality of delivered power.

3.8.1. VSI control strategies

VSI is needed to interface the DG unit to the grid and provide flexible operation. As shown in Figure 3.10, the power circuit of the VSI based DG unit is associated with the control structure, so the controlled operation of the DG unit relies on the inverter control mode. For instance, in the grid-connected mode, DG unit operates as a PQ generator and the inverter should follow the PQ control mode, while voltage and frequency regulation are not required because the grid voltage is fixed. However, in the islanded mode, the DG units are expected to meet the load demand with respect to the quality of power supply. In this case, the voltage and frequency are not fixed and the inverter should follow the (V - f) control mode taking into account the inverter power rating for sharing power issue [66].

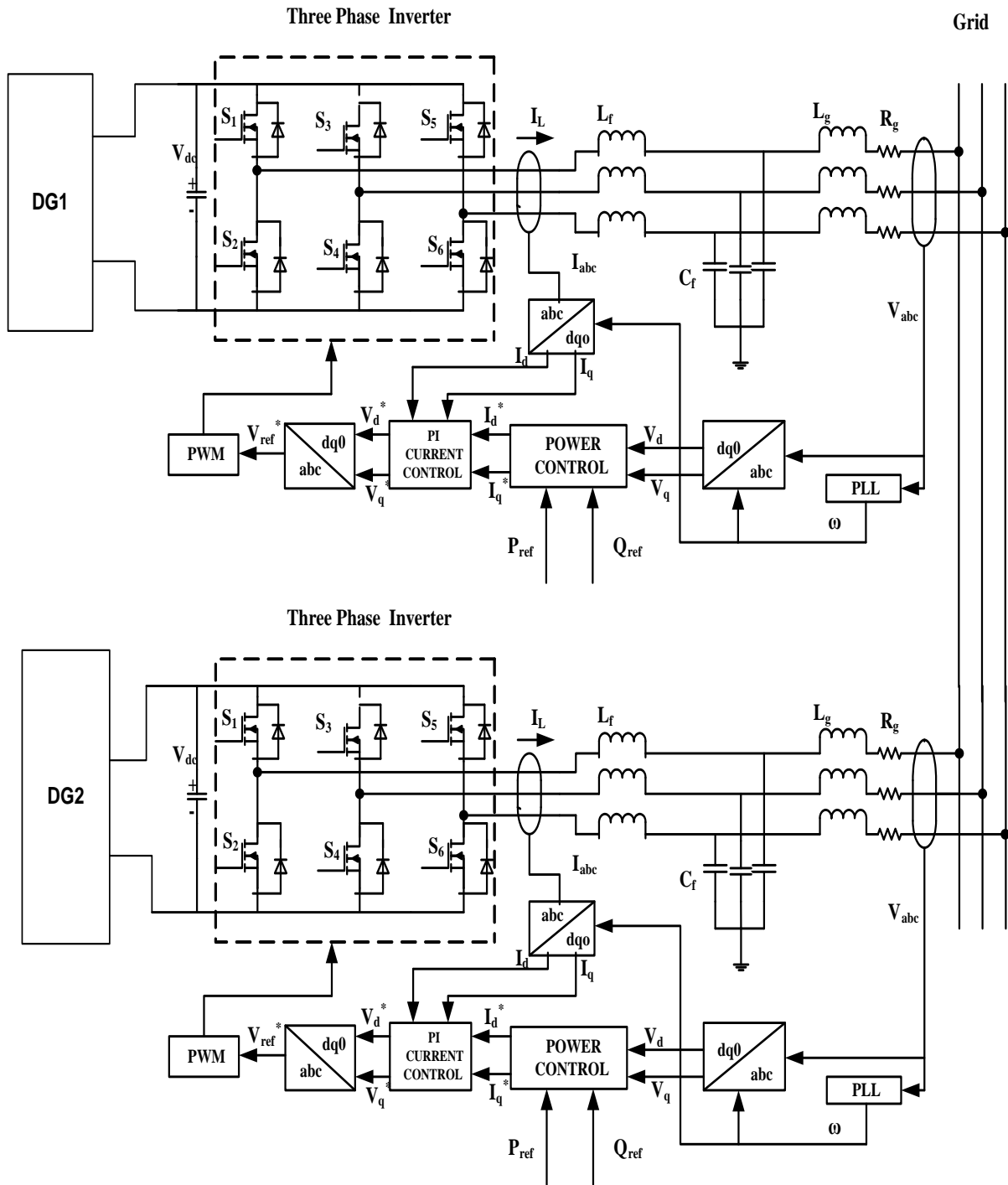


Figure 3.10 Control Structure of Grid-connected VSI

3.8.2. Active and Reactive Power (PQ) Control Strategy

The PQ controller is used in the renewable energy system, including the energy storage system, distributed generation and microgrid. When the inverter uses PQ control strategy, the power source will output stable active and reactive power irrespective of

changes of voltage, frequency and load. When microgrid works in the grid-connected mode, distribution generation can use PQ control; when microgrid operates in the islanded mode, the distribution generation should use the constant voltage and frequency control strategy to support the voltage and frequency for the microgrid [67].

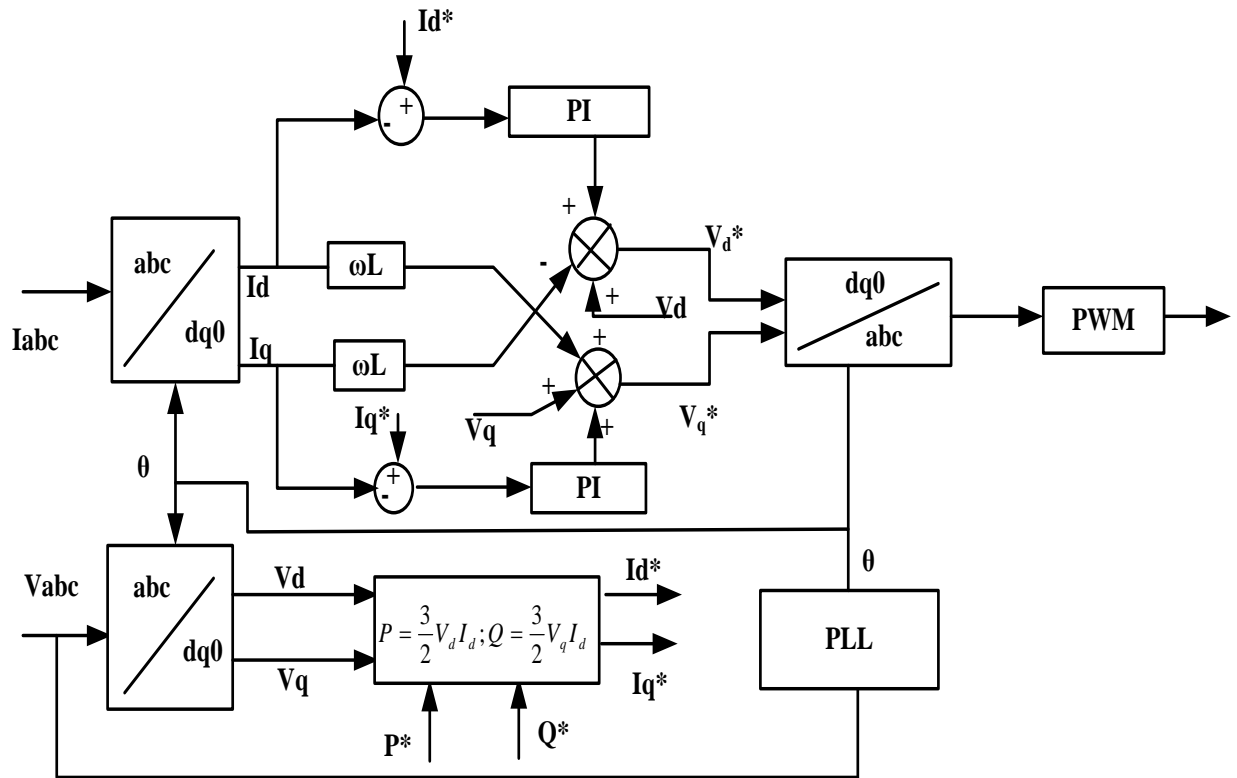


Figure 3.11 Decoupling control of active and reactive power

Here we use second order generalized integrator method to decouple frequency and amplitude control and proposes a simple and precise PQ control strategy with resistive transmission line impedance.

Details of proposed PQ control strategy are shown in Figure.3.11. PQ control output of the active and reactive power respectively as its reference value P_{ref} and Q_{ref} , usually used for grid-connection mode of microgrid[68].

The calculation of PQ is given according to Instantaneous Reactive Power Theory. The simplified measured values of the active and reactive power can be expressed as Real part represents active power (P):

$$P = \frac{3}{2} (V_d * I_d + V_q * I_q) \tag{3.26}$$

Imaginary part represents reactive power (Q):

$$Q = \frac{3}{2}(V_q * I_d - V_d * I_q) \quad (3.27)$$

Where V_d and V_q are the grid voltages in the dq transform. Furthermore, the inverter is able to deliver P and Q , which are the reference active and reactive power, respectively.

With the assumption that the d axis is perfectly aligned with the grid voltage, then $I_q = 0$, the simplified active and reactive powers are calculated as

$$P = \frac{3}{2}V_d I_d \quad (3.28)$$

$$Q = \frac{3}{2}V_q I_d \quad (3.29)$$

Referring to (3.24) and (3.25), the currents of I_d and I_q are compared with I_d^* and I_q^* and if any difference found, adjusted through the PI controller so as to maintain the system voltage (V_d) to be constant. The real power injection from the DG is controlled by the reference signal of I_d^* , whereas the reactive power is set to zero ($I_q=0$) [69-70].

The difference value between the reference current and real current will be adjusted by the PI controller and then process current feedforward compensation. Hence we get the voltage modulating signal. The signal will be modulated by the PWM and as a switch signal to the inverter.

From these parameters, the command voltages V_d and V_q for the inverter gates can be developed using:

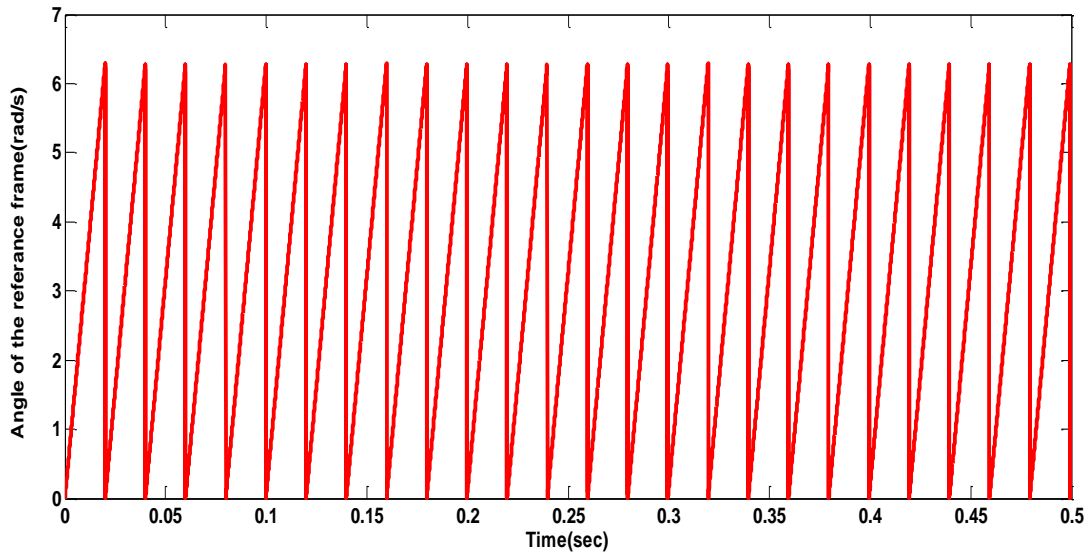
$$V_d^* = K_p(I_d^* - I_d) + K_i \int (I_d^* - I_d)dt - \omega L_f I_q + V_d \quad (3.30)$$

$$V_q^* = K_p(I_q^* - I_q) + K_i \int (I_q^* - I_q)dt - \omega L_f I_d + V_q \quad (3.31)$$

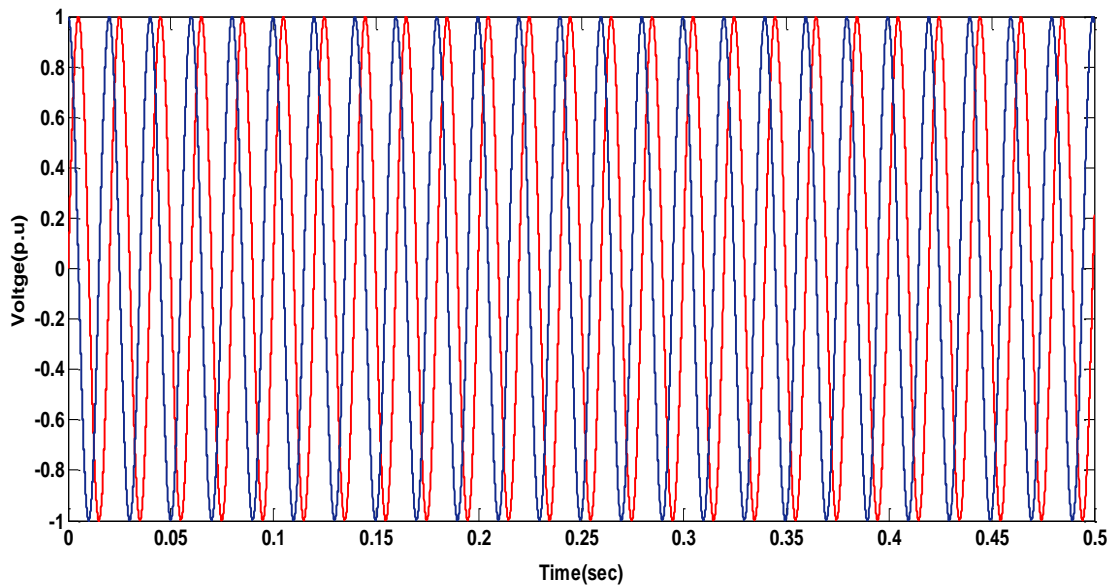
3.9 Simulation Results and discussion

The complete structure of above discussion are simulated with the simulation time $t=0.05$ sec. The simulation study conducted for balanced load condition. Figure 3.12 shows the behaviour of the SRF-PLL, simulated by using Matlab Simulink.

PLL refers the voltage of one of the phases ; the referred voltage per unit value of sine and cosine values (fig 3.12(b) and the magnitude of angular rotation (ω_t) shown in figure 3.12(a) aided by PI regulator provided inside the PLL block adjusted to get the zero angle for the referred phase.



(a)



(b)

Figure 3.12 (a) Angular frequency of reference phase
 (b) Voltage characteristics of grid and Inverter synchronized by PLL

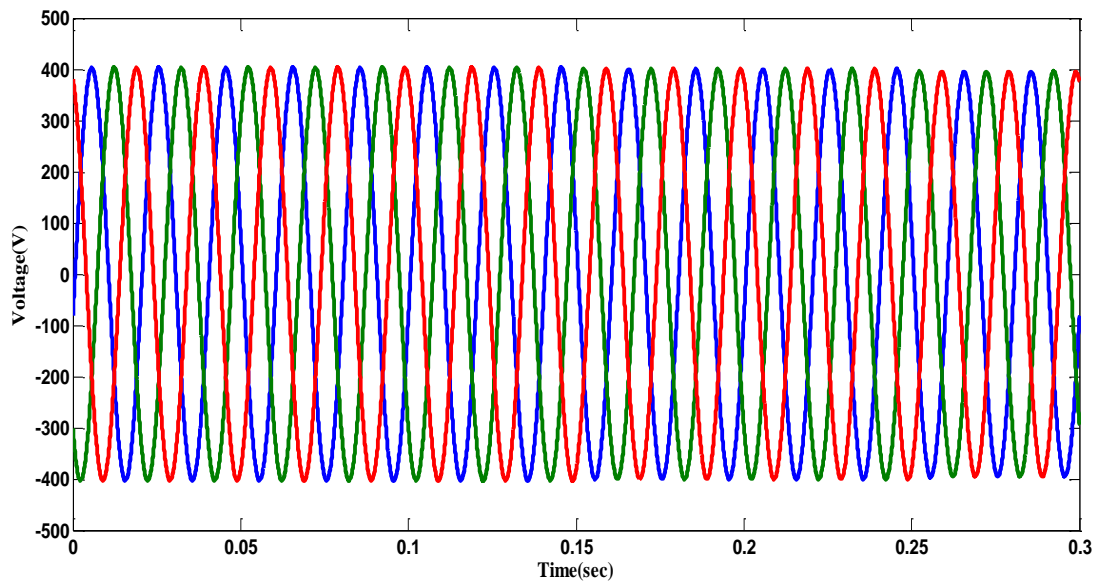


Figure 3.13 Simulated result measured at PCC point - Voltage characteristics

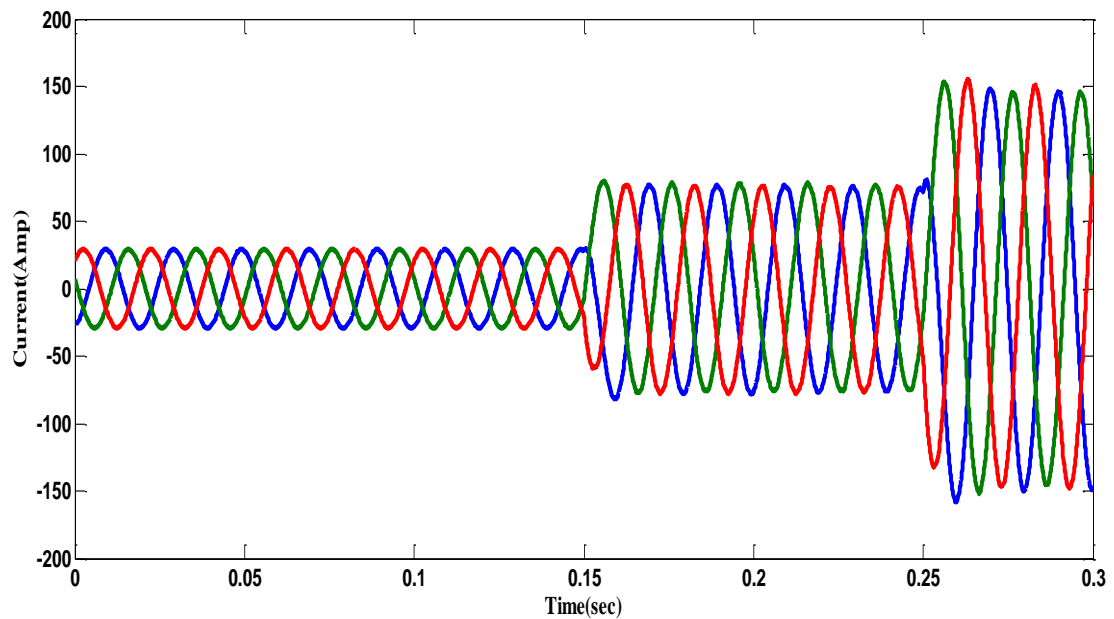


Figure 3.14 Simulated result measured at PCC point - Current characteristics

With incorporation of two DGs, the voltage and current characteristics are studied as shown in figure 3.13 – 3.14. We assumed two DG sources are of the same capacity, each of which is implemented using a separate DC power source. As depicted in figure 3.13, during the course of the entire simulation, the voltage remained in stable condition with the help of

closed loop current control systems even after the loads are changed in regular interval. In this study, the DG1 and DG2 are added to grid at $t=0.15\text{sec}$ and $t=0.25\text{ sec}$ respectively. As it shows from the figure 3.14, it is observed that there is an increase in grid current magnitude due to the injection of the DGs to the grid. The three phase current nature has maintained throughout the study with the help of decoupling current control method incorporated in the study. PWM switchings are controlled on the proper operation of current delivered to the utility grid.

Figure.3.15 shows the active power between the two DG units. The figure3.15 shows the comparative result of conventional method and SRF method. It is observed that there is an increase in the active power value while injecting DG1 and DG2 in regular interval at PCC. For power injection operation, the current control loops parameters are adjusted using PI regulator provided inside the current control loop. *abc to dq* voltage and current values are compared with the PCC current and the error values are adjusted by PI values along with loop inductance value and referred value of *dq* for the proper switching operation condition of SPWM inverter. When compared to conventional method, SRF shows the better performance, smoother and almost tracks the referred values. The nature of I_d current in the discussion is shown in figure 3.16.

Table 3.1 Parameter values for Grid- connected DG under balanced operation

Parameter	Values	Parameter	Values
Grid voltage(Vrms)	400V		
DG1-DC link voltage(Vdc)	700V	DG2-DCLink voltage	600V
DG1-Filter Inductance	4.23e-3H	DG2-Filter inductance	5.6e-3H
DG1-Filter capacitance	500 μF	DG2 Filter Capacitance	3000 μF
DG1-Active power(P)	100Kw	DG2-Active power(P)	50Kw
DG1-Proportional Gain(Kp)	0.514	DG2-Proportional Gain(Kp)	0.263
DG1-Integral Gain(Kp)	7	DG2-Integral Gain(Kp)	7.34
Switching frequency (KHz)	4 KHz	Switching frequency (KHz)	5 KHz

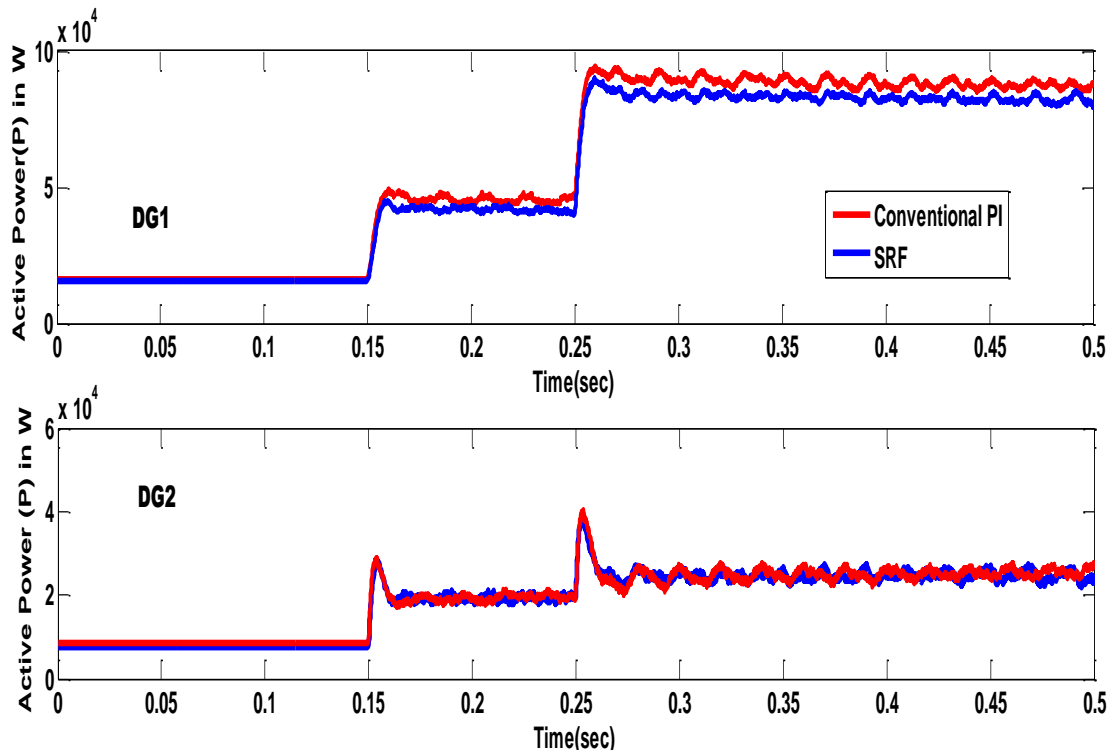


Figure 3.15 Simulated results of Active power delivered by DGs

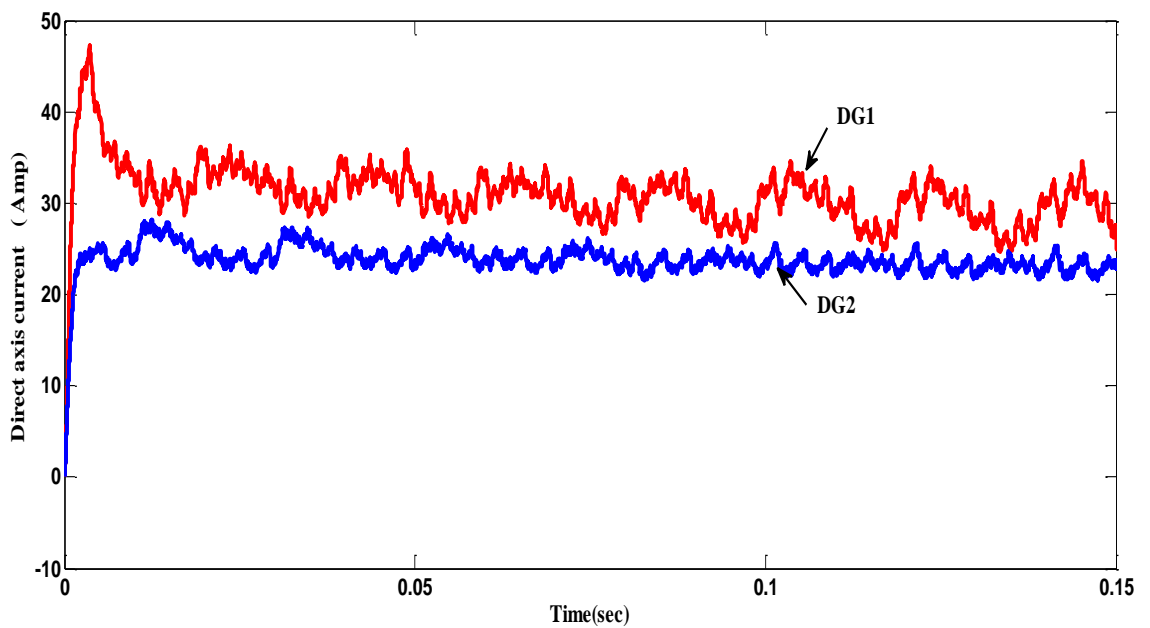


Figure 3.16 Simulated result of d- axis current delivered by DGs

3.10 Conclusion

In this chapter the overview of three phase VSIs various topologies were discussed PWM techniques which are used for inverter switching controller were discussed with necessary waveforms, LC filters and its design. Proportional- Integral (PI) Controller for grid- connected Inverter was discussed with related equations. PLL is used to get the grid frequency, voltage and phase angle information, which is used in the control system.

The SRF-PLL has been considered in this study, which exhibited the better performance under non-ideal grid. Modeling of three-phase Grid-connected VSI system with SRF system was depicted with complete control structure. The comparative simulation result of conventional method and SRF method were studied. . Output power were measured and compared with reference active and reactive power (PQ).It is observed that there is an increase in the active power value while injecting DG1 and DG2 in regular interval at PCC. When compared to conventional method, SRF shows the better performance, smoother and tracks the referred values very closely.

Chapter IV

Proposed Predictive Current Control Method for analysis under unbalanced voltage dip conditions

In this chapter, the predictive current control method under unbalanced voltage dip conditions were proposed and discussed in detail.

The use of power converters has become very popular in the last few decades for a wide range of applications, including drives, energy conversion, traction, and distributed generation. For unbalanced compensation in MGs, one solution could be controlling the loads of MG which is extremely difficult in case of residential loads. Another solution maybe is disconnecting some DG units, which is uneconomical solution. Hence, MPC with suitable control strategy has been proposed to make the MG “grid friendly”. This chapter presents a nonlinear Model-based predictive control (MPC) with continuous set for the current control of three-phase voltage-source converters. Several control schemes have been proposed for the control of power converters and the model is validated under several operating conditions.

4.1 Predictive Current control method

Predictive control presents several advantages that make it suitable for the control of power converters: the concepts are intuitive and easy to understand; it can be applied to a variety of systems; constraints and nonlinearities can be easily included; multivariable cases can be considered; and the resulting controller is easy to implement [71-72].

The main characteristic of predictive control is the use of a model of the system for predicting the future behaviour of the controlled variables. This information is used by the controller to obtain the optimal actuation, according to a predefined optimization criterion.

A classification for different predictive control methods:

- 1) Dead- Beat Control
- 2) Hysteresis Based
- 3) Trajectory Based
- 4) Model Predictive Control(MPC)
 - (a) MPC with finite set
 - (b) MPC with continuous set

In this research study, we focused on the MPC, based on continuous control set [73].

4.2 Overview of Model Predictive Control

The basic ideas present in MPC are:

- The use of a model to predict the future behaviour of the variables until a horizon in time.
- A cost function that represents the desired behaviour of the system.
- The optimal actuation is obtained by minimizing the cost function.[74]

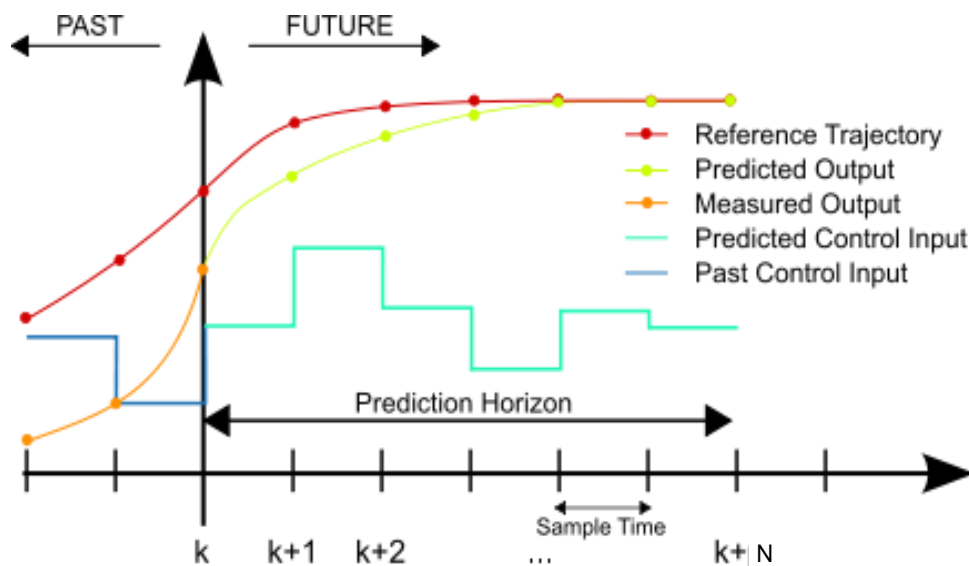


Figure 4.1 Working principle of MPC

The working principle of MPC is summarized in Figure 4.1. The future values of the states of the system are predicted until a predefined horizon in time $k + N$ using the system

model and the available information (measurements) until time k . The sequence of optimal actuations is calculated by minimizing the cost function and the first element of this sequence is applied. This whole process is repeated again for each sampling instant considering the new measured data.

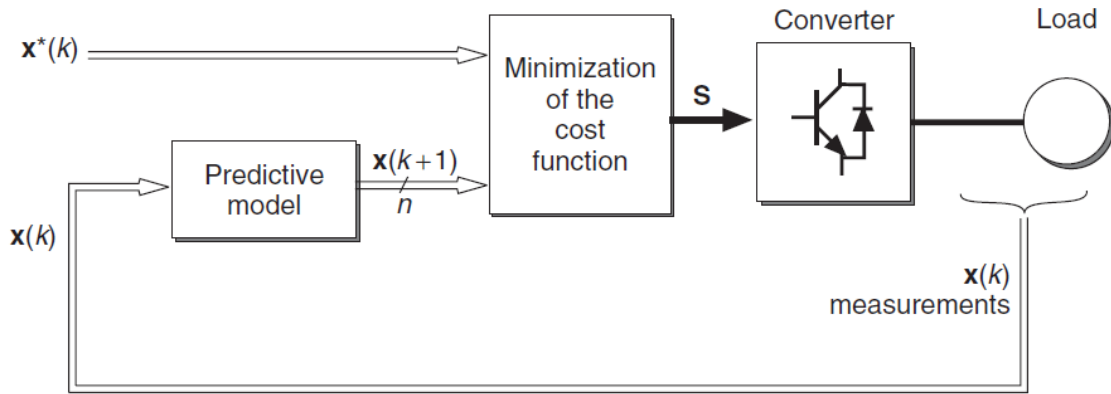


Figure 4.2 General MPC scheme

A general control scheme for MPC applied to power converters and drives is presented in Figure 4.2. The power converter can be from any topology and number of phases, while the generic load shown in the figure can represent an electrical machine, the grid, or any other active or passive load. In this scheme measured variables $\mathbf{x}(k)$ are used in the model to calculate predictions $\mathbf{x}(k + 1)$ of the controlled variables for each one of the n possible actuations, that is, switching states, voltages, or currents. Then these predictions are evaluated using a cost function which considers the reference values $x^*(k)$ and restrictions, and the optimal actuation \mathbf{S} is selected and applied in the converter.[72]-[74].

4.3 Predictive Control of a Three-Phase Inverter

The proposed predictive control strategy is based on the fact that only a number of possible switching states can be generated by a static power converter and that models of the system can be used to predict the behaviour of the variables for each switching state. For the selection of the appropriate switching state to be applied, a selection criterion must be defined. This criterion consists of a cost function that will be evaluated for the predicted values of the variables to be controlled. Prediction of the future value of these variables is

calculated for each possible switching state and then the state that minimizes the cost function is selected [74],[75].

This control strategy can be summarized in the following steps:

- Define a cost function g .
- Build a model of the converter and its possible switching states.
- Build a model of the load for prediction

A discrete-time model of the load is needed to predict the behaviour of the variables evaluated by the cost function, that is, the load currents.

The Predictive Control Algorithm is presented in Table 4.1.

Table 4.1 Predictive Control Algorithm
<ol style="list-style-type: none"> 1. The value of the reference current $\mathbf{i}^*(k)$ is obtained (from an outer control loop), and the load current $\mathbf{i}(k)$ is measured. 2. The model of the system is used to predict the value of the load current in the next sampling interval $\mathbf{i}(k + 1)$ for each of the different voltage vectors. 3. The cost function g evaluates the error between the reference and predicted currents in the next sampling interval for each voltage vector. 4. The voltage that minimizes the current error is selected and the corresponding switching state signals are generated.

4.3.1 Cost Function

The objective of the current control scheme is to minimize the error between the measured currents and the reference values. This requirement can be written in the form of a cost function. The cost function is expressed in orthogonal coordinates and measures the error between the references and the predicted currents:[75],[76].

$$g = |i_d^*(k + 1) - i_d^p(k + 1) + i_q^*(k + 1) - i_q^p(k + 1)| \quad (4.1)$$

where $i_d^p(k+1)$ and $i_q^p(k+1)$ are the real and imaginary parts of the predicted current vector $i^p(k+1)$, for a given voltage vector. This prediction is obtained using the load model. The refer currents $i_d^*(k+1)$ and $i_q^*(k+1)$ are the real and imaginary parts of the reference current vector $i^*(k+1)$. For simplicity, it is assumed that this reference current does not change sufficiently in one sampling interval, so it is considered as $i^*(k+1) = i^*k$.

The cost function selected for the control of d and q components of the load current is given as

$$g = |I_d^*(k) - I_d(k+1)| + |I_q^*(k) - I_q(k+1)| \quad (4.2)$$

A block diagram of the predictive control strategy applied to the current control for a three-phase inverter is shown in Figure 4.3

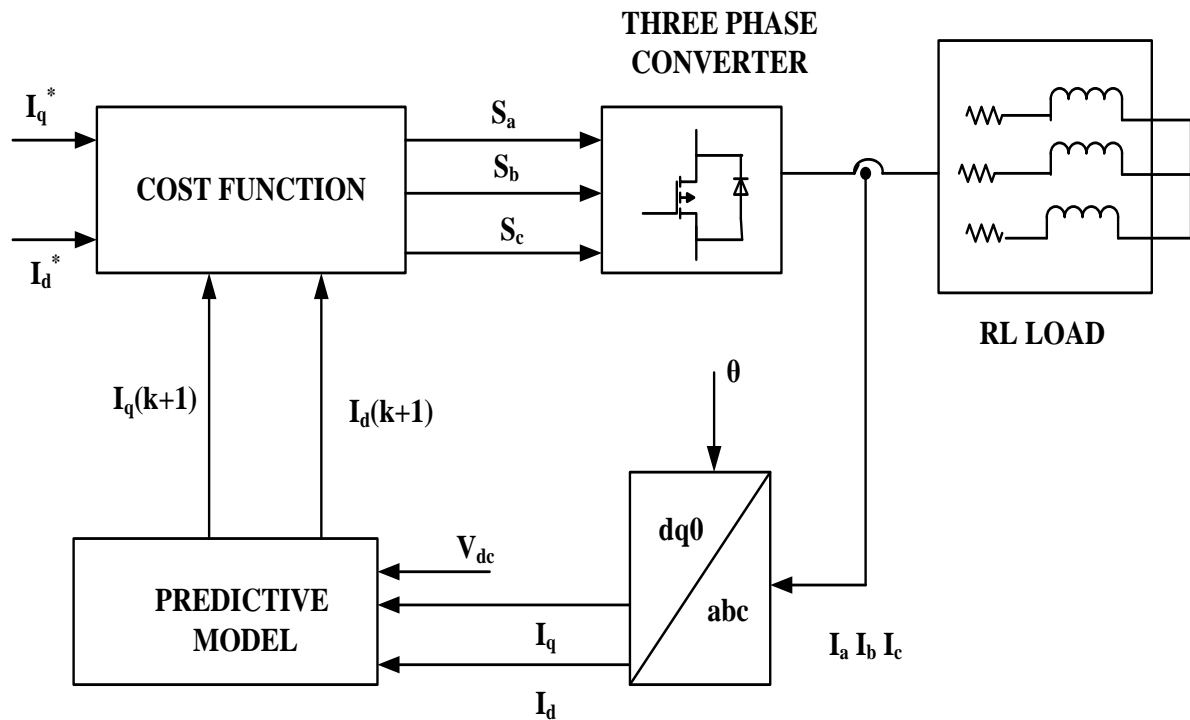


Figure 4.3 Predictive current control block diagram

4.3.2 Converter Model

The power circuit of the three-phase inverter converts electrical power from DC to AC form using the electrical scheme shown in Figure 4.4. Considering that the two switches in each inverter phase operate in a complementary mode in order to avoid short-circuiting the

DC source, the switching state of the power switches S_x , with $x = 1, \dots, 6$, can be represented by the switching signals S_a, S_b , and S_c .

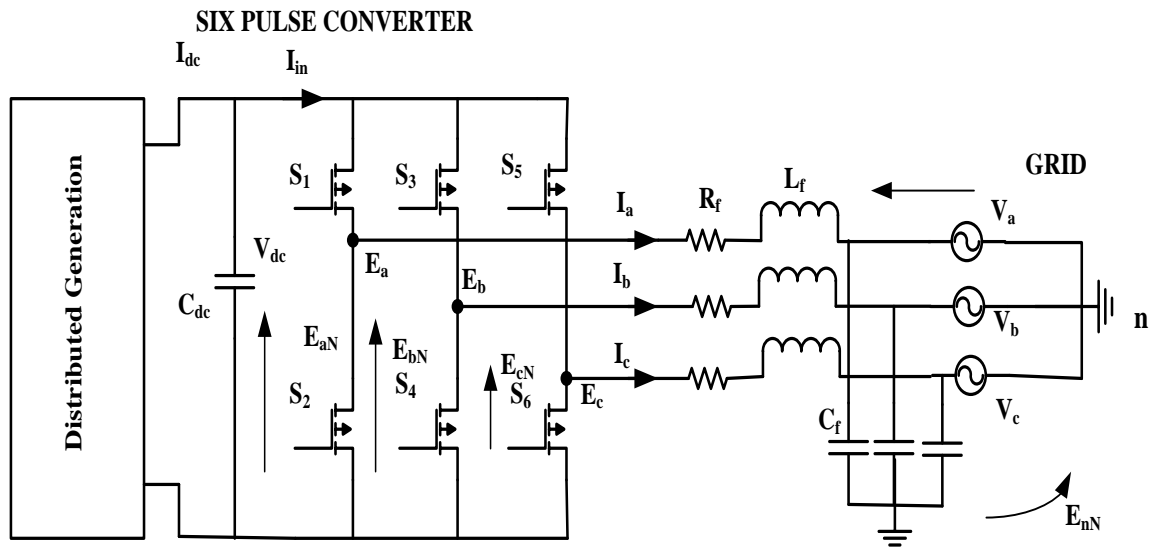


Figure 4.4 Voltage Source inverter Power circuit

The switches have been selected for a clear analysis of a predictive control strategy with RL-Load. It is a three leg inverter operated by switching S_1, S_2, S_3, S_4, S_5 and S_6 . The inverter consists of two pairs of complementary controlled switches in each leg (S_1, S_4), (S_2, S_5) and (S_3, S_6) [77]. The switching states of converter are determined by the gating signals S_a, S_b and S_c as follows:

$$S_a = \begin{cases} 1 & \text{if } S_1 \text{ on and } S_4 \text{ off} \\ 0 & \text{if } S_1 \text{ off and } S_4 \text{ on} \end{cases} \quad (4.3)$$

$$S_b = \begin{cases} 1 & \text{if } S_2 \text{ on and } S_5 \text{ off} \\ 0 & \text{if } S_2 \text{ off and } S_5 \text{ on} \end{cases} \quad (4.4)$$

$$S_c = \begin{cases} 1 & \text{if } S_3 \text{ on and } S_6 \text{ off} \\ 0 & \text{if } S_3 \text{ off and } S_6 \text{ on} \end{cases} \quad (4.5)$$

These switching signals define the value of the output voltages

$$E_{aN} = S_a V_{dc} \quad (4.6)$$

$$E_{bN} = S_b V_{dc} \quad (4.7)$$

$$E_{cN} = S_c V_{dc} \quad (4.8)$$

where V_{dc} is the DC source voltage.

Considering the unitary vector $= e^{j2\pi/3} = -\frac{1}{2} + j\sqrt{3}/2$, which represents the 120° phase displacement between the phases, the output voltage vector can be defined as

$$V = \frac{2}{3}(E_{aN} + aE_{bN} + a^2E_{cN}) \quad (4.9)$$

where E_{aN} , E_{bN} , and E_{cN} are the phase-to-neutral (N) voltages of the inverter.

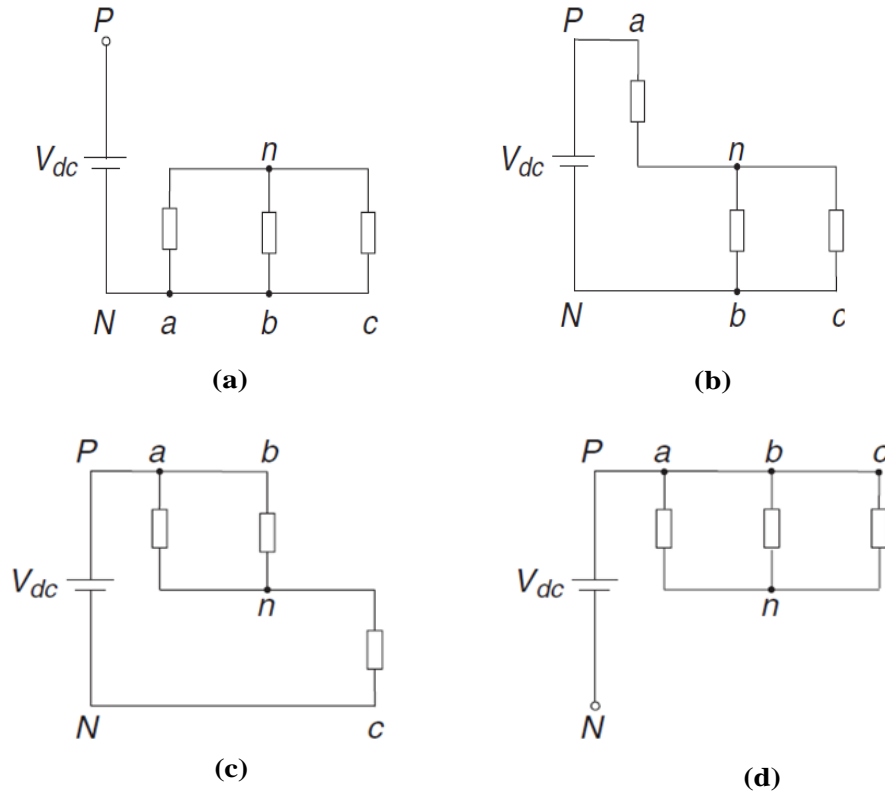


Figure 4.5 Equivalent load configurations for different switching states.

(a) Switching state (0, 0, 0) (Voltage vector V_0) where $E_{aN} = 0$, $E_{bN} = 0$, and $E_{cN} = 0$	(c) Switching state (1, 1, 0) (Voltage vector V_2) where $E_{aN} = 1/3V_{dc}$; $E_{bN} = 1/3V_{dc}$; $E_{cN} = -2/3V_{dc}$
(b) Switching state (1, 0, 0) (Voltage vector V_1) where $E_{aN} = 2/3V_{dc}$; $E_{bN} = -1/3V_{dc}$; $E_{cN} = -1/3V_{dc}$	(d) Switching state (1, 1, 1) (Voltage vector V_7) where $E_{aN} = 0$, $E_{bN} = 0$, and $E_{cN} = 0$

In this way, switching state $(S_a, S_b, S_c) = (0, 0, 0)$ generates voltage vector V_0

$$V_0 = \frac{2}{3}(0 + a0 + a^20) = 0 \quad (4.10)$$

and corresponds to the circuit as shown in figure 4.5(a)

Switching state (1, 0, 0) generates voltage vector V_1 defined as

$$V_1 = \frac{2}{3}(V_{dc} + a0 + a^20) = \frac{2}{3}V_{dc} \quad (4.11)$$

Voltage vector V_2 is generated by switching state (1, 1, 0) and is defined as

$$\begin{aligned} V_2 &= \frac{2}{3}(V_{dc} + aV_{dc} + a^20) \\ &= \frac{2}{3}\left(V_{dc} + \left(-\frac{1}{2} + j\frac{\sqrt{3}}{2}\right)V_{dc}\right) = \frac{V_{dc}}{3} + j\frac{\sqrt{3}}{3}V_{dc} \end{aligned} \quad (4.12)$$

and corresponds to the circuit shown in Figure 4.5(b).

Switching state (1, 1, 1) generates voltage vector V_7 that is calculated as

$$V_7 = \frac{2}{3}(V_{dc} + aV_{dc} + a^2V_{dc}) = \frac{2}{3}(1 + a + a^2) = 0 \quad (4.13)$$

Considering all the possible combinations of the gating signals S_a , S_b , and S_c , eight switching states and consequently eight voltage vectors are obtained, as shown in Table 4.2. In Figure 4.4 However, that $V_0 = V_7$, resulting in only seven different voltage vectors in the complex plane.[78]

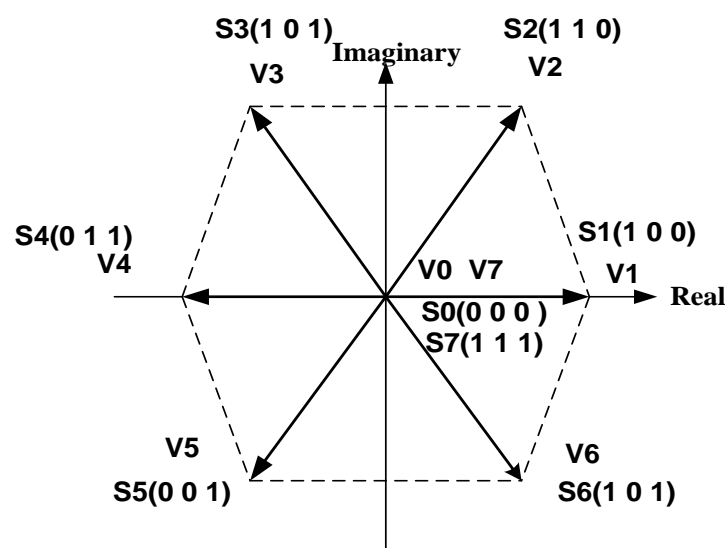


Figure 4.6 Voltage vectors in complex plane

Table 4.2 Switching states and voltage vectors

X	S_a	S_b	S_c	Voltage vector V
1	0	0	0	$V_0 = 0$
2	1	0	0	$V_1 = \frac{2}{3}V_{dc}$
3	1	1	0	$V_2 = \frac{1}{3}V_{dc} + j\frac{\sqrt{3}}{3}V_{dc}$
4	0	1	0	$V_3 = -\frac{1}{3}V_{dc} + j\frac{\sqrt{3}}{3}V_{dc}$
5	0	1	1	$V_4 = -\frac{2}{3}V_{dc}$
6	0	0	1	$V_5 = -\frac{1}{3}V_{dc} - j\frac{\sqrt{3}}{3}V_{dc}$
7	0	1	1	$V_6 = \frac{1}{3}V_{dc} - j\frac{\sqrt{3}}{3}V_{dc}$
8	1	1	1	$V_7 = 0$

Taking into account modulation techniques, like PWM, the inverter can be approximated as a linear system. Nevertheless, throughout this study the inverter will be considered as a non-linear discrete system with only seven different states as possible outputs.

4.3.3 Load Model

Taking into account the definitions of variables from the circuit shown in Figure 4.4, the equations for load current dynamics for each phase can be written as

$$E_{aN} = L \frac{di_a}{dt} + Ri_a + V_a + E_{nN} \quad (4.14)$$

$$E_{bN} = L \frac{di_b}{dt} + Ri_b + V_b + E_{nN} \quad (4.15)$$

$$E_{cN} = L \frac{di_c}{dt} + Ri_c + V_c + E_{nN} \quad (4.16)$$

where R_f is the load resistance and L_f the load inductance.

By substituting in eq. (4.9) a vector equation for the load current dynamics can be obtained

$$V = L_f \frac{d}{dt} \left(\frac{2}{3} (i_a + ai_b + a^2 i_c) \right) + R_f \left(\frac{2}{3} (i_a + ai_b + a^2 i_c) \right) + \frac{2}{3} (V_a + aV_b + a^2 V_c) + \frac{2}{3} (E_{nN} + aE_{nN} + a^2 E_{nN}) \quad (4.17)$$

Considering the space vector definition for the inverter voltage given by (4.9), and the following definitions for load current and space vectors,

$$i = \frac{2}{3} (i_a + ai_b + a^2 i_c) \quad (4.18)$$

$$V_L = \frac{2}{3} (V_a + aV_b + a^2 V_c) \quad (4.19)$$

and assuming the last term of eq. (4.17) equal to zero

$$\frac{2}{3} (E_{nN} + aE_{nN} + a^2 E_{nN}) = E_{nN} \frac{2}{3} (1 + a + a^2) = 0 \quad (4.20)$$

then the load current dynamics can be described by the vector differential equation

$$V = R_f i + L_f \frac{di}{dt} + V_L \quad (4.21)$$

where V is the voltage vector generated by the inverter, i is the load current vector, and V_L the load vector [79-80].

4.4 Discrete-Time Model for Prediction

The detailed discussion of discretization process of the load current equation (4.21) is presented for a sampling time T_s . The discrete-time model will be used to predict the future value of load current from voltages and measured currents at the k^{th} sampling instant. Several discretization methods can be used in order to obtain a discrete-time model suitable for the calculation of predictions. Considering that the load can be modeled as a first order system, the discrete-time model can be obtained by a simple approximation of the derivative. However, for more complex systems this approximation may introduce errors into the model and a more accurate discretization method is required.[81]

The load current derivative di/dt is replaced by a forward Euler approximation as

$$\frac{di}{dt} \approx \frac{i(k+1) - i(k)}{T_s} \quad (4.22)$$

By substituting in (4.21) to obtain an expression that allows prediction of the future load current at time $k+1$, for each one of the seven values of voltage vector $\mathbf{V}(k)$ generated by the inverter[82]. This expression is

$$i^p(k+1) = \left(1 - \frac{R_f T_s}{L_f}\right) i(k) + \frac{T_s}{L_f} (V(k) - V_L^*(k)) \quad (4.23)$$

where $V_L^*(k)$ denotes the estimated load vector. p denotes the predicted variables. The vector load can be calculated from (4.21) considering measurements of the load voltage and current with the following expression;[83-85]

$$V_L^*(k-1) = V(k-1) - \frac{L}{T_s} i(k) - \left(R - \frac{L}{T_s}\right) i(k-1) \quad (4.24)$$

4.5 Principle of MPC controller

Load currents i_d , i_q , and their references are shown for a complete period of the reference. Using the measurement $\mathbf{i}(k)$ and all switching states of the voltage vector $\mathbf{v}(k)$, the future currents $\mathbf{i}(k+1)$ are estimated, $\mathbf{i}_p(k+1)$. The complete overall structure of MPC scheme is shown in Figure 4.7 illustrates the cost function as a measure of error or distance between reference and predicted vectors [89-90]. It is easy to view these errors and distances for the case of current control, but these plots become difficult or impossible to build for more complex cost functions. Current $i_d^p(V_{0,7})$ corresponds to the predicted current if the voltage vector \mathbf{V}_0 or \mathbf{V}_7 is applied at time k . It can be seen in this figure that vectors \mathbf{V}_2 and \mathbf{V}_6 are the ones that minimize the error in the i_d current, and vectors \mathbf{V}_2 and \mathbf{V}_3 are the ones that minimize the error in the i_β current, so the voltage vector that minimizes the cost function g is \mathbf{V}_2 .

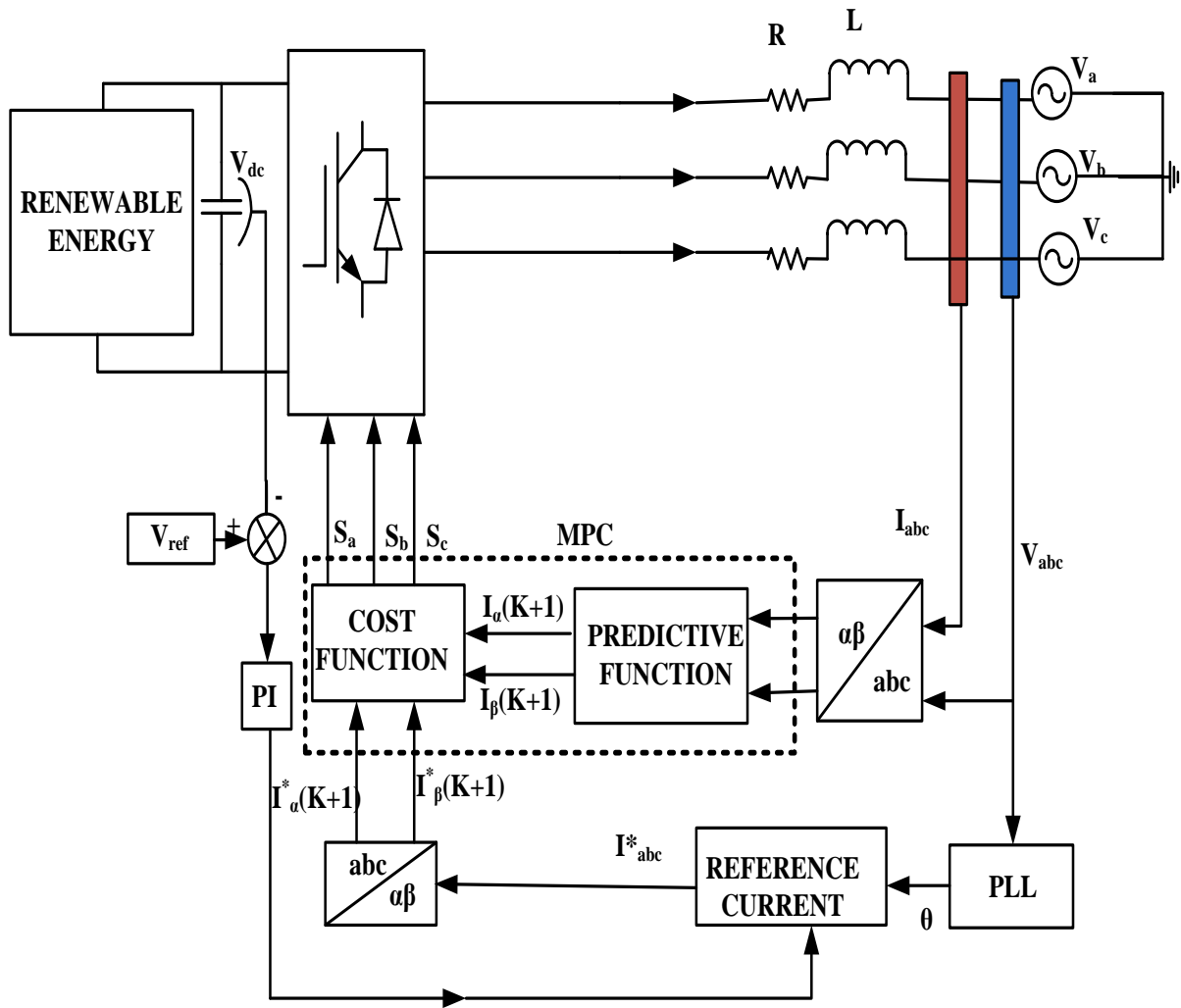


Figure 4.7 Structure of the proposed control scheme with a disturbance observer

A flow diagram of the different tasks performed by the predictive controller is shown in Figure 4.8. Here, the outer loop is executed every sampling time, and the inner loop is executed for each possible state, obtaining the optimal switching state to be applied during the next sampling period. The control results of proposed predictive control can be obtained from evaluation of the cost function by using a flowchart of the optimization process.[85-88]

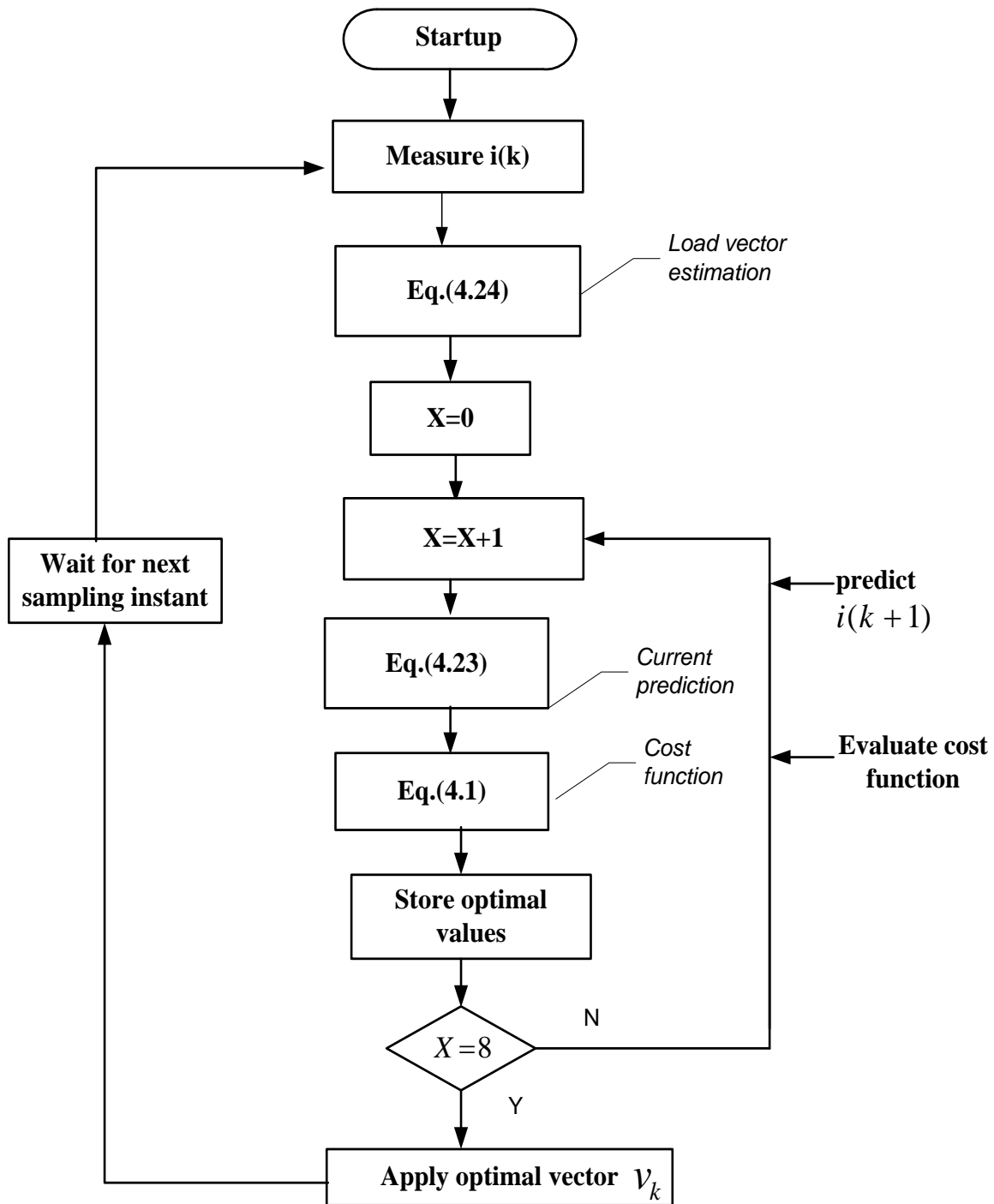


Figure 4.8 Predictive control algorithm flow diagram

4.6 Matlab Code

The predictive current control strategy is implemented for simulation in MATLAB, containing the following code:

```
function [g_opt, Sa, Sb, Sc] = MC_control(I_ref,I_meas)

%Variables defined in the parameters file

%Sampling time for the predictive control algorithm [s]
Ts = 50e-6;
% Load parameters
R = 25; %Resistance [ohm]
L = 25e-3; %Inductance [H]
e = 550; % amplitude [V]
f_e = 50 * (2*pi) ;% frequency [rad/s]
Vdc = 600; %DC-link voltage [V]

% %Current reference
i_ref = 10;
w_ref = 2*pi*50;

%Voltage vectors
v0 = 0;
v1 = 2/3 *Vdc;
v2 = (1/3) * Vdc + 1j*(sqrt(3)/3)* Vdc;
v3 = -(1/3) * Vdc + 1j*(sqrt(3)/3) * Vdc;
v4 = -(2/3) * Vdc;
v5 = -(1/3) * Vdc - 1j*(sqrt(3)/3) *Vdc;
v6 = (1/3) * Vdc - 1j*(sqrt(3)/3) *Vdc;
v7 = 0;
v = [v0 v1 v2 v3 v4 v5 v6 v7];

%Switching states
states=[0 0 0; 1 0 0; 1 1 0; 0 1 0; 0 1 1; 0 0 1; 1 0 1; 1 1 1];

% Optimum vector and measured current at instant k-1
persistentx_oldi_old
% Initialize values
```

```

if isempty(x_old), x_old = 1; end
if isempty(i_old), i_old = 0 + 1j*0; end
g_opt = 1e10;
% Read current reference inputs at sampling instant k
ik_ref = I_ref(1) + 1j*I_ref(2);

% Read current measurements at sampling instant k
ik = I_meas(1) + 1j*I_meas(2);

% Back-emf estimate
e = v(x_old) - L/Ts*ik - (R - L/Ts)*i_old;
% Store the measured current for the next iteration
i_old = ik;
% Initialize x_opt
x_opt = 0;

for i = 1:8
% i-th voltage vector for current prediction
    v_o1 = v(i);
% Current prediction at instant k+1
    ik1 = (1 - R*T_s/L)*ik + T_s/L*(v_o1 - e);
% Cost function
    g = abs(real(ik_ref - ik1)) + abs(imag(ik_ref - ik1));
% Selection of the optimal value
    if (g < g_opt)
        g_opt = g;
        x_opt = i;
    end
end
% Store the present value of x_opt
x_old = x_opt;

% Output switching states
    Sa = states(x_opt, 1);
    Sb = states(x_opt, 2);
    Sc = states(x_opt, 3);

```


4.7 Results and Discussion

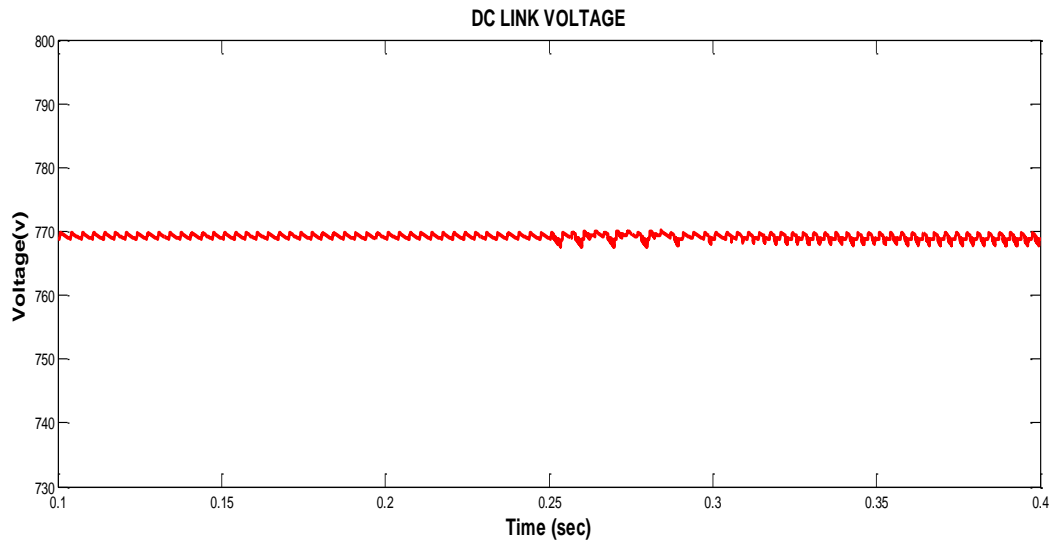
In order to verify the performance of the proposed predictive current control method on a voltage source inverter, simulation studies were conducted in the Matlab/Simulink software tool under unbalance voltage dip condition. This simulation model consists of PV panels connected with high value of capacitor. Inverter is used to convert DC supply in to AC supply which is connected to LC filter. All these components are connected to PCC with proper control loops, like voltage and current control loops respectively to control the active and reactive power in the utility grid.

The simulation study is carried out for sample of signal duration $50\mu s$ at unbalanced voltage dip conditions. In this study, proposed Predictive Current Control method has been implemented for control of VSI. The system parameters used in the simulation is listed in Table 4.3.

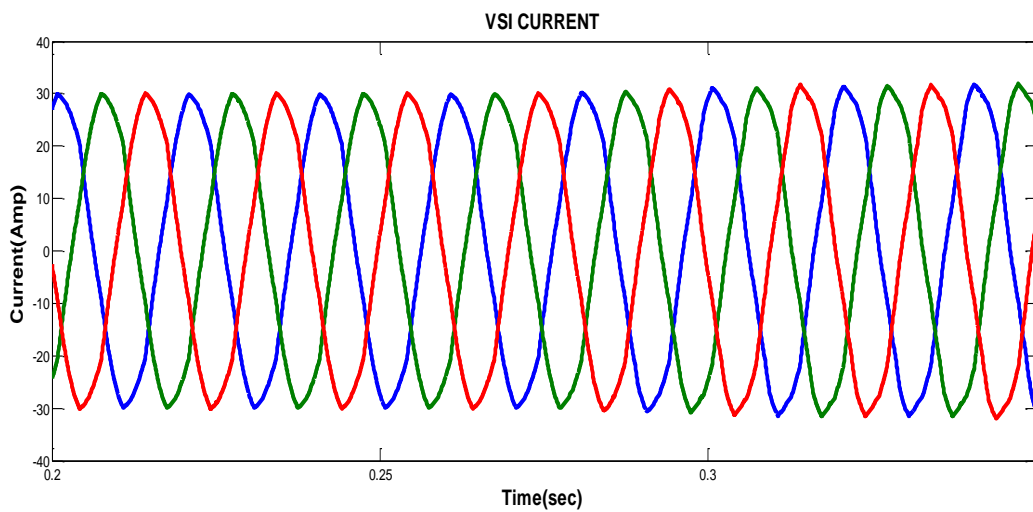
Table 4.3 System Parameters for MPC control DGs

Parameters	Variables	Values
Grid voltage (Line to line)	V_{abc}	$400V_{rms}$
DC link voltage	V_{dc}	$850V$
Supply frequency	f	$50Hz$
Sampling period	T_s	$50\mu s$
Grid side inductor	L	$9mH$
PV Module Detail	V_{MM}	$55V$
	I_{MM}	$7.35A$
	P_{MM}	$400W$
	N_s	12
	N_p	70
Load Detail	P_L	$10KW$
	Q_L	$0.5KW$
PI Parameters	k_p	0.0265
	k_i	0.524
Switching Frequency	f_s	$10Kz$

The DG connected with very high value parallel capacitors produce DC voltage so as to maintain the reliable input voltage to VSI. Figs.4.9(a) shows the level of voltage connected to the input side of VSI and the instantaneous current flows through the inverter are measured before the occurrence of the unbalance in the system voltage as shown in Fig. 4.9(b).



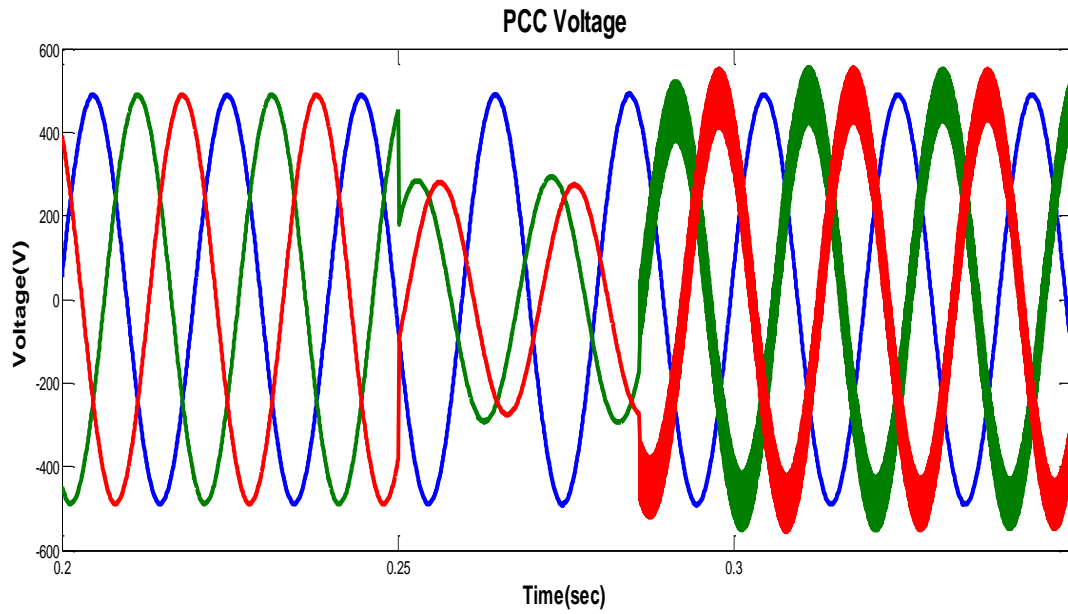
(a)



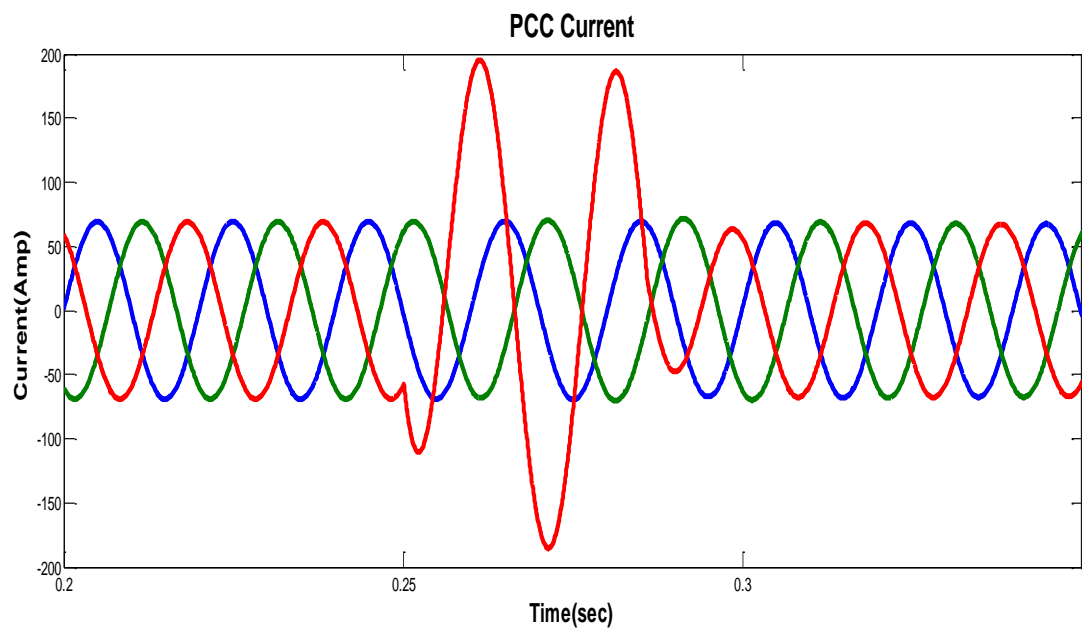
(b)

Figure 4.9 Simulation results of Three-phase Grid connected inverter.

(a) DC link voltage measured across the capacitor, **(b)** Inverter current waveform



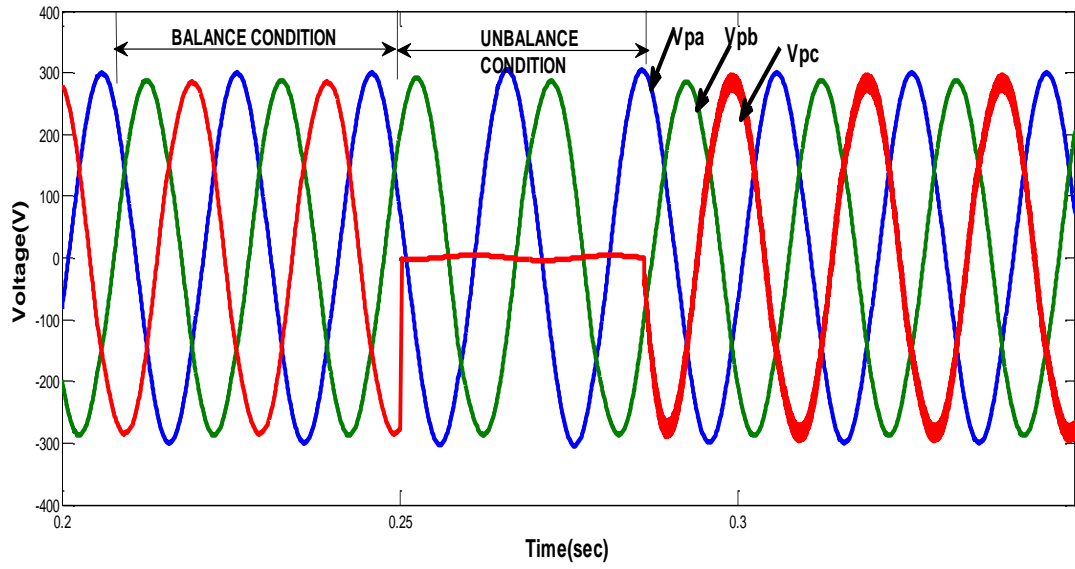
(a)



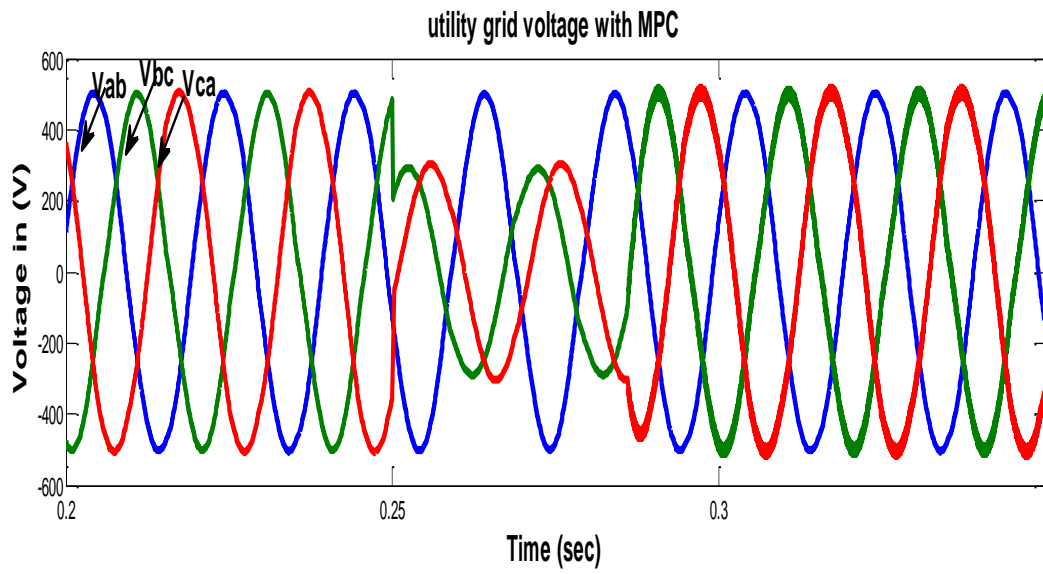
(b)

Figure 4.10 Simulation results of implementation of SRF

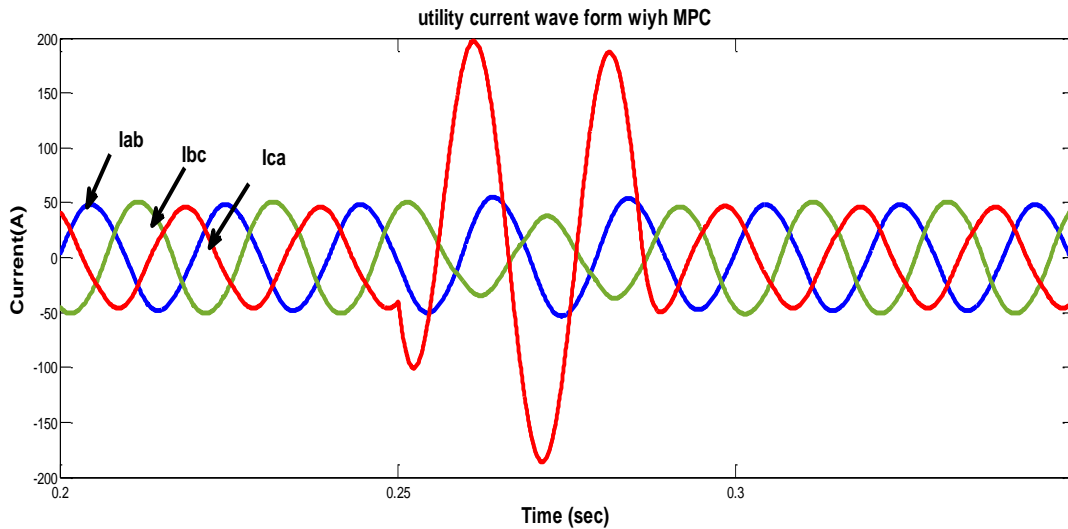
(a) Voltage wave form during voltage dip (b) corresponding current wave form during dip



(a)



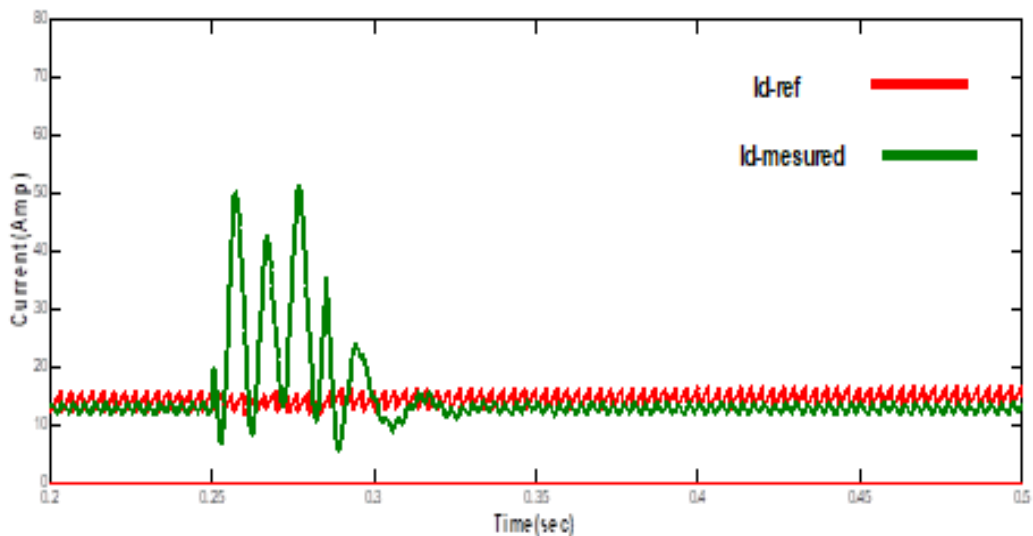
(b)



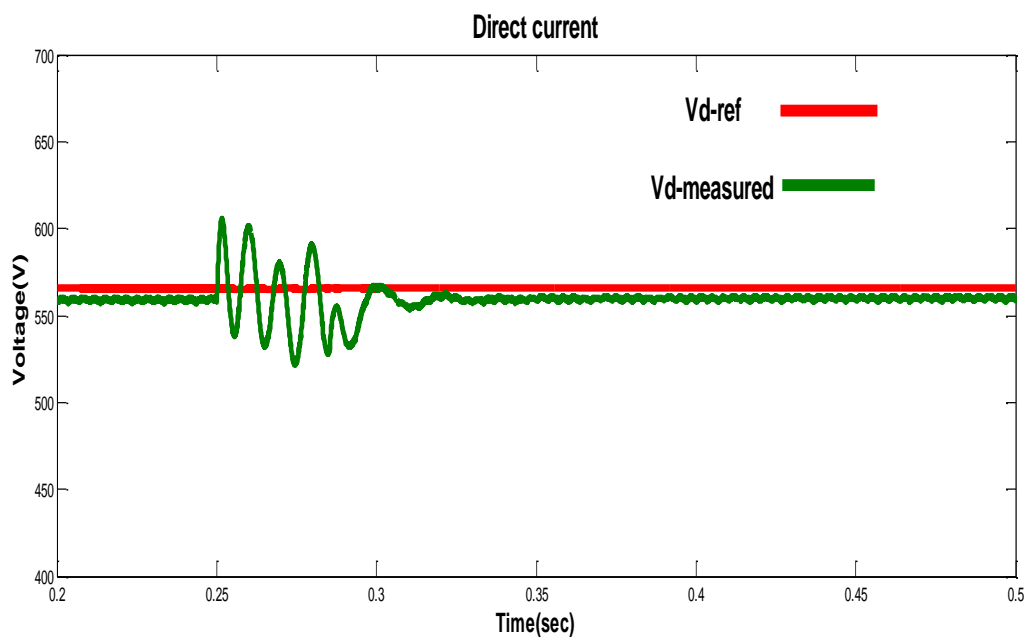
(c)

Figure.4.11. Simulation results of Three- phase Grid connected inverter with MPC
 (a) Phase voltage waveform, (b) Line voltage waveform, (c) Line current waveform

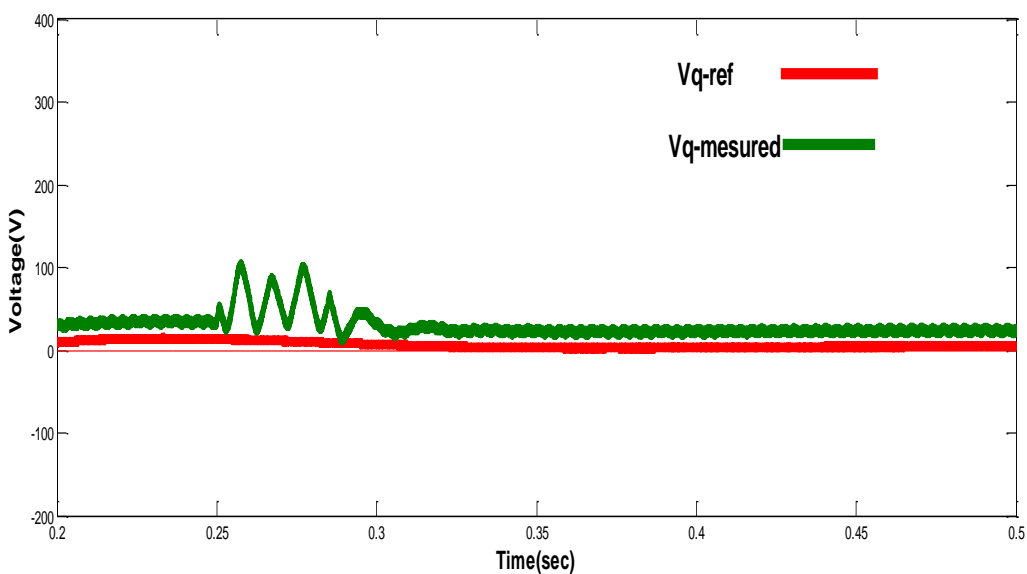
PI controller is implemented for the grid to synchronise VSI and the results observed as shown in Figs.4.10.(a-b). As is shown, the abnormality is injected in the system and it is studied for the time interval 0.2s to 0.3s. It is observed that the system voltage becomes unbalanced and sags from its magnitude in the subsequent other two phases. After the distortion, the voltage level decreases to 180V, however the normal voltage is 400Vrms. The three phase current becomes transient in nature and subsequently the magnitude of grid current increases from 30A to 200A.



(a)



(b)



(c)

Figure 4.12 Variations in the parameters of d and q values during the occurrence of disturbance in the system(a) Direct current,(b) Direct voltage,(c) Quadrature voltage

The simulation results of MPC is shown in Fig.4.11. The Simulink model is presented as shown in figure 5.13. The inverter operated at rated power, and the reference current of each phase set as 30A. As is shown in Fig.4.11c, the amplitude of reference currents and the output currents are altered so as to get the better comparison of dynamic performance of

MPC and PI. From the Fig.4.10b and Fig.4.11c, the significant differences among the two methods could be observed. The simulation results of Figs.4.12.(a-c) show the variations in the parameters of d and q values during the occurrence of disturbance in the system. As it shows, the tracking time of MPC is very short, which is much shorter than that of PI controller. Moreover, overshoot of MPC is much smaller than overshoot of PI. The current tracking error of MPC is 2.02A, which is almost one-sixth of the reference current. Compared with PI control, output current of MPC is obviously smoother. Output currents of MPC are closer to expected currents. In conclusion, the MPC strategy has smaller steady state error, less overshoot, faster response speed and provides higher quality power.

Simulation studies are performed to verify the performance of the MPC control method and its strategy. The results show that the proposed technique not only has an excellent steady-state and transient performances, and also compares the results of conventional control under unbalance voltage conditions.

4.8 Conclusion

In this chapter the Proposed Predictive Current Control Method under unbalanced and voltage dip conditions were discussed with its basic working principle. Different predictive control techniques and their merits have also been discussed. The three phase six pulse inverter is used for grid connected operation in combination with SVPWM with proper switching pulses. The proposed model was designed and validated under several operating conditions. Simulation studies were performed to verify the performance of the MPC control method and its strategy. The steady-state and transient performances were studied and the results of proposed predictive control method were compared with the results of conventional control under unbalance voltage conditions. The results of various stages of voltages and currents for MPC method shows good response under voltage unbalance and voltage dip conditions.

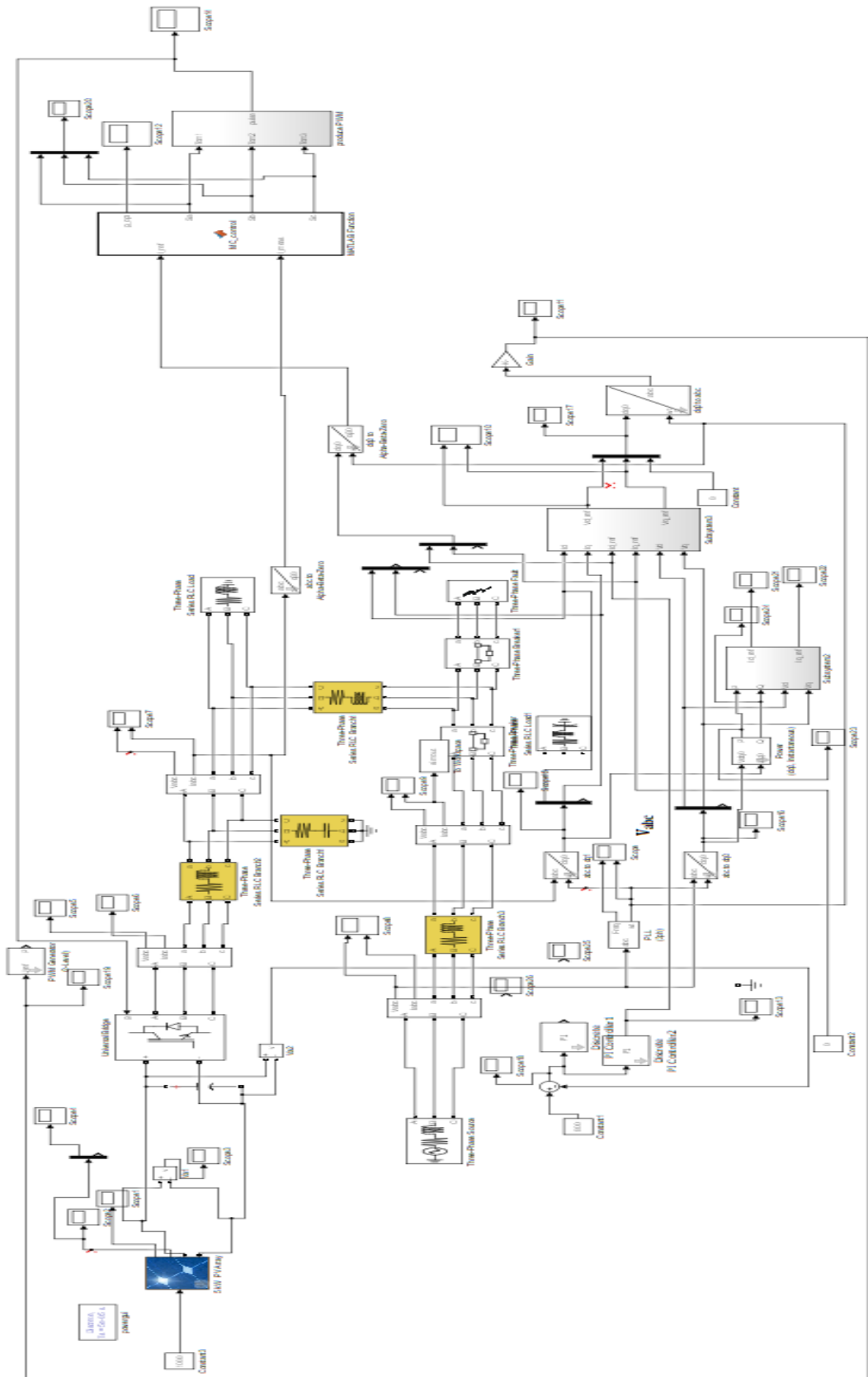


Figure 4.13 Simulink Model of proposed control scheme

Chapter V

Proposed Power system Control design for Parallel Inverters

In this chapter, the improved control strategy is proposed to maintain the grid parameters during the transition between MGs and main grid. The frequency droop controller is discussed for a smooth transfer between grid connected mode and islanded mode operations. The detailed discussion of this method is given below

5.1 Introduction

In the islanding operation of distributed AC power supply systems, DG units are usually connected through inverters to an AC distribution system. Different methods have been developed to control the parallel inverters or more specifically the power sharing among different DGs. One of the common methods for controlling inverters in the islanding mode is the droop method, which has an advantage of being a wireless control method [91]. This is an important benefit for the droop control method especially when different DGs are located far from each other and there is no possibility of building a communication link between these units [92]. One of the issues associated with conventional droop control method to control the parallel inverters is the reactive power sharing while supporting the bus voltage, which results in bus voltage drop.

During fluctuations in load capacity, the grid-connected system must be able to supply balanced power from the utility grid side and micro-grid side. Therefore, Droop control is implemented to maintain a balanced power sharing. The inverter operates in voltage control mode in order to control the filter capacitor voltage. An adjusted droop control method for equivalent load sharing of parallel connected Inverters, without any communication between individual inverters has been proposed to supply the demanded active power and support the reactive power within the converter constraints.

5.2 Various control methods of the Parallel Inverters

There are four types of control methods for power control of inverters in parallel operation as follows:[93-96]

1. Instantaneous current sharing using master/slave method.
2. The deviation from average active/reactive powers method.
3. Harmonic and reactive currents injection method.
4. Frequency and voltage Droop method.

5.2.1. Instantaneous Current Sharing Using Master/Slave Method

In order to share the identical power between parallel inverters, the instantaneous current sharing technique utilizes the load current as the feedback signal to the parallel units. In this method one of the inverters operates as the master unit which provides and stabilizes the required voltage for the load, and the other units tries to inject the same current in their output as their feedback load-current signal, these unites operate as slave controllers.

Weakness - In the case of fault occurrence in the master unit the whole system will collapse. Therefore, the requirement of a unit as the master unit is one of the major weaknesses of this method which degrades the reliability of the system. Recently, it is tried to enable the control system to replace the master unit with one of the slave unites in the case of fault in master unit to increase the reliability of the system and to keep the continuity of the power transferring. This approach will increase the complexity and the cost of the control system comparing with common master/slave method. Moreover, the physical wiring between parallel units is the other weakness of this system which also declines the system reliability.

5.2.2 The Deviation from average Active/Reactive Powers Method

This power sharing technique is designed based on the AC systems power flow theory, in which the transmission lines are considered dominantly inductive; therefore, the active power flow and reactive power flow will be a function of phase angle and voltage, respectively .in this power control method there is no need for master unit, the reliability of the system is higher than the master/slave technique. Moreover, the accurate active and

reactive power sharing between inverters in this method results in lower circulation currents between units.

Weakness - This approach affects only the fundamental component of the load current. Therefore, in the case of nonlinear loads this method would not be able to share the harmonic current between the inverters. The other weakness associated with this method is the communication link between units which deteriorates the system reliability.

5.2.3 Harmonic and Reactive Current Injection Method

The injection signal approach makes it possible to share the harmonic and reactive power between parallel inverters. In this technique two signals with the frequencies different from fundamental frequency is injected to the reference voltage, in which one of them is for controlling the disturbance power and the other helps to control the reactive power.

Weakness - the inverter output voltage quality degradation, resulting from the injected signals. Moreover, the harmonic currents sharing are in the cost of system stability reduction (reduction in bandwidth). Utilizing the high frequency signals in this approach limits its application to low power inverters, where the switching frequency is higher. In high power inverters the switching frequency is lower and subsequently the LC filters with lower cut-off frequency are used; therefore, the high frequency signals, controlling harmonic and reactive powers, may affect the output of the units.

5.2.4 Frequency and Voltage Droop Method

This technique employs the same concept as the multiple generators in power system take over the load sharing. The main idea of this method is the mimicking of the synchronous generator governor behaviour. In power systems, the synchronous generators share the change in load by the frequency drop, proportional to their governor droop characteristic. This makes it possible for synchronous generator to react to the load changing in a determined manner and utilize the system frequency as the communication link [97]. The droop technique is applicable to the parallel inverters by frequency and voltage amplitude drop at the output of the inverters proportional to active and reactive power, respectively.

Weakness - System frequency and voltage amplitude drop, Lack of the ability to share the harmonic currents, High sensitivity to the transmission lines, slow dynamic response.

The main advantage of droop control is elimination of the need for communication by use of local measurements. During lack of the communication link for control signals may result in higher reliability for the system. Moreover, the maintenance of the system is feasible without any problem for the system. Since it is assumed that the transmission of control signals between units is not possible while designing the control system, the **droop methodology** is selected as the power control system.

5.3 Concise introduction of Droop Control

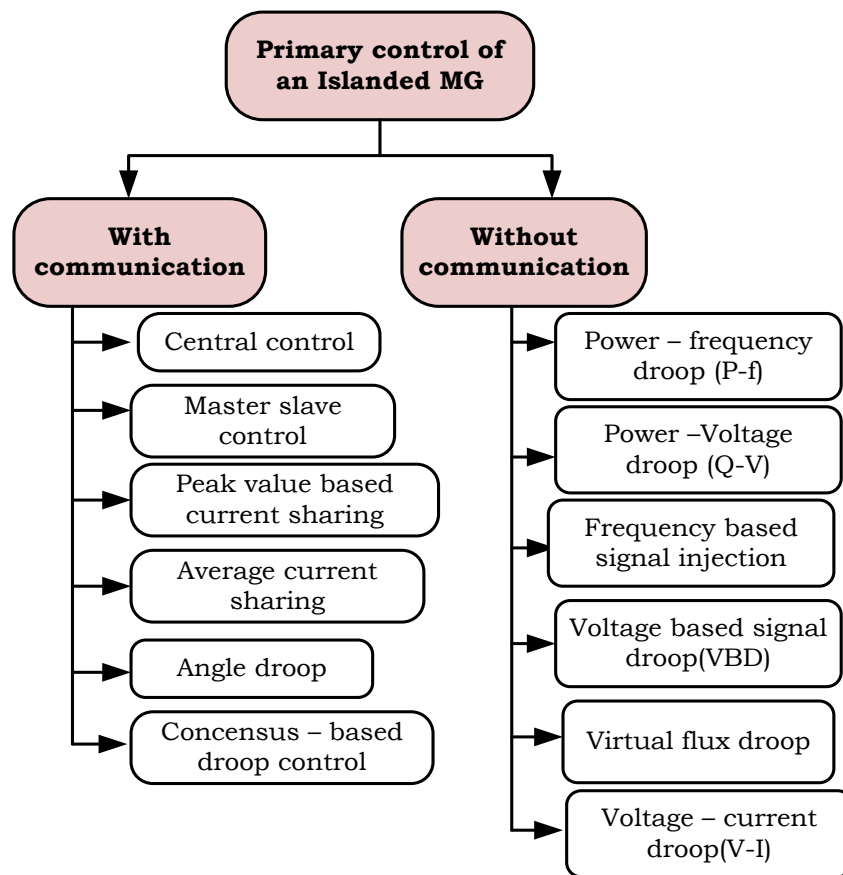


Figure 5.1 Various power control strategies for an islanded microgrid

The basic control objective in a microgrid operating in island mode is to achieve accurate power sharing while maintaining close regulation of the microgrid voltage magnitude and frequency. Numerous control methods, as shown in Figure5.1, are

developed to improve the power quality, disturbance rejection and voltage/current tracking of the inverter output. The different developed control strategies are used according to the characteristics of microgrids. The control strategies are developed from simple approaches to complex analytical methods [96]. The control methods are described below.

1. *Communication-based control (wired methods)*

These control schemes use high speed communications between inverters to achieve accurate power sharing by making one inverter take the master role of voltage control inverter (VCI) to control the frequency and voltage of the microgrid while the other inverters operate as current controlled inverters (CCI). The main disadvantages of this system are the dependence on high-speed communications which is costly and decreases the system reliability and expandability. Moreover, it does not provide seamless mode transition from grid-connected mode to island mode and vice-versa. During transition, the voltage across the load can become very low or very high [97],[101].

2. *Non-communication-based control (wireless methods) that relies on droop control.*

The name wireless comes up as this method does not need communications between the inverters. The advantage is that no external communication mechanism is needed among the inverters. However, communication can still be used between each unit and a supervisory central controller, for monitoring and management issues. This enables good sharing of linear and/or nonlinear loads. In addition, its ease of implementation, based merely on local voltage and current information, enables plug-and-play operation. Thus, it increases redundancy and simplicity of system expansion.

In the primary control level, the control approaches of DG units are expected without communication to maintain high reliability, reduce costs, avoid communication complexity, and apply plug and play features of each unit. The communication-based operations are unsuitable, especially, if DG units are placed in remote areas because of high bandwidth communication and infrastructure, which is very costly. In this case, droop based control approaches can be applied, and are able to handle different ratings of DG units with great flexibility and reliability. However, this has some drawbacks, such as power (P - Q) control coupling, voltage and frequency deviation, dependence on network impedance, and issues with non-linear loads and accuracy [94].

To overcome these problems, different control approaches are adopted in our study based on their comparative advantages.

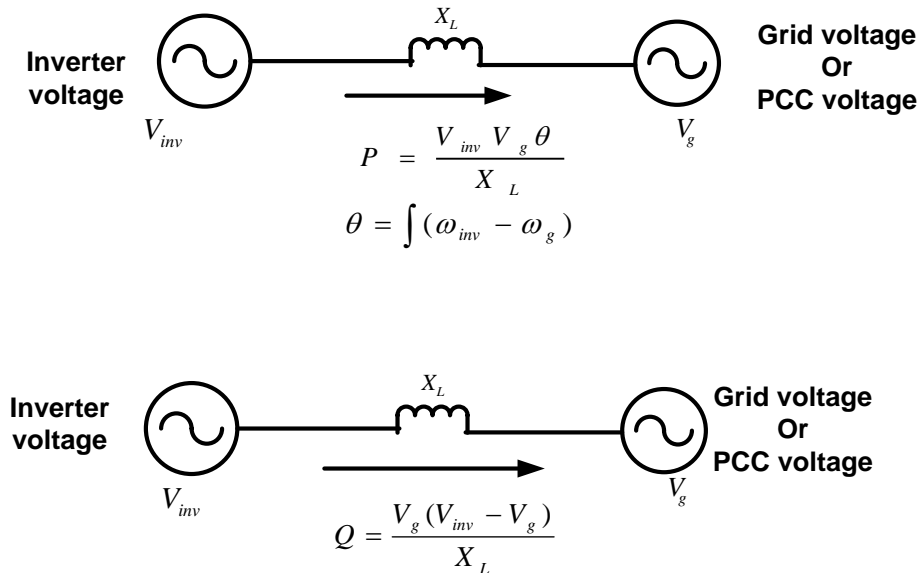


Figure 5.2 Power flow control between two voltage sources nodes

The droop control replaces the need of communication in particular in island mode. In grid-connected mode the control of power generated to the grid can be easily implemented using droop control or other controllers. However, the strength of droop control appears in island mode, when all units need to share power according to its rating without the need to communicate to other units. This supports the seamless transfer between the microgrid modes. Figure 5.2 illustrates the power system flow between two voltage sources separated by an inductor and how the active power can be controlled by the phase angle between the voltage signals of each source and the reactive power by changing the amplitude difference between these sources. In practical scenarios, the output impedance can't be purely inductive as a resistive value might affect its performance.

A grid-forming unit within a microgrid is assigned to regulate the voltage at the PCC, dominantly set the system frequency, and provide a reference to other vector controlled inverters. Its function is similar to a traditional slack bus generator and is a necessary component for operation of other vector controlled inverters. Conventionally, frequency-droop and voltage-droop control strategies without using vector control mechanism were used to share real and reactive powers among two or more DG units.

5.4 Load-sharing control of Parallel Power converters

The droop technique [98] has been widely used as a load-sharing scheme in conventional power system with multiple DGs. In this droop method, the generators share the system load by drooping the frequency of each generator with the real power (P) delivered by the generator. This allows each generator to share changes in total load in a manner determined by its frequency droop characteristic and essentially utilizes the system frequency as a communication link between the generator control systems. Similarly, a droop in the voltage amplitude with reactive power (Q) is used to ensure reactive power sharing. This load sharing technique is based on the power flow theory in an AC system, which states that the flow of the active power (P) and reactive power (Q) between two sources can be controlled by adjusting the power angle and the voltage magnitude of each system—i.e., the active power flow (P) is predominantly controlled by the power angle, while the reactive power (Q) is predominantly controlled by the voltages magnitude.

Figure.5.3 indicates critical variables for load-sharing control of paralleled power converters. It shows two inverters represented by two voltage sources connected in parallel and supplying common load through line impedance represented by pure inductances. Each inverter is connected via output impedance to the load bus. The active and reactive power that is exported from each inverter is subject to one of two forms according to the kind of output impedance. The output impedance can be dominantly inductive or resistive and this determines how the inverter would control the exported power [100].

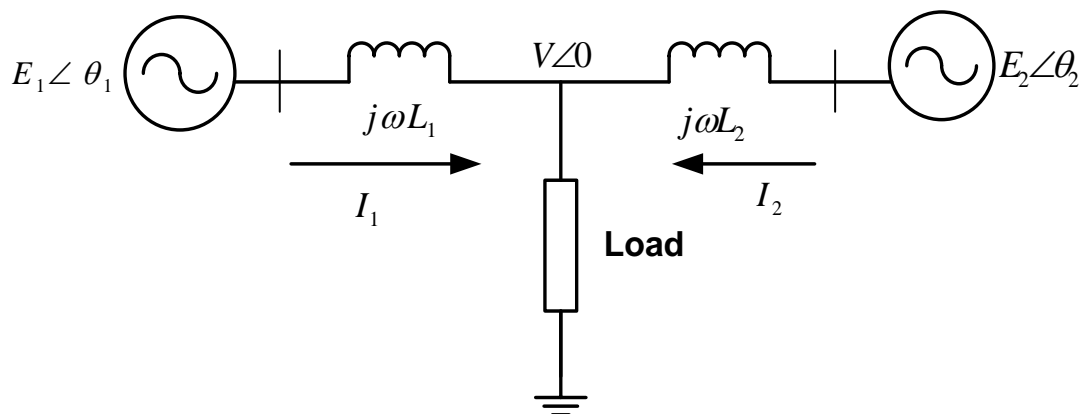


Figure 5.3 Parallel connection of two inverters to a common load

The complex power at the load due to inverter is given by

$$S_i = P_i + jQ_i = V \cdot I_i^* \quad (5.1)$$

where $i=1, 2$, and I^* is the complex conjugate of the inverter current and is given by

$$I^* = \left[\frac{E_i \cos \theta_i + jE_i \sin \theta_i - V}{j\omega L_i} \right] \quad (5.2)$$

$$S_i = V \left[\frac{E_i \cos \theta_i + jE_i \sin \theta_i - V}{j\omega L_i} \right]^* \quad (5.3)$$

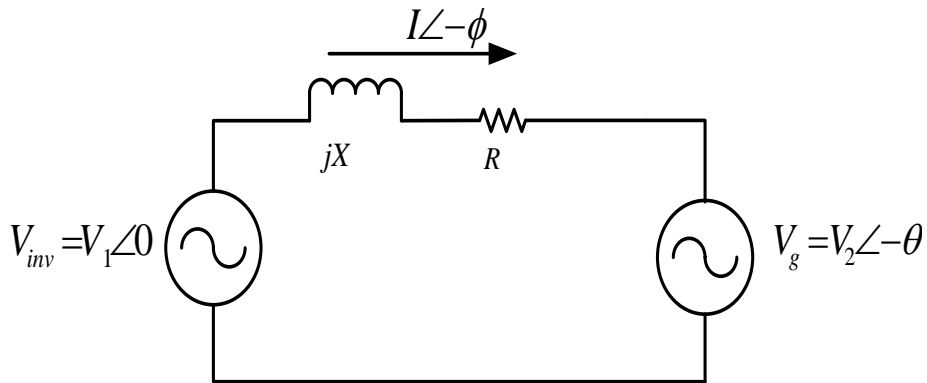
$$P_i = \frac{VE_i}{\omega L_i} \sin \theta_i \quad (5.4)$$

$$Q_i = \frac{VE_i \cos \theta_i - V^2}{\omega L_i} \quad (5.5)$$

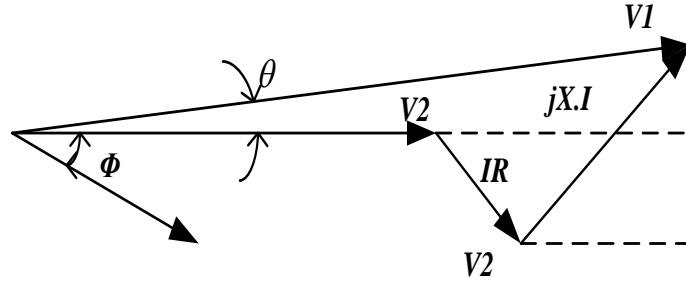
The droop regulation techniques are implemented in grid-supporting power converters to regulate the exchange of active and reactive powers with the grid, in order to keep the grid voltage frequency and amplitude under control. The main idea to support the droop control comes from mimic the self-regulation capability of the synchronous generator in grid-connection mode, decreasing the delivered active power when the grid frequency increases and decreasing the injected reactive power when the grid voltage amplitude increases.

5.4.1 Grid Impedance Influence on Droop Control

Considering the power converter as an ideal controllable voltage source that is connected to the mains through a given line impedance [102], as shown in Figure. 5.4(a) the active and reactive powers that it will deliver to the grid can be written as based on the single phase equivalent circuit of the network and the current and complex power equations (5.2 - 5.3), the phasor diagram is obtained as given in Figure 5.4(b).



(a)



(b)

Figure 5.4 Simplified model of power convector connection to a distribution network
 (a) Equivalent circuit (b) phasor diagram

Further, considered the power converter as an ideal voltage source connected to the main grid through a given line impedance, the active and reactive powers is delivered to the grid as given by

$$P_1 = \frac{V_1}{R^2 + X^2} [R(V_1 - V_2 \cos\theta) + XV_2 \sin\theta] \quad (5.6)$$

$$Q_1 = \frac{V_1}{R^2 + X^2} [-RV_2 \sin\theta + X(V_1 - V_2 \cos\theta)] \quad (5.7)$$

where P_1 and Q_1 are the active and reactive powers, respectively, flowing from the source I (power converter) to 2 (grid), V_1 and V_2 are the voltage values of these sources, θ corresponds to the phase-angle difference between the two voltages, $Z = R + jX$ is the interconnection line impedance and ϕ is the impedance angle. As $R = Z \cdot \cos(\theta)$ and $X = Z \cdot \sin(\theta)$. The performance of this simplified electrical system can be depicted by its vector representation, as shown in Figure 5.4(b).

Further, considered the power converter as an ideal voltage source connected to the main grid through a given line impedance [103], the active and reactive powers is delivered to the grid (as shown in figure 5.1) as given by

Assuming $\sin\theta \approx \theta$ and $\cos\theta \approx 1$, (5.6) and (5.7) can be rewritten as,

$$P_1 = \frac{V_1}{\omega L} (V_2 \sin\theta) \Rightarrow \theta = \frac{\omega L P_1}{V_1 V_2} \quad (5.8)$$

$$Q_1 = \frac{V_1}{\omega L}(V_1 - V_2 \cos\theta) \Rightarrow V_1 - V_2 = \frac{\omega L Q_1}{V_1} \quad (5.9)$$

The direct relationship between the power angle θ and the active power P as well as the voltage difference $V_1 - V_2$ and the reactive power Q can be observed from above equations. These relationships permit regulating the grid frequency and voltage at the point of connection of the power converter [105], by controlling the value of the active and reactive powers delivered to the grid. Hence, the droop control expressions can be given for inductive lines as

$$f = f_o + m_i(P - P^*) \quad (5.10)$$

$$V = V_o + n_i(Q - Q^*) \quad (5.11)$$

where f is grid supply frequency, f_o is nominal frequency, V is grid voltage and V_o is nominal voltage. It is noted that $(f-f_o)$ and $(V-V_o)$ represent the grid frequency and the voltage deviations, respectively from their rated values and $(P - P^*)$ and $(Q - Q^*)$ are the variations in the active and reactive powers delivered by the power converter to compensate such deviations. These relationships can be graphically represented by the droop characteristics as shown in Figure 5.5.

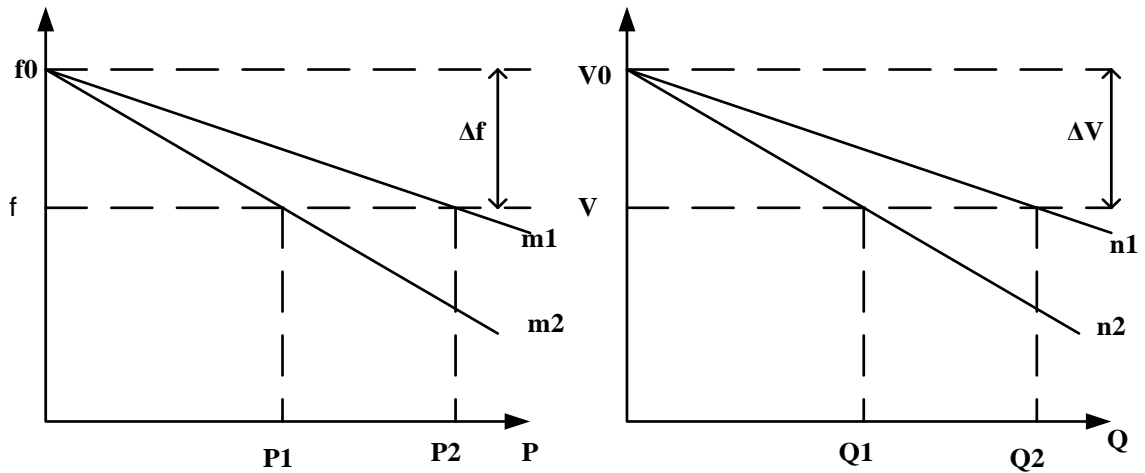


Figure 5.5 Droop characteristics of voltage and frequency

As stated in (5.10) and (5.11), the gain of the control action in each case, i.e., the slope of the frequency and voltage droop characteristic, is set by V and f parameters respectively. Therefore, as depicted in Figure 5.5, each of the grid-supporting power converters operating in the microgrid will adjust its active and reactive power references

according to its P - f and Q - V droop characteristic to contribute in the regulation of the microgrid frequency and voltage, respectively.

In droop control method the $P - f$ (Active power - Frequency) and the $Q - V$ (Reactive power - Voltage amplitude) droop characteristics for a system including several inverters are expressed as follows

$$f_i = f_o - m_i P_i \quad (5.12)$$

$$V_i = V_o - n_i Q_i \quad (5.13)$$

where f_i and V_i are the angular frequency and voltage amplitude of the i^{th} inverter respectively, and the ω_o and V_o are the nominal angular frequency and voltage amplitude. m_i and n_i are called droop coefficients.

In case of multiple inverters, the proportion of the load shared by each inverter can be adjusted by choosing the droop coefficient, depending on its apparent power rating as $m_1 \cdot S_1 = m_2 \cdot S_2 = \dots = m_n \cdot S_n$ and $n_1 \cdot S_1 = n_2 \cdot S_2 = \dots = n_n \cdot S_n$.

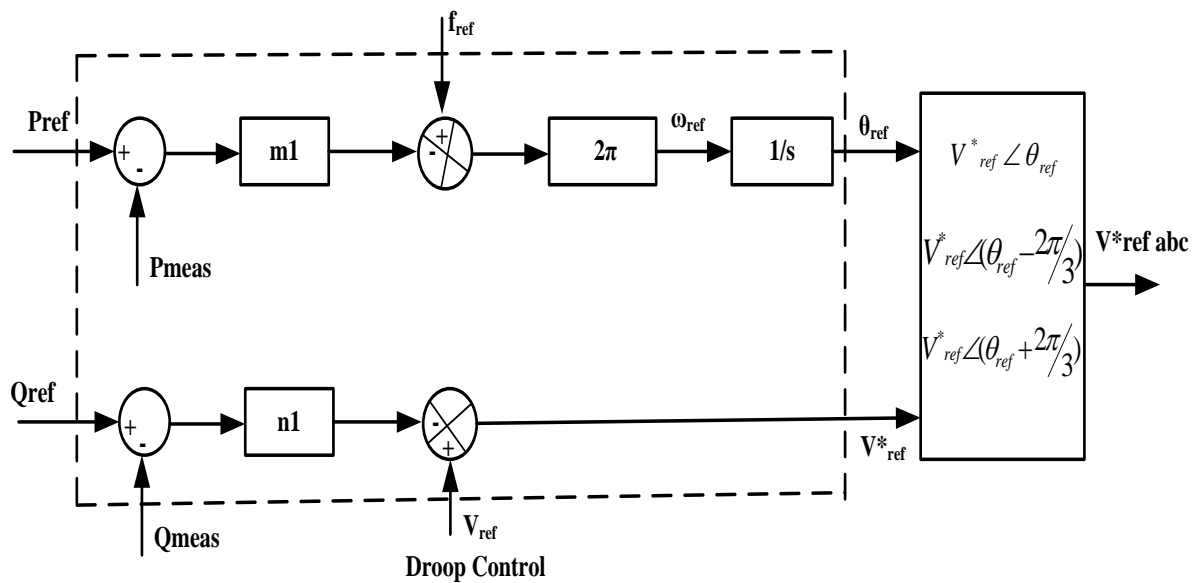


Figure 5.6 Reference voltage and frequency of Droop characteristics

Figure 5.6 shows the block diagram of reference voltage by droop method. This is the reference signal generated with phase angle (θ_{ref}) by the real power (P) and amplitude (V_{ref}) by the reactive power (Q), and this is used for the reference voltage of each power converter.

5.4.2 VSI control strategies

VSI is needed to interface the DG unit to the grid and provide flexible operation. As shown in Figure 5.7, the power circuit of the VSI based DG unit is associated with the control structure, so the controlled operation of the DG unit relies on the inverter control mode. For instance, in the grid-connected mode, DG unit operates as a PQ generator and the inverter should follow the PQ control mode, while voltage and frequency regulation are not required because the grid voltage is fixed. However, in the islanded mode, the DG units are expected to meet the load demand with respect to the quality of power supply. In this case, the voltage and frequency are not fixed and the inverter should follow the ($V-f$) control mode taking into account the inverter power rating for sharing power issue [101].

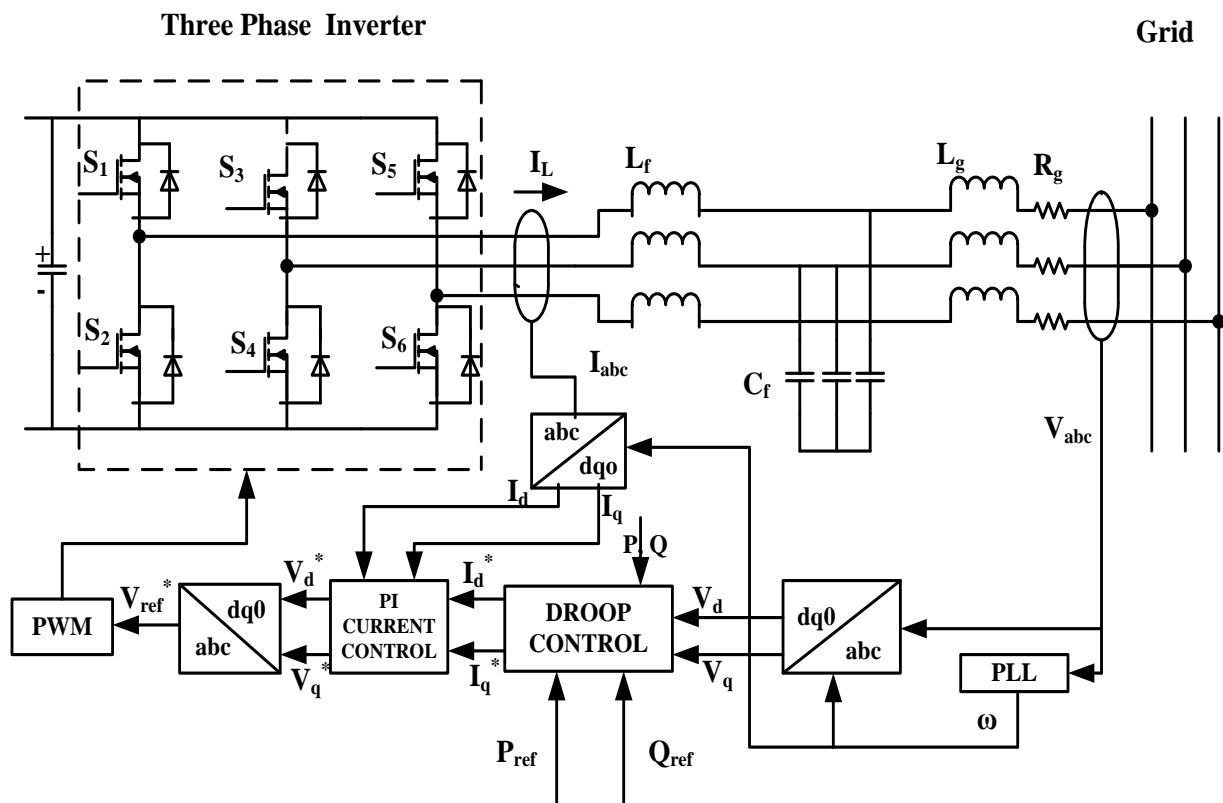


Figure 5.7 Droop Control Structure of Grid-connected VSI

5.4.3 PQ Control Strategy

For both microgrid operation modes, as long as the voltage and frequency are in stable condition, the PQ control mode is an application that can be used either to import less

power from the utility (Peak Shaving) in grid-connected mode or to inject a stable active and reactive power in a standalone mode. The PQ mode is usually applied to the DG units which supply a constant power. In this case, the amplitude and phase angle of the inverter current is controlled in order to inject the pre-set active and reactive power values which can be defined locally or by the Microgrid Control Centre (MGCC). Figure 5.7 shows the block diagram of the PQ control strategy [104].

The calculation of PQ is given according to Instantaneous Reactive Power Theory. The simplified measured values of the active and reactive power can be expressed as

Real part represents active power (P):

$$P = \frac{3}{2}(V_d * I_d + V_q * I_q) \quad (5.14)$$

Imaginary part represents reactive power (Q):

$$Q = \frac{3}{2}(V_q * I_d - V_d * I_q) \quad (5.15)$$

where V_d and V_q are the grid voltages in the dq transform. Furthermore, the inverter is able to deliver P and Q , which are the reference active and reactive power, respectively.

The variation in frequency and voltage are considered to adjust the active and reactive power. The droop adjustment in voltage and frequency to control the current loop and voltage loop

$$\omega = \omega^* - \left(k_p + \frac{k_i}{s}\right)(P - P^*) \quad (5.16)$$

$$V = V^* - \left(k_p + \frac{k_i}{s}\right)(Q - Q^*) \quad (5.17)$$

5.4.4 V-f Control strategy

For a reliable operation of the microgrid, it is necessary to ensure the continuous transition between the microgrid modes and keep a stable operation during the islanding mode in terms of regulating the microgrid voltage and frequency with respect to the load demand. In this case, the DG units must follow the load demand and maintain the voltage and frequency within threshold limits, so that V - f control mode has to be adopted by one or more

DG units in order to satisfy the above requirements [102]. The block diagram of the application is shown in Figure 5.8.

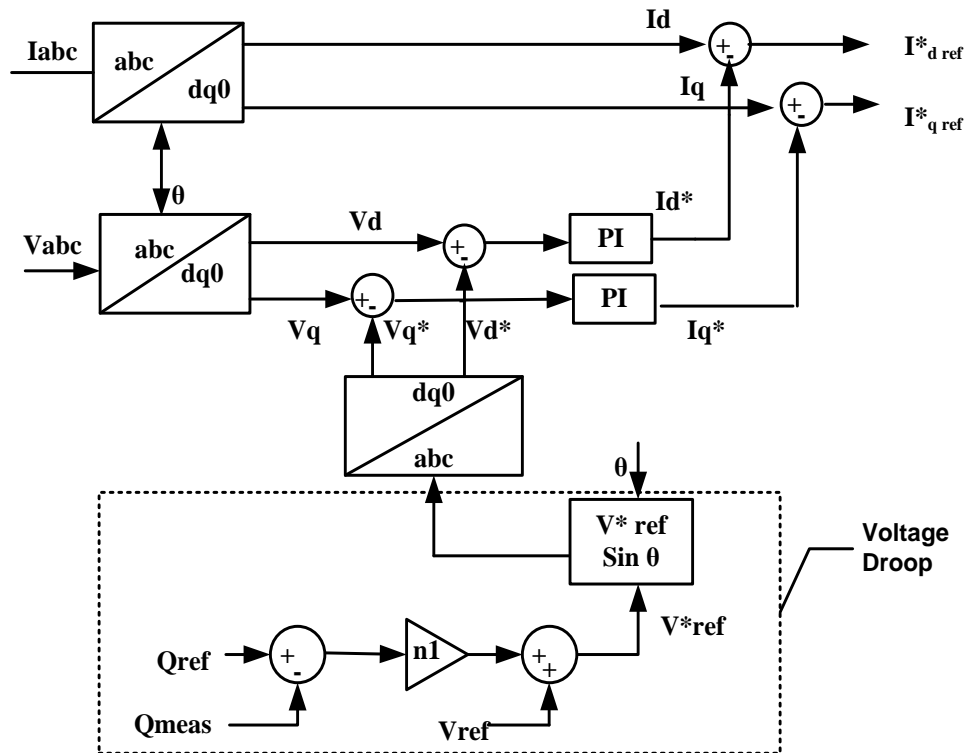


Figure 5.8 Structure of voltage and frequency droop control

Since the reference voltage and frequency values can be defined locally, the frequency can be measured by the PLL application as

$$V_d^* = I_d^* - \omega I_d + V_d \quad (5.18)$$

$$V_q^* = I_q^* - \omega I_q + V_q \quad (5.19)$$

The system turns in to grid-connected mode when there is drop in frequency and voltage, the reason behind is the change in impedance value and the disturbance in the PLL. The measured reactive is compared with reference reactive power to regulate the voltage. The measured difference combined with droop co-efficient produces direct axis and quadrature axis voltage. The d and q voltages are compared and regulated through PI controller in order to obtain the new d and q current reference values. The change of d and q axis currents are represented as .

$$I_d^* = (k_p + k_i/s)(V_d^* - V_d) \quad (5.20)$$

$$I_q^* = (k_p + k_i/s)(V_q^* - V_q) \quad (5.21)$$

5.4.5 Control of the DC link voltage

The *dc* link voltage control must be well regulated in order to facilitate the inverter control. This strategy ought to keep the *dc* link close to the reference value, even under variations on the grid source voltage or loads impact. Therefore, an active power control is proposed to maintain the *DC* voltage close enough to the given reference. The DC-link voltage controller is responsible for keeping the DC-link voltage constant by balancing the injected active power and the output active power of DC-link [104-105].

The power balance across the DC link shown is expressed as

$$\frac{d}{dt} \left(\frac{1}{2} C V_{DC}^2 \right) = P_{DC} - P_{outDC} - \frac{V_{DC}^2}{R_{loss}} = P_{inv} - P_{outDC} - \frac{V_{DC}^2}{R_{loss}} \quad (5.22)$$

where V_{DC} is the DC- link voltage, C is the DC- link capacitance, $P_{DC} = V_{DC} I_{DC}$, which is equal to the rectifier AC- side terminal power P_{inv} . P_{outDC} is the external power that flows out of the DC- capacitor. R_{loss} represents the total switching loss of the system. If the instantaneous power of AC- side filter is not considered, P_{inv} is equal to the grid side power P_{grid} .

Considering the fact (5.22) can be rewritten as,

$$\frac{d}{dt} \left(\frac{1}{2} C V_{DC}^2 \right) = P_{grid} - P_{outDC} - \frac{V_{DC}^2}{R_{loss}} \quad (5.22)$$

Taking the Laplace transform on the both the side of (5.22),

$$V_{DC}^2(s) = \frac{2R_{loss}}{CR_{loss}s + 2} P_{grid}(s) - \frac{2R_{loss}}{CR_{loss}s + 2} P_{outDC}(s) \quad (5.23)$$

where V_{DC}^2 and P_{grid} are the system output and control input respectively, and P_{outDC} acts like a disturbance input.

5.5 Simulation results and discussion

The complete block diagram of the control structure developed is given in Figure 5.9 and the system parameters are given in Table 5.1

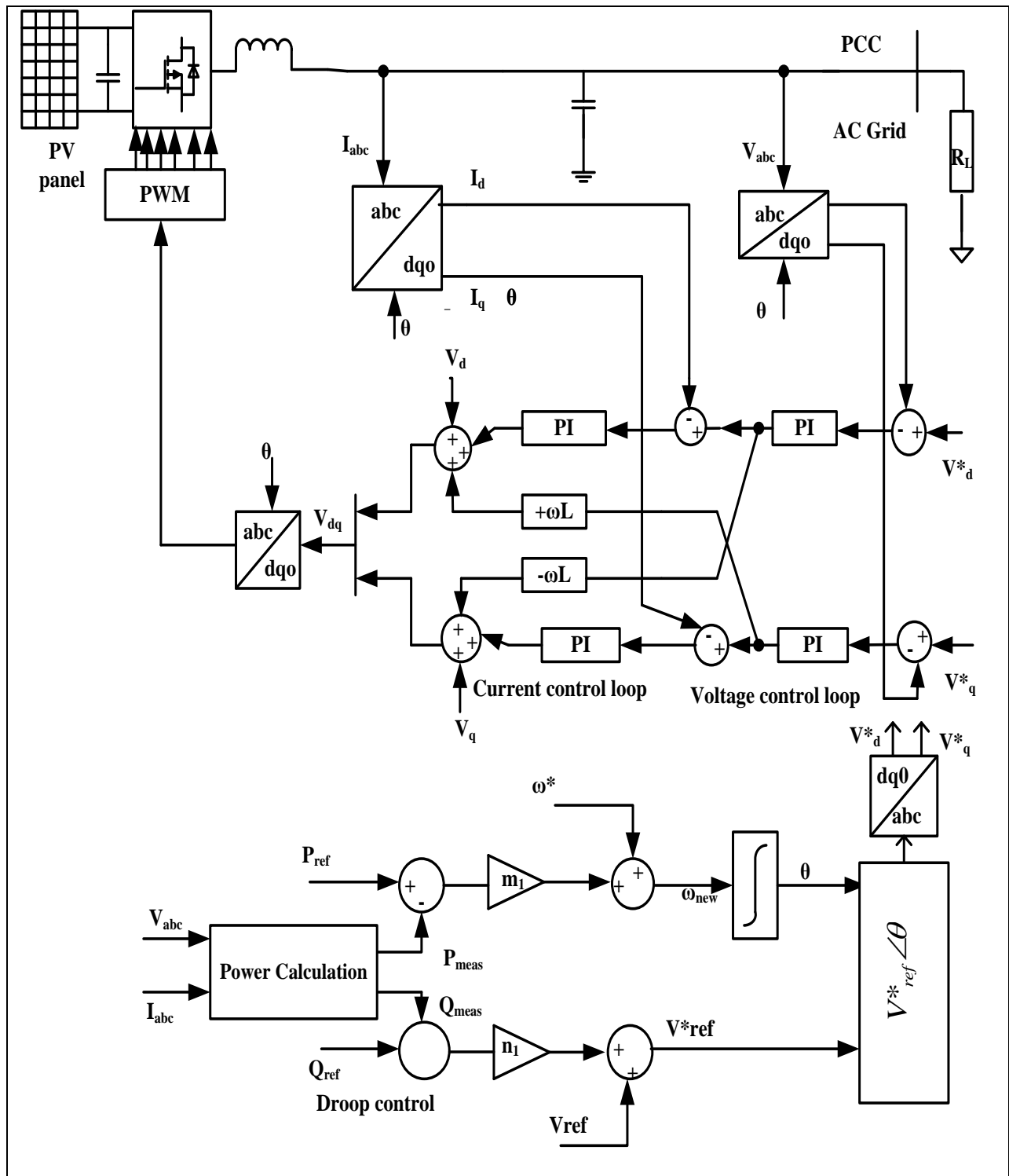
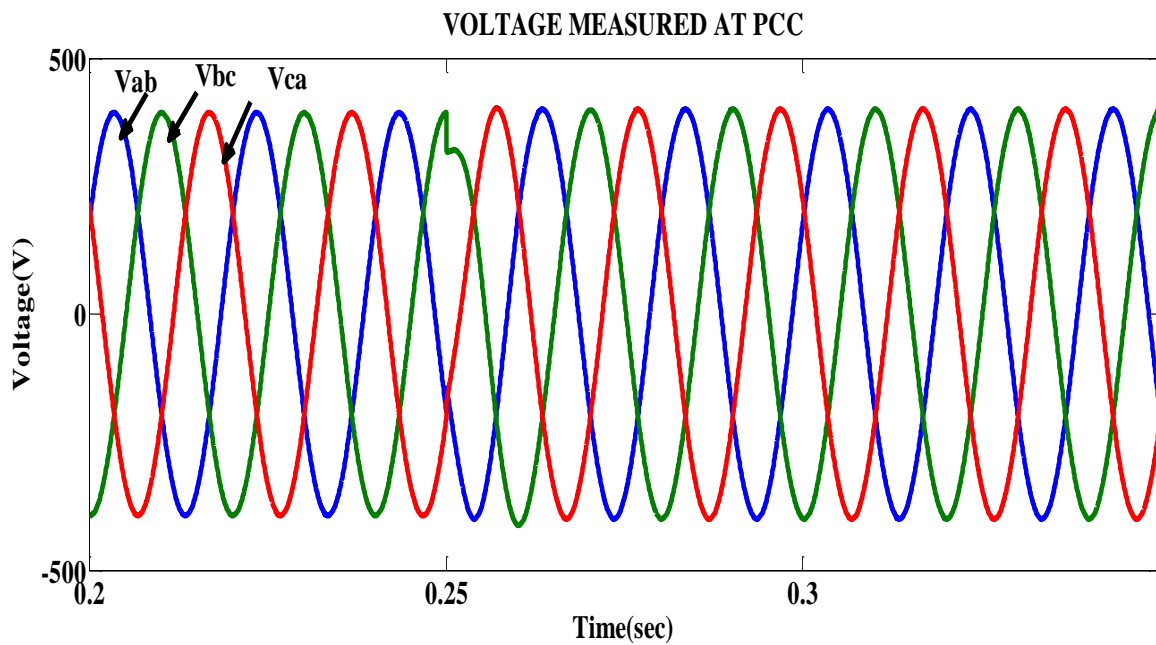


Figure 5.9 Block diagram of Complete Control structure of the study

Table 5.1. Simulation parameters for droop control DGs

Parameter	Value	Description
V_g	400V(rms)	Grid voltage(rms)
V_{dc}	750 V	DC voltage
C_{dc}	800 μ F	DC link capacitor
DG power	10Kw	PV Arrays
F_s	10KHz	Switching Frequency
L_f	45mH	Filter inductor
C_f	500 μ F	Filter capacitor
L_l	4 μ F	Link inductor
f	50Hz	Grid supply frequency

To verify the effectiveness of the active and reactive power and droop control, the controller testing is conducted in two different modes, grid-connected mode and island mode. The complete control structure discussed in the study is tested with different active and reactive load conditions. The transition from islanded mode to grid-connected mode using proposed schemes have been analyzed. The test has been conducted for the time duration of 0.5sec.



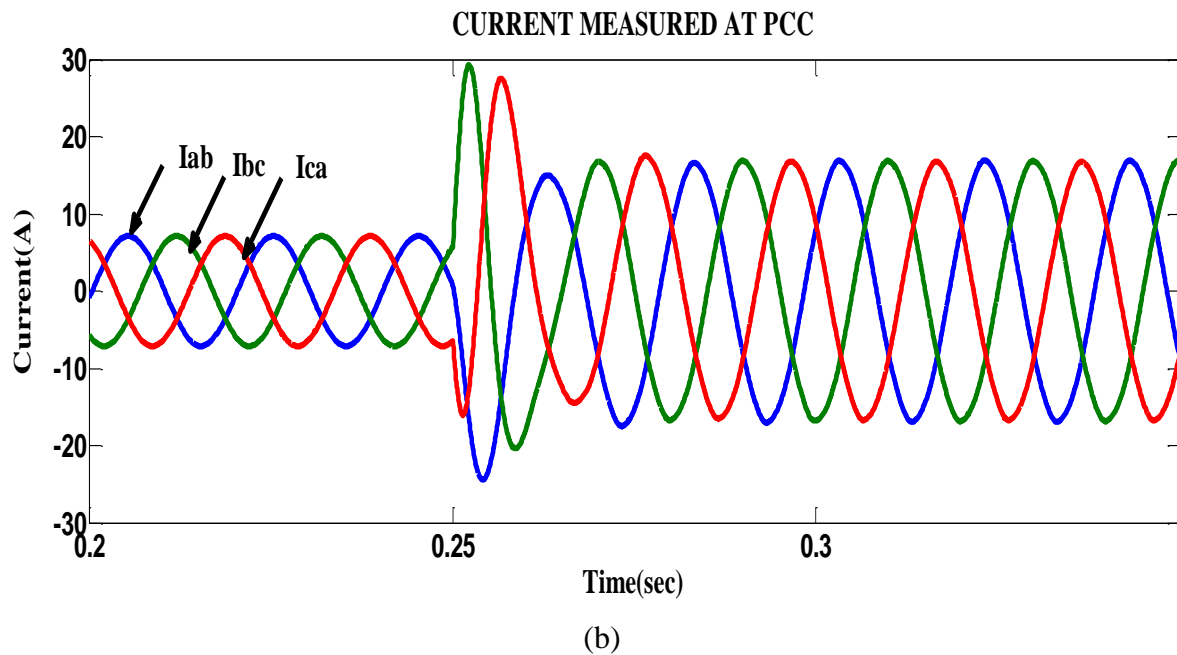


Figure 5.10 Simulation results of (a) voltage waveform and (b) current waveform during the transition

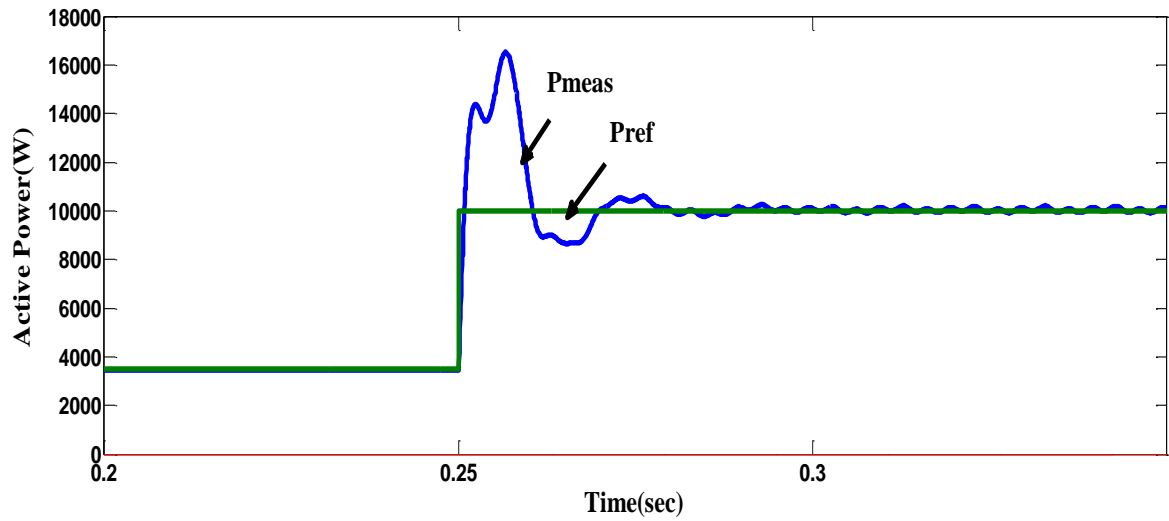
The following sequence of occurrences is observed. Initially, the system starts to operate in an islanded mode at $t=0$ sec, the system transits to grid-connected mode at $t=0.25$ sec.

Initial operating conditions: At $t=0$ sec, the real and reactive power set points of DG is set to 3.5 kW and 2.2kVar ($Pf 0.85$).

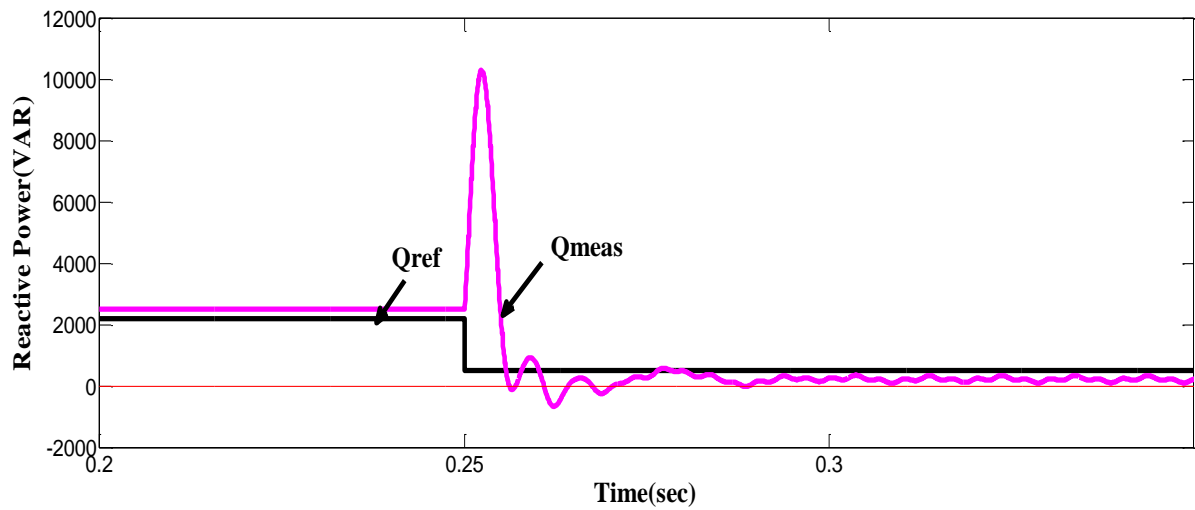
Occurrence (i): At $t=0.25$ sec, the real and reactive power set points of DG are changed from 3.5kW and 2.2kVar to 10 kW and 0.5kVar (upf), the system transits to grid-connected mode.

Occurrence (ii): During $t=0.25$ sec to $t=0.28$ sec, change of phase angle and drop in voltage are observed. In view of the change, a decrease in frequency value and change in active power is observed. Due to the drop in voltage the reactive power decreases gradually. The increase in current values (see Figure 5.10(b)) shows; the VSI supports the main grid when it is connected to grid-connected mode of operation.

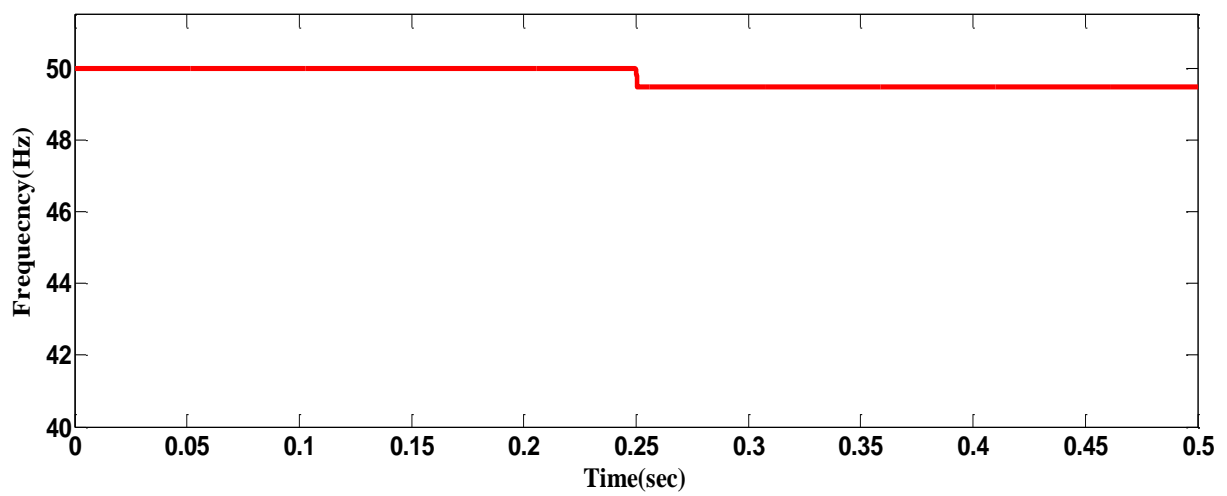
Occurrence (iii): At $t=0.28$ sec, the power remains unchanged. The settling time of 0.03sec is achieved as per the design. The voltage measured at PCC shows, the voltage values are nearer to the grid set voltage.



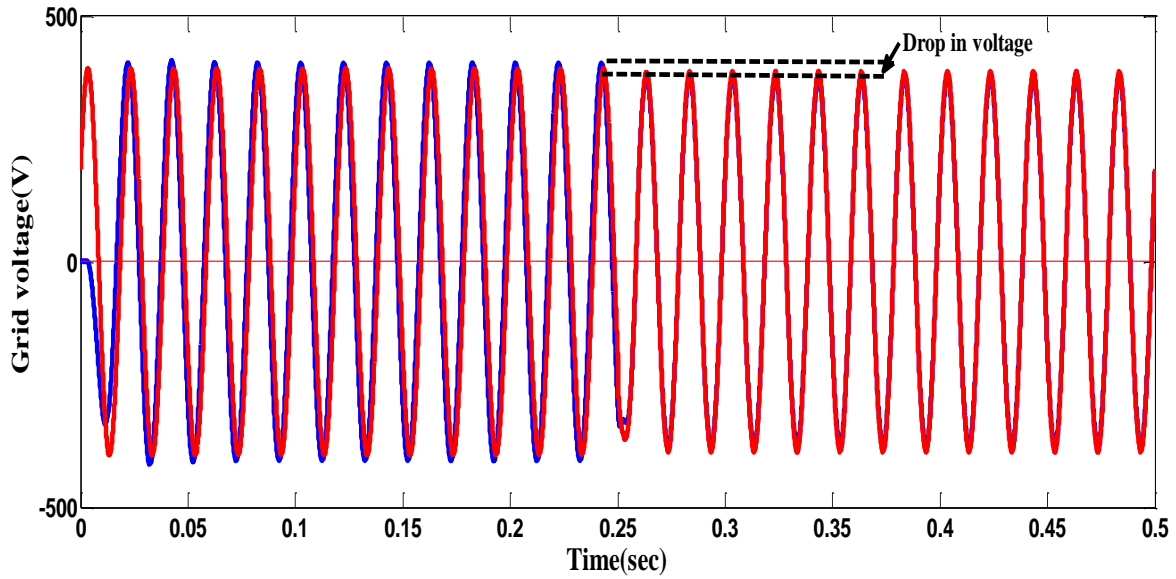
(a)



(b)



(c)



(d)

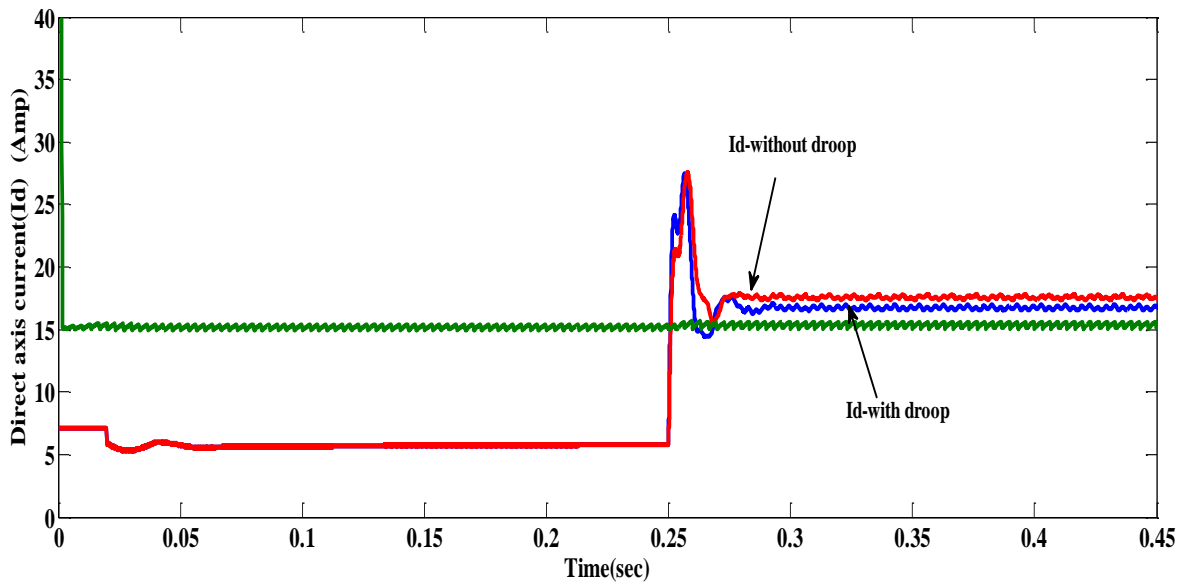
Figure 5.11 Simulation results of power sharing

(a) Active power (b) Reactive power (c) Frequency (d) Drop in Voltage

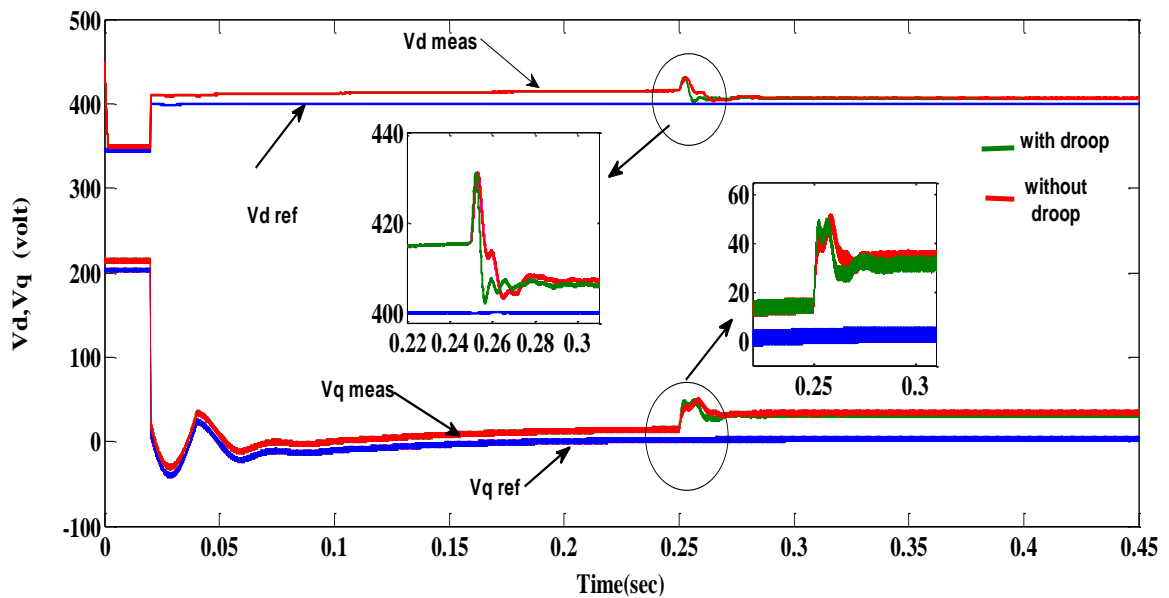
The performance of active synchronizing control scheme is evaluated in the micro grid as shown in the figure 5.11(a-d). The current controller, voltage controller, and droop controller are collectively engaged to validate the control loops of active and reactive power so as to support the grid-connected DG operation. The active power controller test is performed with support unit step signal. During grid synchronizing or dynamic operation, there is a drop in frequency which is managed with support of direct axis current in addition to the droop co-efficient. The predetermined power values show, (see Figure.5.11(a), (c)) with the efficient smooth tracking of set values, the load sharing in the grid, manage the frequency drop during the sudden change in loads. The reactive power controller effort is based on the reactive power difference between Q_{ref} and Q measured and grid voltage drop. The variance in voltage is controlled by voltage and frequency control loop. The droop controller controls the variance in reactive power through PI controller and droop co-efficient provided in the droop control loop.

Figure 5.12 shows the comparison of the variations in the current and voltage during the islanded and grid connected modes of operation between the proposed model and

conventional method. During the transition, DG injects the active power to grid which increases the grid current (see figure 5.12(a)). The droop is implemented during the transition for the system stabilization. Droop control maintains the smoother operation of current controller and reduces the settling time. The variation in the voltage during the transition controlled through V - f controller and droop control and nature of d - axis and q -axis voltage is represented in figure 5.12(b). The Simulink model is presented as shown in figure 5.13.



(a)



(b)

Figure 5.12. Simulation results of direct axis quadrature axis values of
a) direct axis current b) direct and quadrature axis voltage

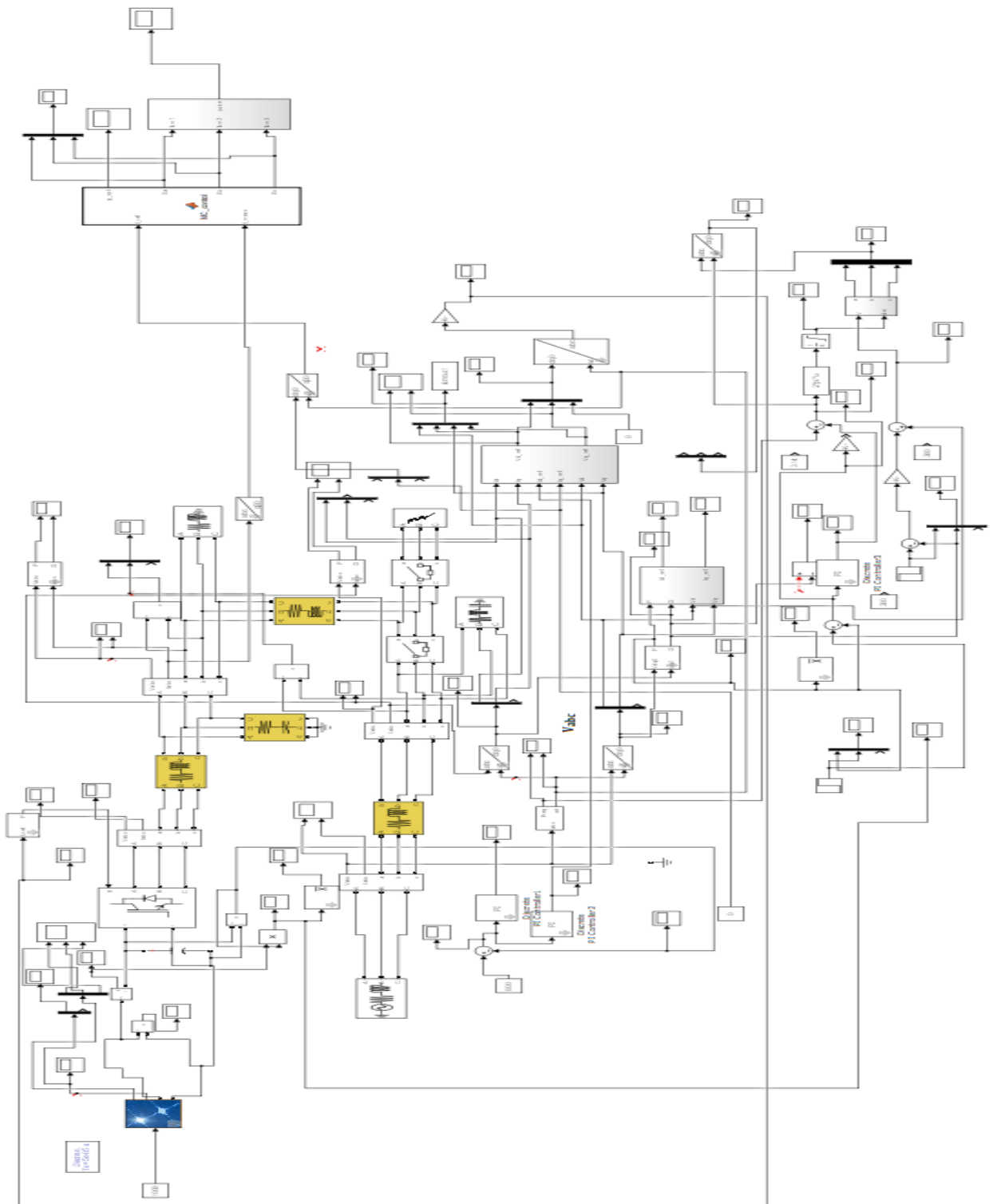


Figure 5.13: Simulink Model of Complete Control structure of the study

5.6 Conclusion

The proposed droop control method dynamically coordinates between frequency/active power and voltage/ reactive power generation and consumption to keep the PCC point frequency and voltage close to their nominal values. The use of PQ control ensures that DGs can generate certain power in accordance with real and reactive power references. Droop controller was implemented to ensure the quick dynamic frequency response and proper power sharing between DGs when a forced islanding occurs or load changes. Compared to pure $V-f$ control and master-slave control, the proposed control strategy have the ability to operate without any on-line signal communication between DGs and make the system fast responding to load changes. Droop control maintains smoother operation of current controller and reduces the settling time.

The simulation results depicted that when compared to existing methods; the proposed controller is more effective in performing real and reactive power tracking, voltage control and power-sharing during both grid-connected mode and islanded mode, and their makes the system more resilient, fast and adaptive under frequent load shedding and can restore rapidly.

Chapter VI

Conclusion

6.1 Conclusion

In this thesis, the various issues, challenges and potential drawbacks of DG when it is connected to utility grid or the main grid were discussed. The two DG units (PEMFC, PV) characteristics were studied under various operating conditions. These DGs are interfaced with main grid with the assumptions of balance load condition. It is observed that the performance of control loops were better even under highly unbalanced and poor power factor conditions.

The MPC scheme for control of PV based three phase grid connected inverter had been proposed to attain control of converter under balanced and unbalanced dip in voltage with extraordinary response. Simulation studies were performed to verify the performance of the MPC control method and its strategy. It is observed that compared with PI control, output current of MPC is obviously smoother. Output currents of MPC are closer to expected currents. In conclusion, the MPC strategy has smaller steady state error, less overshoot, faster response speed, and provides higher quality power, when compared with the results of conventional control under unbalance voltage conditions.

The different methods applied to the power control of the parallel inverters were presented and pros and cons of each method were investigated. The proposed droop control method dynamically coordinates between frequency/active power and voltage/ reactive power generation and consumption to keep the PCC point frequency and voltage close to their nominal values. The use of PQ control ensures that DGs can generate certain power in accordance with real and reactive power references. Droop controller was implemented to ensure the quick dynamic frequency response and proper power sharing between DGs when a forced islanding occurs or load changes. Compared to pure $V-f$ control and master-slave control, the proposed control strategies have the ability to operate without any on-line signal

communication between DGs and make the system fast responding to load changes. Droop control maintains the smoother operation of current controller and reduces the settling time.

The simulation results obtained show that when compared to existing method; the proposed controller is effective in performing real and reactive power tracking, voltage control and power-sharing during both grid-connected mode and islanded mode, makes the system more resilient, fast and adaptive under frequent load shedding and restore rapidly.

Although, the droop technique benefits from being a wireless control system, there are negligible weaknesses inherent in this technique. One of these is the voltage drop held by reactive power control, and the other one is being sensitive to transmission lines impedance.

6.2 Future Scope of Study

This thesis investigates locally controlled DG systems to regulate feeder voltage. The future study will be investigating on how to mitigate the voltage sag/swell during transient or disturbed condition and the study of transition between grid-connected mode and islanding mode.

1. The co-ordinated control approaches can be explored in this case as well to further improve the dynamic performance and effectiveness of the overall control of the system. The co-ordinated control of the load and the DG power is yet to be explored fully to identify the stability limitations of the control scheme
2. Protection of converters in case of fault in utility or microgrid may be further investigated
3. Improvement in supplementary droop control for enhanced system damping under different operating conditions.
4. A modified droop control can be derived for frequency dependent loads.

References

- [1] Huang Jiayi, Jiang Chuanwen, Xu Rong, “A review on distributed energy resources and MicroGrid ” ,*Renewable and Sustainable Energy Reviews*,2008,12(9): 2472–2483
- [2] Mudathir Funsho Akorede , Hashim Hizam, Edris Pouresmaeil, “Distributed energy resources and benefits to the environment”, *Renewable and Sustainable Energy Reviews*, 2010,14(2) : 724–734
- [3] P. Tenti, T. Caldognetto, “Chapter-4 master/slave power-based control of low-voltage microgrids – Microgrid”, *Elsevier Ltd.*, 2017
- [4] Ahmed Alabdulwahab, Mohammad Shahidehpour, “Microgrid networking for the monitoring, control and protection of modern power systems”, *The Electricity Journal*, 2016, 29(10) : 1–7.
- [5] Mudathir Funsho Akorede , Hashim Hizam, Edris Pouresmaeil, “Distributed energy resources and benefits to the environment”,*Renewable and Sustainable Energy Reviews*,2010,14(2): 724–734.
- [6] G. Bhuvaneswari and R. Annamalai , “Development of a Solar Cell model in Matlab For PV Based Generation System”, *INDICON IEEE conf*, 2011: 1-5.
- [7] Ali Reza Reisi , Mohammad H. Moradi , Hemen Showkati, “Combined photovoltaic and unified power quality controller to improve power quality”, *Solar Energy*, 2013, 88: 154–162.
- [8] Yahia Bouzelata , Erol Kurt , Rachid Chenni , Necmi Altın , “ Design and simulation of a unified power quality conditioner fed by solar energy”, *International Journal of Hydrogen Energy*, 2015,40(44):15267-15277.
- [9] Alexis B. Rey-Boué , Rafael García-Valverde, “An integrative approach to the design methodology for 3-phase power conditioners in Photovoltaic Grid-Connected systems”, *Energy Conversion and Management* ,2012,56 :80–95.
- [10] L. Hassaine , E.O.Lias , J.Quintero , V.Salas , “Overview of power inverter topologies and control structures for grid connected photovoltaic systems”, *Renewable and Sustainable Energy Reviews*, 2014,30:796–807.
- [11] Kazmierkowski M, Krishnan R, Blaabjerg F, “Control in power electronic selected problems”, *Elsevier Ltd*, 2003.
- [12] Molina.M.G , Mercado .PE., “ Modeling and control of grid-connected photovoltaic energy conversion system used as a dispersed generator”, *IEEE Transmission and Distribution conference and exposition*, 2008.

- [13] N.A.Rahim , Selvaraj J, Krismadinata.C., “Five-level inverter with dual reference modulation technique for grid-connected PV system”, *Renewable Energy*, 2010, 35: 712–720.
- [14] Martinez JA, Garcia JE, Arnaltes S, “Direct power control of grid-connected PV systems with three level NPC inverter”, *Solar Energy*, 2010, 84:1175–1186.
- [15] Turitsyn K, et al., “Options for control of reactive power by distributed photovoltaic generators.”, *Proc. IEEE*, 2011, 99:1063–1073.
- [16] Svensson J. Synchronisation , “Methods for grid-connected voltage source converters”, *Proc Inst Electr Eng - Gener Transm Distrib*,”, 2011,48:229–35.
- [17] Tsengenes Georgios, Adamidis Georgios., “Investigation of the behavior of a three phase grid-connected photovoltaic system to control active and reactive power”, *Electr Power Syst Research*, 2011,81:177–188
- [18] Boualem Boukezata , Jean-Paul Gaubert , “Predictive current control in multi-functional grid connected inverter interfaced by PV system”, *Solar Energy*,2016, 139:130–141.
- [19] N. Hamrouni, M. Jraidi, A. Che´rif, “New control strategy for 2-stage grid-connected photovoltaic power system”, *Renewable Energy*,2008, 33: 2212–2221.
- [20] Junbiao Han¹, Sarika Khushalani- Solanki, “Study of unified control of STATCOM to resolve the Power quality issues of a grid connected three phase PV system”, *IEEE conf. Innovative Smart Grid Technologies (ISGT)*, 2012
- [21] Yang Du, Dylan Dah-Chuan Lu, “A Study on the Harmonic Issues at CSIRO Microgrid”, *IEEE 9th conf on Power Electronics and drives*, 2011.
- [22] Ehsan Afshari, Gholam Reza Moradi, “Control Strategy for Three-Phase Grid Connected PV Inverters Enabling Current Limitation under Unbalanced Faults,” *IEEE Transactions on Industrial Electronics*”, 2017, 64: 8908 – 8918.
- [23] Zhang Guowei, Wei Tongzhen, Huang Shengli and Kong Lingzhi, “The Control for Grid Connected Inverter of Distributed Generation under Unbalanced Grid Voltage”, *IEEE Int Conf on Sustainable Power Generation and Supply*, 2009: 1 – 5.
- [24] Farhad Shahnia, Ritwik Majumder*, Arindam Ghosh, Gerard Ledwich, Firuz Zare. “Operation and control of a hybrid microgrid containing unbalanced and nonlinear loads”, *Electric Power Systems Research*,2010, 80 :954–965.
- [25] Jaume Miret, , Miguel Castilla, Antonio Camacho, Lu´ıs Garc´ıa de Vicu˜na, and Jos´e Matas, “Control Scheme for Photovoltaic Three-Phase Inverters to Minimize Peak Currents During Unbalanced Grid-Voltage Sags”, *IEEE Transactions on Power Electronics*,2012,27:4262-4271.
- [26] Gustavo Hunter, Iván Andrade, “Active and Reactive Power Control during Unbalanced Grid Voltage in PV systems” ,*42nd IEEE conf on Industrial Electronics society*,2016.

- [27] Mitra Mirhosseini, Josep Pou, , Baburaj Karanayil, , “Resonant Versus Conventional Controllers in Grid-Connected Photovoltaic Power Plants Under Unbalanced Grid Voltages”, *IEEE Transactions on Sustainable Energy*,2016, 7:1124-1134.
- [28] Zhilei Yao and Lan Xiao, and Vassilios G. Agelidis, , “Control of Single-Phase Grid-Connected Inverters with Nonlinear Loads”, *IEEE Trans on Industrial Electronics* , 2013, 60:1384-1389.
- [29] Y. C. Zhang, W. Xie, Z. X. Li, and Y. C. Zhang, “Model predictive direct power control of a PWM rectifier with duty cycle optimization”, *IEEE Trans. Power Electron*, 2013, 28: 5343–5351.
- [30] Tobias Geyer, “A Comparison of Control and Modulation Schemes for Medium-Voltage Drives: Emerging Predictive Control Concepts Versus PWM-Based Schemes”, *IEEE Trans on Industry Applications*, 2011, 47(3):1380-1389.
- [31] Fernand Diaz Franco , Tuyen V. Vu, David Gonsulin, Hesam Vahedi, Chris S. Edrington, “Enhanced performance of PV power control using model predictive control,” *Solar Energy* , 2017,158: 679-686.
- [32] A. Nami, J. Liang, F. Dijkhuizen, G.D. Demetriades,“ Modular multilevel converters for HVDC applications: review on converter cells and functionalities”, *IEEE Trans. Power Electron.*,2015,30:18–36.
- [33] Changliang Xia, , Meng Wang, Robust Model Predictive Current Control of Three-Phase Voltage Source PWM Rectifier With Online Disturbance Observation,” *IEEE Transactions on Industrial Informatics*,2012 ,8: 459-469.
- [34] Xunwei Yu, *Student Member, IEEE*, Xu She, *Student Member, IEEE*, Xiaohu Zhou, “Power Management for DC Microgrid Enabled by Solid-State Transformer”, *IEEE Transactions on Smart Grid*, 2014, 5:954- 965.
- [35] M. Uzunoglu, , M. S. Alam, “Dynamic Modeling, Design, and Simulation of a Combined PEM Fuel Cell and Ultracapacitor System for Stand-Alone Residential Applications,” *IEEE Trans on Energy Conversion*,2006, 21: 767-775.
- [36] Wei Yuan, Yong Tang, Minqiang Pan, Zongtao Li, Biao Tang, “Model prediction of effects of operating parameters on proton exchange membrane fuel cell performance,” *Renewable Energy* ,2010,35: 656–666.
- [37] Serkan Bahceci , Seyfullah Fedakar, Tankut Yalcinoz, “Examination of the grid-connected polymer electrolyte membrane fuel cell’s electrical behaviour and control,” *IET Renew. Power Gener.*, 2016,10: 388–398.
- [38] Qi Li , Weirong Chen, Zhixiang Liu, Guohua Zhou, Lei Ma, “ Active control strategy based on vectorproportion integration controller for proton exchange membrane fuel cell grid-connected System,” *IET Renew. Power Gener.*,2015 , 9:991–999.

- [39] Guiying Wu, Kwang Y. Lee, , “Modeling and Control of Power Conditioning System for Grid-connected Fuel Cell Power Plant”, *IEEE conf. Power and Energy Society General Meeting*, 2013 .
- [40] Vipin Dasa, Sanjeevikumar Padmanaban, “Recent advances and challenges of fuel cell based power system architectures and control – A review”, *Renewable and Sustainable Energy Reviews*, 2017, 73:10–18.
- [41] G.K. Singh, “Solar power generation by PV (photovoltaic) technology: A review,” *Energy* , 2013, 53: 1-13
- [42] Hongmei Tian , Fernando Mancilla-David , Kevin Ellis , Eduard Muljadi , Peter Jenkins , “A cell-to-module-to-array detailed model for photovoltaic panels,” *Solar Energy* , 2012, 86: 2695–2706.
- [43] Aissa Chouder , Santiago Silvestre , Nawel Sadaoui , Lazhar Rahmani , “Modeling and simulation of a grid connected PV system based on the evaluation of main PV module parameters”, *Simulation Modelling Practice and Theory* , 2012, 20: 46–58.
- [44] R.Ayaz, I. Nakir, and M. Tanrioven, “An Improved Matlab-Simulink Model of PV Module considering Ambient Conditions” , *International Journal of Photoenergy*,” 2014, 1:1- 6.
- [45] A. Ravi , P.S. Manoharan , J. Vijay Anand, “Modeling and simulation of three phase multilevel inverter for grid connected photovoltaic systems”, *Solar Energy*, 2011, 85 : 2811–2818.
- [46] M. Bouzguenda, T. Salmi, A. Gastli and A. Masmoudi, “Evaluating Solar Photovoltaic System Performance using MATLAB,” *IEEE, 1st Int. Conf. on Renewable Energies and Vehicular Technology*, 2012.
- [47] Ioulia T. Papaioannou , Arturs Purvins, “Mathematical and graphical approach for maximum power point modelling,” *Applied Energy*, vol. 91 (2012), pp. 59–66.
- [48] Arun Kumar Verma, Bhim Singh, and D.T Shahani. “Fuzzy-Logic Based MPPT Control of Grid Interfaced PV Generating System with Improved Power Quality,” *IEEE 5th conf. Power India*, 2012.
- [49] Kun Ding, XinGao Bian, HaiHao Liu, and Tao Peng, “A MATLAB-Simulink-Based PV Module Model and Its Application Under Conditions of Nonuniform Irradiance ,” *IEEE Transactions on Energy Conversion*, 2012, 27(4):864-872.
- [50] Ram Krishan, Yog Raj Sood , “The Simulation and Design for Analysis of Photovoltaic System Based on MATLAB,” *IEEE Conf. Energy Efficient Tech.s for Sustainability*, 2013.
- [51] N. Hamrouni, M. Jraidi, “Current control for inverter-interfaced grid-connected photovoltaic generator,” *16th IEEE Electrtechnical Conf*, 2012 :296-299.

- [52] A. Ebrahimi, S. H. Fathi, N. Farokhnia, "Novel Topology for Power Quality Improvement of Grid-Connected Photovoltaic System," *IEEE Conf on Power Engineering and Renewable Energy*, 2012.
- [53] M. Bobrowska-rafał, K. Rafał, "Control of PWM rectifier under grid voltage dips," *bulletin of the polish academy of sciences technical sciences*, 2009,57(4).
- [54] Santanu K. Mishra, Adda Ravindranath, "Analysis and PWM Control of Switched Boost Inverter," *IEEE Transactions on Industrial Electronics*, 2013, 60(12): 5593 -5602.
- [55] A. Ruiz-Gonzalez; M. J. Meco-Gutierrez, "Reducing Acoustic Noise Radiated by Inverter-Fed Induction Motors Controlled by a New PWM Strategy," *IEEE Trans on Industrial Electronics*, 2010, 57: 228 – 236.
- [56] Giovanni Lo Calzo; Alessandro Lidozzi, "LC Filter Design for On-Grid and Off-Grid Distributed Generating Units," *IEEE Trans. on Industry Applications*, 2015, 51: 1639 -1650.
- [57] Ravi Nath Tripathi., Alka Singh., Tsuyoshi Hanamoto, "Design and control of LCL filter interfaced grid connected solar photovoltaic (SPV) system using power balance theory," *Elect. Power Energy Syst.*, 2015, 69 : 264-272.
- [58] Mohammad Monfared a,n, SaeedGolestan, "Control strategies for single-phase grid integration of small-scale renewable energy sources: A review," *Renewable and Sustainable Energy Reviews*, 2012,16:4982–4993.
- [59] Waleed Al-Saedi, Stefan W. Lachowicz, Daryoush Habibi, Octavian Bass, "Power quality enhancement in autonomous microgrid operation using Particle Swarm Optimization," *Electrical Power and Energy Systems*, 2012,42:139–149.
- [60] Alka Singh, Bhim Singh, "Multifunctional Capabilities of Converter Interfaced Distributed Resource in Grid Connected Mode," *IEEE 5th Conf on Power Electronics*, 2012.
- [61] Antonio Camacho, Miguel Castilla, Jaume Miret, Ramon Guzman and Angel Borrell, "Reactive Power Control for Distributed Generation Power Plants to Comply with Voltage Limits During Grid Faults," *IEEE Trans on Power Electronics*, 2014, 29(11):6224-6234.
- [62] Mourad Tiar, Achour Betka, "Optimal energy control of a PV-fuel cell hybrid System", *Int j. of Hydrogen Energy*, 2017,42: 1456-1465.
- [63] Nayan Kumar, Tapas Kumar Saha, Jayati Dey, "Modeling, control and analysis of cascaded inverter based grid-connected photovoltaic system," *Electrical Power and Energy Systems*, 2016,78:165–173.
- [64] L. Hassaine E. OLias, J. Quintero, V. Salas, "Overview of power inverter topologies and control structures for grid connected photovoltaic systems," *Renewable and Sustainable Energy Reviews*, 2014, 30: 796–807.

- [65] Nattapong Chayawatto , Krissanapong Kirtikara, “DC–AC switching converter modelings of a PV grid-connected system under islanding phenomena,” *Renewable Energy* ,2009,34: 2536–2544.
- [66] A. Vijayakumari , A.T. Devarajan , N. Devarajan, “Decoupled control of grid connected inverter with dynamic online grid impedance measurements for micro grid applications,” *Electrical Power and Energy Systems*, 2015, 68: 1–14.
- [67] Irvin J. Balaguer, , Qin Lei, Shuitao Yang, Uthane Supatti, “Control for Grid-Connected and Intentional Islanding Operations of Distributed Power Generation,” *IEEE Transactions on Industrial Electronics*, 2011,58:147-157.
- [68] Amr Ahmed A.Radman,Y.Abdal Rady I.Mohammad, “Power Synchronization for Grid-connected current – source Inverter based PV Systems”,*IEEE Trans on Energy Conversion*,2016,31(3):1023-1036.
- [69] Zhilei Yao; Lan Xiao; Josep M. Guerrero, “Improved control strategy for the three-phase grid-connected inverter,” *IET Renewable Power Generation*, 2015, 9:587-592.
- [70] Mohammad Hadi Andishgar, Eskandar Gholipour, Rahmat-allah Hooshmand, “An overview of control approaches of inverter-based microgrids in islanding mode of operation,” *Renewable and Sustainable Energy Reviews*, 2017, 80:1043–1060.
- [71] Yongchang Zhang., Changqi Qu. “Model predictive direct power control of PWM rectifiers under unbalanced network conditions”, *IEEE Trans.Ind. Electron*, 2015, 62(7): 4011- 4022.
- [72] Hang Gao., Bin Wu., Dewei (David) Xu.,et.al: “Common mode voltage reduced model predictive control scheme for current-source converter fed induction motor drives”, *IEEE Trans. Power Electron*, 2017, 32, (6):4891 – 4904.
- [73] Sabir Ouchen,Sabrina Abdeddaim,Achour Betka, Abdelkrim Menadi, “Experimental validation of sliding mode-predictive direct power control of a grid connected photovoltaic system, feeding a nonlinear load”, *Solar Energy*, 2016 ,137:328-336 .
- [74] Ahmed El-Naggar, István Erlich, “Control approach of three-phase grid connected PV inverters for voltage unbalance mitigation in low-voltage distribution grids”, *IET Renew Power Gener.*,2016 , 10,(10):1577-1586.
- [75] Aditi Chatterjee, Kanungobarada Mohanty, et.al “Design and experimental investigation of digital model predictive current controller for single phase grid integrated photovoltaic systems”, *Renew. Energy* , 2017,108 :438-448.
- [76] Guerrero-Rodriguez NF, Herrero-de Lucas LC, De Pablo- Gomez S, Rey-Bou AB. “Performance study of a Synchronization algorithm for a 3-phase photovoltaic grid connected system under harmonic distortions and unbalances”, *Elect. Power Syst. Research*, 2014, 65:252-265.

- [77] Hector Young, Marcelo A.Perez,Jose Rodriguez.,“Analysis of finite-control-set model predictive current control with model parameter mismatch in a three-phase inverter”, *IEEE Trans. Ind. Electron.*,2016, 63,(5) :3100- 3107.
- [78] Marco Rivera, Venkata Yaramasu, “Digital predictive current control of a three-phase four-leg inverter”, *IEEE Trans.Ind. Electron.*, 2013, 60, (11):4903 -4912.
- [79] Rachid Errouissi, S. M. Muyeen,“Experimental validation of a robust continuous nonlinear model predictive control based grid-interlinked photovoltaic inverter”, *IEEE Trans. Ind. Electron.*,2016, (7): 4495 - 4505 .
- [80] Patricio Cortes, Jose Rodriguez, Cesar Silva, Alexis Flores, “Delay compensation in model predictive current control of a three-phase inverter”, *IEEE, Trans. Ind. Electron.*, 2012, 59(2):1323- 1325.
- [81] Ikram Maaoui-Ben Hassine, Mohamed Wissem Naouar, “Model based predictive control for three-phase grid connected converter”, *J.Electrical Systems*, 2015,1:11-24.
- [82] Thomas John., Y. Wang.: “Model predictive control of distributed generation inverter in a Microgrid”, *IEEE Conf. Innovative Smart Grid Technology*, 2014, pp.657-662.
- [83] Boualem Boukezata. ,Jean-paul Gaubert., Abdelmadjid chaoui. , Mabrouk Hachemi .: “Predictive current control in multifunctional grid connected inverter interfaced by PV system”, *Solar energy* , 2016,139:130-141.
- [84] Yongchang Zhang, Changqi Qu , “Model Predictive Direct Power Control of PWM Rectifiers Under UnbalancedNetwork Conditions,” *IEEE Transactions on Industrial Electronics*,2015, 62(7):4011-4022.
- [85] Rodríguez,J.,Cortés,C., “Predictive Control of Power Converters and Electrical Drives”,*Wiley & Sons Ltd*, 2012.
- [86] Sze sing lee, Yeh en Heng, “Optimal VF-PDPC of grid connected inverter under unbalanced and distorted grid voltages”, *Elect.Powr Syst. Research*, 2016,140, 1–8.
- [87] Sabir Ouchen, Achour Betka, Sabrina Abdeddaim, Abdelkrim Menadi, “Fuzzy-predictive direct power control mplementation of a grid connected photovoltaic system, associated with an active power filter”, *Energy Conver. Manag.* 2016,122: 515-525.
- [88] Zhanfeng Song., Changliang Xia.,Tao Liu.: “Predictive current control of three-phase grid-connected converters with constant switching frequency for wind energy systems”, *IEEE Trans.Ind. Electron.*, 2013,60, (6): 2451 -2464.
- [89] Alejandro Calle-Prado., Salvador Alepuz., Jose Rodriguez.: “Model predictive current control of grid- connected neutral-point clamped converters to meet low voltage ride-through requirements”, *IEEE Trans. Ind. Electron.*, 2014,62 (3):1503- 1514.

- [90] Marco Rivera, Venkata Yaramasu, Maurice Fadel, “Digital predictive current control of a three-phase four-leg inverter,” *IEEE Trans. Ind. Electron.*, 2013, 60(11):4903- 12.
- [91] Mohammad Hadi Andishgar, Eskandar Gholipour, Rahmat-allah Hooshmand, “An overview of control approaches of inverter-based microgrids in islanding mode of operation,” *Renewable and Sustainable Energy Reviews*, 2017, 80: 1043–1060.
- [92] G. Shankar, V. Mukherjee, “Load-following performance analysis of a micro turbine for islanded and grid connected operation,” *Electrical Power and Energy Systems*, 2014, 55:704-713.
- [93] Usman Bashir Tayaba, Mohd Azrik Bin Roslana, “A review of droop control techniques for microgrid,” *Renewable and Sustainable Energy Reviews*, 2017, 76:717–727.
- [94] H. R. Pota , M. J. Hossain , M. A. Mahmud , R. Gadh, “Islanded Operation of Microgrids with Inverter Connected Renewable Energy Resources,” 19th IFAC World Congress Cape Town, 2014 , pp.6368-6373.
- [95] Ritwik Majumder, Balarko Chaudhuri, “Improvement of Stability and Load Sharing in an Autonomous Microgrid Using Supplementary Droop Control Loop,” *IEEE Transactions on Power Systems*, 2010, 25(2): 796-808.
- [96] Joan Rocabert, Alvaro Luna, “Control of Power Converters in AC Microgrids,” *IEEE Trans on Power Electronics*, 2012, 27(11): 4734 – 4749.
- [97] Alaa Mohda, Egon Ortjohanna, Danny Mortonb, Osama Omaric, “Review of control techniques for inverters parallel operation,” *Electric Power Systems Research*, 2010, 80: 1477–1487.
- [98] Lu Xiaonan, Guerrero Josep M, Teodorescu, et.al., “ Control of parallel-connected bidirectional AC-DC converters in stationary frame for microgrid application”, *3rd IEEE Energy Conversion Congress and Exposition*, pp. 4153-4160 .
- [99] V. Ravikumar Pandi , A. Al-Hinai , Ali Feliachi , “Coordinated control of distributed energy resources to support load frequency control”, *Energy Conv. and Mgmt*, 2015, 105 : 918–928 .
- [100] Jing Wang, *et al.*, “Design of a generalized control algorithm for parallel inverters for smooth microgrid transition operation,” *IEEE Trans. Industrial Electronics*, 2015, 62:4900-4914.
- [101] Partha Pratim Das, *et al.*, “A d-q voltage droop control method with dynamically phase shifted phase locked loop for inverter paralleling without any communication between inverters , *IEEE Trans on Industrial Electronics*, 2017, 64:4591 - 4600 .
- [102] Seul-Kim, “Voltage shift acceleration control for anti-islanding of distributed generation inverters,” *IEEE Trans. Power Delivery*, 2011, 26:2223 – 2234.
- [103] Mohammad A, *et al.*, “Improved droop control strategy for grid-connected inverters,” *Sustainable Energy, Grids and Networks*, 2015, 1:10–19.

- [104] Wenlei Bai , *et al.*, “ Distributed generation system control strategies with PV and fuel cell in microgrid operation”, *Control Engineering Practice*,2016,53:184-193.
- [105] Ali Bidram, *et al.*, “Distrbuted cooperative secondary control of Microgrid Using Feedback linearization”, *IEEE Trans. Power Systems*, 2013, 28(3):3462-3470.